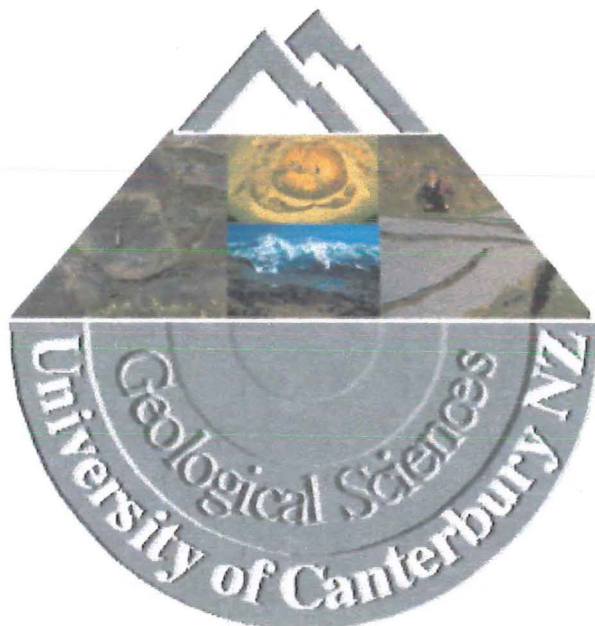


Investigation of Potentially Expansive Soils, 'The Birches' Subdivision, Rangiora, New Zealand

A thesis
submitted in partial fulfilment
of the requirements for the degree
of
Bachelor of Science with Honours in Engineering Geology
at the
University of Canterbury
By
NICHOLAS CLENDON



University of Canterbury,
July 2001

Abstract

'The Birches' is a recently developed subdivision in the township of Rangiora. Early in 1997 a Benkelman Beam test on Lowes Place, one of the two major access roads into 'The Birches', produced deflection results as high as 12.76 mm. In addition to this was the raising of a section of footpath 10-20 mm up from the curb. Early 1998 saw longitudinal shrinkage cracks appear in a house access driveway, while later in 1998 two houses experienced cracking and movement of the interior wall linings, subsequently requiring redecoration.

These types of damage are typical of the damage caused by expansive soils, and an investigation was put in place to evaluate these potentially expansive soils. There are no previous cases of swelling soil problems in Rangiora or on the Canterbury Plains, so a field investigation program using crack monitoring, shallow moisture pits and trenches was implemented. A range of samples were gathered from three trenches, including bulk, long and short tube, and block samples. The laboratory methods for analysing these samples included a scanning electron microscope for the identification of microscopic layering, the plotting of grading curves to establish grain distribution, the establishment of dry density, and laterally confined vertical swell levels. The aim of this was to establish both a cause, and the controlling factors of the observed soil volume expansion.

The trenches revealed massive, homogenous, silty clay units, with numerous rootlets throughout. The SEM study showed no layering or bedding to be present, but showed evidence of possible bioturbation or leaching. XRD analysis discerned the clay mineralogy was, on average, 20% kaolinite and 80% muscovite. Both of these are very stable minerals, and showed no swelling properties when glycolated. This indicates the causes of volume expansion in these soils are structural. Remoulded samples were also tested, and proved to be more susceptible to volume expansion when moisture content was increased. This is because the process of remoulding destroys the stability of the lattice structure of the soil, which has formed through repetition of the shrink/swell process. The presence of leaching and bioturbation, and the presence of kaolinite, indicates acidic leaching. The historical data, combined with the evidence of previously high levels of vegetation in the area, as indicated by the presence of rootlets in the silty clay unit, suggests the depositional environment was that of a swamp margin.

Acknowledgements

During this most exciting time in my life many people took time out from their own busy day to make my journey a little easier.

Thanks to Dave Bell for using up all his red pens on my draft copies, both the many ticks and crosses were of much assistance in eliminating the nonsense.

Marton Sinclair for lending both an ear and an idea or two, and organising the much needed money for digging holes.

Too all the technicians: Cathy Knight, Arthur Nicholas, Jane Guise, Neil Richards and Siale Faitotonu.

Mum for all the care packages she felt she needed to send me.

The rest of the family for sounding interested.

My Flatemates, Ginge, Mutt, Hutt, for their never ending support and honest care for my well-being. Also for making sure dinner was cooked by the time I got home.

Thanks to my roommates Backdoor, Loose Hiney and Mr Squeal for being quiet, considerate, caring and highly motivated towards academic achievement. I feel we all deserve first class honours.

Last but not least, Bex, for everything (editing, cooking breakfast, humouring me and putting up with me).

Thanks.

Contents

	<u>Chapter 1: Introduction</u>	<u>Page</u>
1.1	Project Background	1
1.2	Regional Setting	1
	1.2.1 Location	1
	1.2.2 Basement	3
	1.2.3 Late Cretaceous to Cenozoic Cover Sequence	3
	1.2.4 Quaternary Deposits	5
1.3	Subdivision History	
	1.3.1 Road and Pavement Deflections	6
	1.3.2 House Foundations and Damage	9
	1.3.3 Probable Causes	10
1.4	Specific Project Objectives	12
1.5	Previous Investigations	12
	1.5.1 Expansive soils	12
	1.5.2 Site Specific Works	14
1.6	Project Format	14
	 <u>Chapter 2: Review of Soil Behaviour</u>	
2.1	Introduction	16
2.2	Field Evidence	17
2.3	Mineralogical Considerations	18
	2.3.1 Clay Mineralogy	18
	2.3.2 Ion Exchange	21
	2.3.3 Soil Structure	23
2.4	Geotechnical Factors	24
	2.4.1 Particle Size	24
	2.4.2 Suction	24
	2.4.3 Environmental Conditions	25
	2.4.4 Shrinkage	27
2.5	Evaluation of Shrink/Swell Behaviour	28
	2.5.1 Identification and Location	29
	2.5.2 Evaluation of the Soil	29
	2.5.3 Evaluation of the Extent of Influence of Environmental Conditions	30
2.6	Deflection	30
2.7	Project Methodology	31
2.8	Synthesis	34
	 <u>Chapter 3: Field Investigations</u>	
3.1	Introduction	35
3.2	Ashley Fan Geomorphology	35
3.3	Site History	38
3.4	Fieldwork	39
	3.4.1 Field Program	39
	3.4.2 Crack Monitoring	41
	3.4.3 Shallow Pits	44
	3.4.4 Trenches	46

3.5	Data Interpretation	48
3.6	Synthesis	49

Chapter 4: Laboratory Testing

4.1	Introduction	50
4.2	Scanning Electron Microscope	51
4.3	Atterberg Limits and Grading Curves	53
	4.3.1 Method	53
	4.3.2 Results	53
4.4	Dry/Bulk Density and Vertical Swell	57
	4.4.1 Method	57
	4.4.2 Results	57
4.5	X-Ray Diffraction Analysis	60
	4.5.1 Method	60
	4.5.2 Results	60
4.6	Tri-axial Testing	62
4.7	Swell Tests on Re-compacted Samples	64
	4.7.1 Method	64
	4.7.2 Results	65
4.8	Synthesis	67

Chapter 5: Conclusions

68

References

71

Appendix

A – Tectonics-Ashley Fault	A-1
B – Subdivision History-General Sequence	B-1
C – Test Method Review	C-1
D – fieldwork Results	D-1
E – XRD Results	E-1
F – Laboratory Results	F-1

List of Figures

<u>Figure</u>	<u>Page</u>
1.1 Physical Setting of the Ashley Catchment and Location of 'The Birches Subdivision	2
1.2 Geology and Structural Setting	4
1.3 Location of Fill and Services in The Birches Subdivision	7
1.4 Photo of Driveway to lots 67, 66.	9
1.5 Deflection of Lowes Place in "The Birches" Subdivision	11
1.6 Shrinkage Cracks in "The Birches" Subdivision	11
1.7 Swelling of Subsoil in "The Birches" Subdivision	13
2.1 Clay minerals	20
2.2 Effect of varying density on volume change for constant moisture content samples	25
2.3 Shrinkage Diagram	28
3.1 Sketch of the Rangiora and Ashley Fans	36
3.2 Geomorphic Map of the Rangiora Township and Surrounding Area	37
3.3 The Birches Subdivision Field Work Map	40
3.4 Shallow Moisture Pits	41
3.5 Crack Diagram	41
3.6 Percentage Change in Spacing Between Two Nails Spanning a Surface Crack	43
3.7 Moisture content vs. Time for Soil Samples Taken at Varying Depths	45
3.8 Excavation Logs	47
4.1 SEM Sample One	52
4.2 SEM Sample Two	52
4.3 SEM Sample Three	52
4.4 Casagrande Plot with Unified Soil Classification System (USCS) for Soil from 'The Birches' Subdivision	54
4.5 Grading Curves	55
4.6 Dry Density Versus Confined Vertical Swell for Natural Samples	56
4.7 Confined Vertical Swell Versus Initial Moisture Content for Natural Samples	58
4.8 Block Diagram of the Geological Setting During Deposition of the Silty Clay Unit Beneath 'The Birches' Subdivision.	63
4.9 Undrained Triaxial Shear Stress versus Normal Stress for Soils Recovered from Trench R3, 'The Birches' Subdivision	64
4.10 Determination of the Dry Density/Water Content Relationship, Combined Sample	66
4.11 Confined Vertical Swell on Re-compacted Samples Versus Natural Samples	66

List of Tables

<u>Table</u>	<u>Page</u>
1.1 Quaternary Deposits of the Ashley River Floodplain	6
2.1 Summary of Clay Mineral Characteristics	22
2.2 Summary of Environmental Conditions and Affects	26
2.3 Effect of Varying Moisture Content on Volume Change And Swelling Pressure for Constant Density Samples	27

3.1	Table 3.1 Summary of Shallow Moisture Pits Data	44
4.1	Laboratory Program	50
4.2	Atterberg Limits and Clay Size Fraction	56
4.3	Result of Dry/Bulk Densities and Vertical Swell	59
4.4	XRD Results	61

Chapter 1 Introduction

1.1 Project Background

This project is concerned with the presence of potentially expansive soils in the Rangiora area, North Canterbury. Eliot Sinclair and Partners Limited identified the possible existence of such soils during development of a new subdivision called 'The Birches'. The construction of this subdivision has been divided into three stages, with the first two stages already complete. During the construction of Stage One, in early 1997, two incidents caused minor concern to the engineers. These were high deflection of one of the access roads, and the lifting of a footpath out of alignment with the curb. Stage Two, in early 1998, problems occurred with an access driveway developing longitudinal cracks. Additionally, two Stage Two houses constructed later that year suffered cracking and movement in the interior wall linings. Both houses required redecorating at the expense of the developers.

Subsoil testing was carried out prior to construction, with the conclusion that the soil was satisfactory, consistent with the New Zealand Standard 4431:1989. Therefore there were no special requirements for the construction of the foundations under the provisions of New Zealand Standards: 3604:1990 - 'Code of Practice for Light Framed Timber Buildings not requiring Specific Design'. At the time, the expansive potential of the soil had not been recognised, so expansive soils were not tested for. The above events occurring in Stages One and Two of the subdivision development are consistent with the kinds of damage caused by the expansive behaviour of soils (see Section 2.2). Therefore, this expansive soil behaviour is the focus of this project. Specifically, the project examines the nature, distribution and origin of the potentially (or apparently) expansive soils, and evaluates their geotechnical characteristics and possible remediation.

1.2 Regional Setting

1.2.1 Location

'The Birches' subdivision lies within the township of Rangiora, which is situated south of the Ashley River on its floodplain (Figure 1.1). The Canterbury Regional Council describes the Ashley River, as "...a steep braided river, which

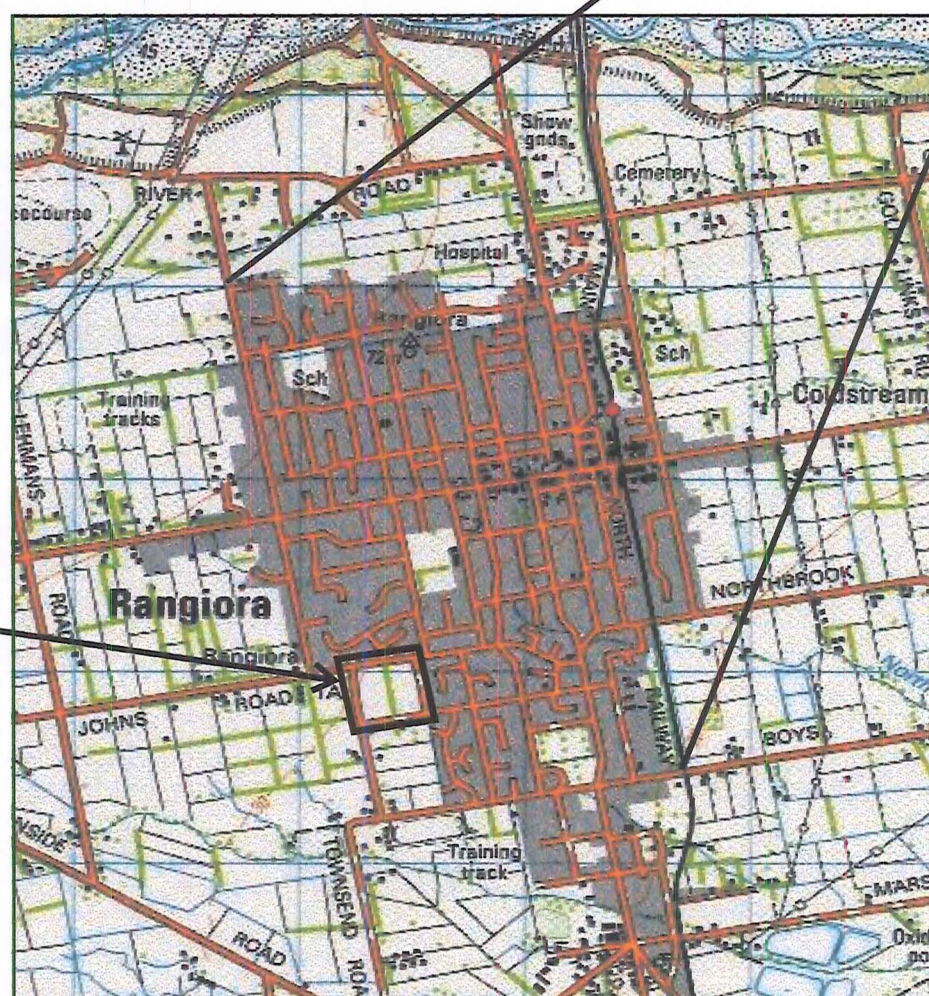
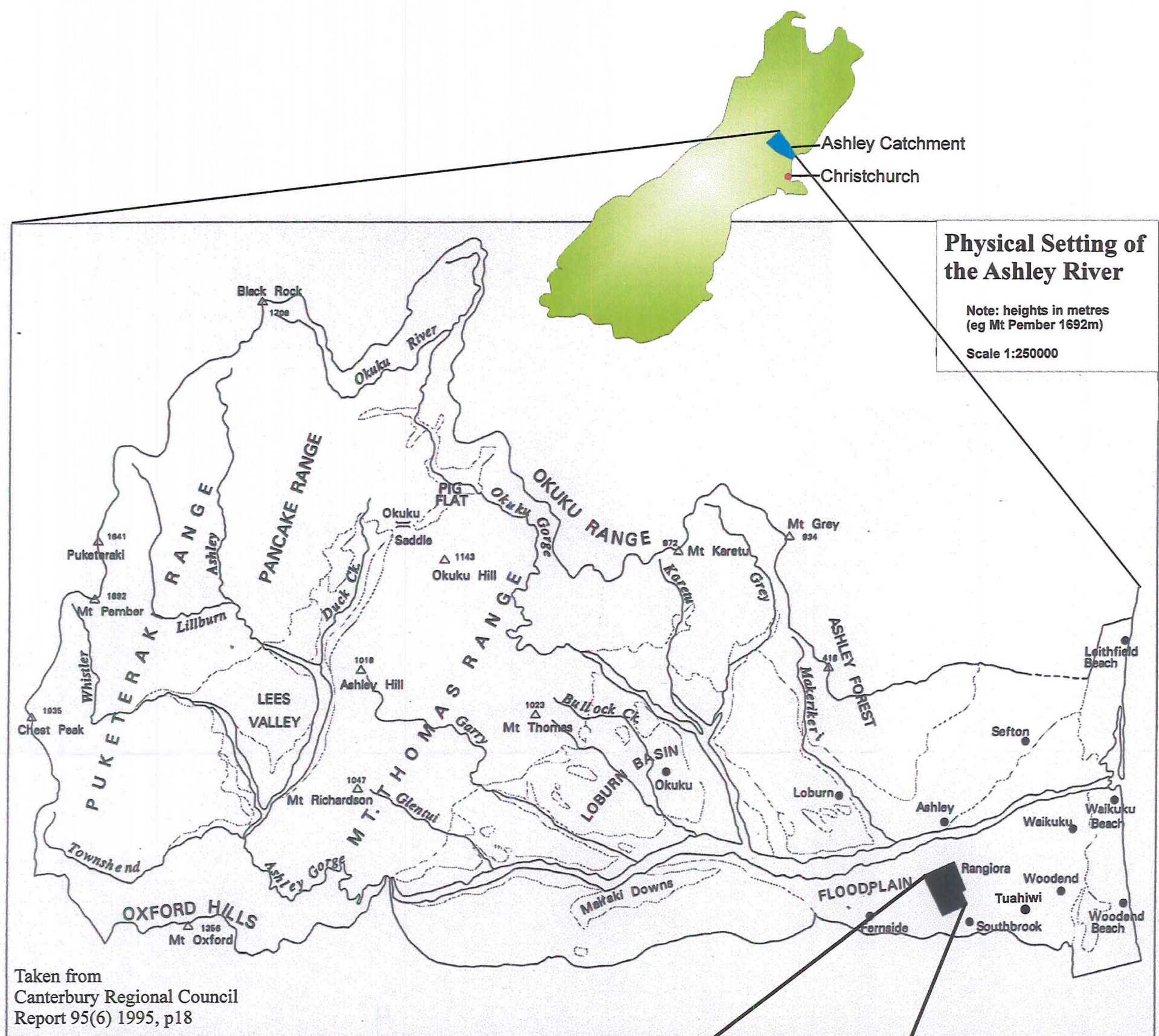


Figure 1.1 Physical Setting of the Ashley River and Location of 'The Birches' Subdivision

together with its major tributary the Okuku, drains a catchment of 1,340 square kilometres” (Canterbury Regional Council Report 95(6), 1995, p17).

The headwaters of the Ashley River are located within the Puketeraki Range. The river then flows down through Lees Valley, through the Ashley Gorge and over Loburn Basin, to where it meets the Okuku River. The Ashley Floodplain, referred to earlier, begins seaward of the junction of the Okuku and Ashley Rivers (Figure 1.2).

The geomorphic features of the existing Ashley Floodplain, as well as many of the older geological formations (as described in Table 1.1), have been controlled not only by the tectonic and geological setting (Figure 1.2), but also by the post-glacial climate. The tectonic setting is described in Appendix A.

The geological setting can be separated into three periods: the Basement, the late Cretaceous to Cenozoic cover sequence, and the Quaternary deposits. These will be discussed separately in the following sections.

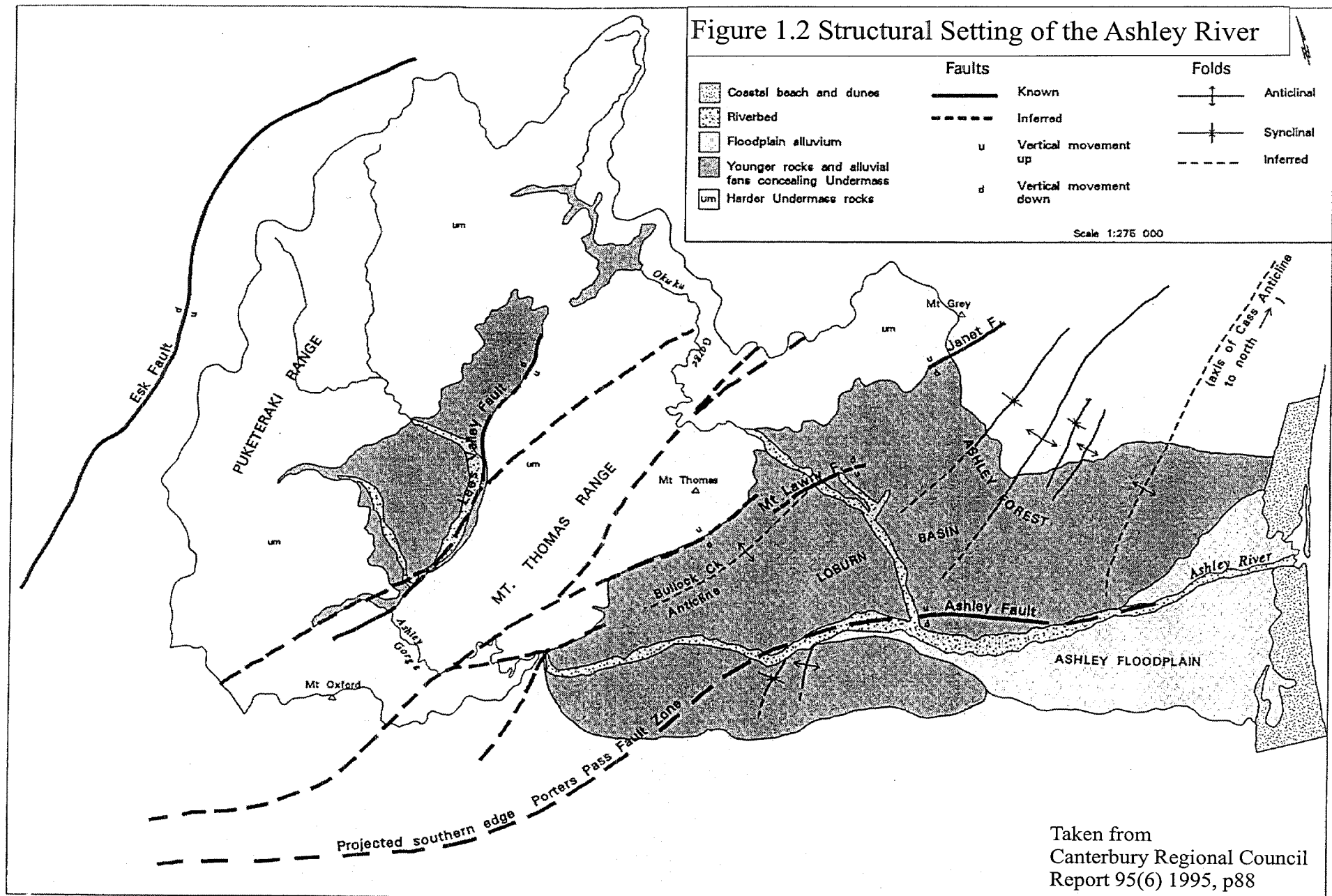
1.2.2 Basement

The basement rock of the Ashley Catchment is made up of the Rakaia and Pahau terranes, which are collectively known as the Torlesse Supergroup. The Rakaia and Pahau terranes account for 98% of the Torlesse lithology, with the other 2% coming from exotics, such as minor volcanics of Mesozoic era (Sisson, 1999). The basement rock is well exposed in the upper catchment, with the exception of Lees Valley which has alluvial fans and younger rocks concealing the Torlesse. The Torlesse Supergroup is noted on Figure 1.2 as harder undermass (um) (Canterbury Regional Council Report 95(6), 1995).

1.2.3 Late Cretaceous to Cenozoic Cover Sequence

This sequence comprises three major units. First is the late Cretaceous-mid Oligocene Eyre Group, which is essentially a transgressive shelf unit including predominantly sandy rocks at or near the base of the Cretaceous-Cenozoic sequence in Canterbury. Unconformably overlying the Torlesse basement, these rocks range in age from Haumurian (65-69million years ago) to Whaingaroan (32-38 million years ago). This is discussed by Sisson (1999), and Browne and Field (1985).

Conformably overlying the Eyre Group is the early-to-mid Oligocene Amuri Limestone. This is overlain by the Motunau Group of the mid Oligocene to early



Quaternary age, which represents the beginnings of the marine regression. The Motunau Group deposits are represented on Figure 1.2 as younger rock and alluvial fans concealing undermass. They have not been separated from the Quaternary deposits that are also represented as younger rock and alluvial fans concealing undermass.

1.2.4 Quaternary Deposits

The Quaternary-aged deposits overlying the Cretaceous to Cenozoic sequence are closely related to changes in climatic conditions and reflect both glacial and interglacial periods. These formations have also been influenced by regional and local tectonic activity. Unlike the Waimakariri and Rakaia Valleys, the Ashley catchment has never been glaciated and therefore lacks a moraine sequence to which down valley aggradation surfaces could be traced (Suggate, 1965). The Quaternary deposits are shown on Table 1.1.

Springston Formation <14000 years includes Holocene	
Yaldhurst Member	Gravels, sand or silt deposited in flood channels of the lower Ashley, both before and after the recent development of stopbanks and groynes. Member probably less than 300 years old.
Yaldhurst-Halkett Member	Gravel, sand or silt mapped undivided as Yaldhurst to Halkett in the vicinity of Rangiora. Deposited in the last 3000 years, it is the member which relates to that underlying 'The Birches' subdivision.
Halkett Member and older	Undifferentiated alluvium underlying terraces mostly situated above boundary banks of present-day floodplain. Member between the ages of 3000 to 10,000 years.
Pleistocene 1.64 Ma - 14000 years ago	
Burnham Formation	Fluvioglacial outwash gravel composed almost entirely of greywacke pebbles with creamy matrix of sand and silt; gravel typically coarse and poorly sorted; surface is relatively flat to gently sloping and capped by loess averaging 0.7 metres thick. Formation was deposited in the last glacial period, in the interval c.1500 to 27000 years. Soils are Lismore age (>14,000 years).
Windwhistle Formation	Fluvioglacial outwash gravel composed of cream-brown pebbles with of sand and silt matrix; gravel typically poorly sorted; surface slightly rolling and dissected with a loess cover averaging 1.0 metre thick. Formation is considered older than 45,000 years and correlates with cold climate conditions c.40,000 to 70,000 years ago.
Woodlands Formation	Fluvioglacial outwash composed of brown, silty, poorly sorted gravel; surface is moderately rolling and dissected, with a loess cover averaging 1.5-2.0 metres thick. Formation correlates with a cold climate inferred at c.150,000 years ago.
Horoata Formation	Brown, friable, dissected high level gravel; loess up to 15 metres thick. Age of formation uncertain.
Pliocene-Pleistocene 5.2 – 1.64 Ma	
Kowai Formation	Top of the Motunau Group, the Kowai formation is the oldest deposits and is exposed at the surface of the Loburn basin. Brown, weathered, soft, silty gravel interbedded with grey, moderately soft silt mudstone and fine sand.

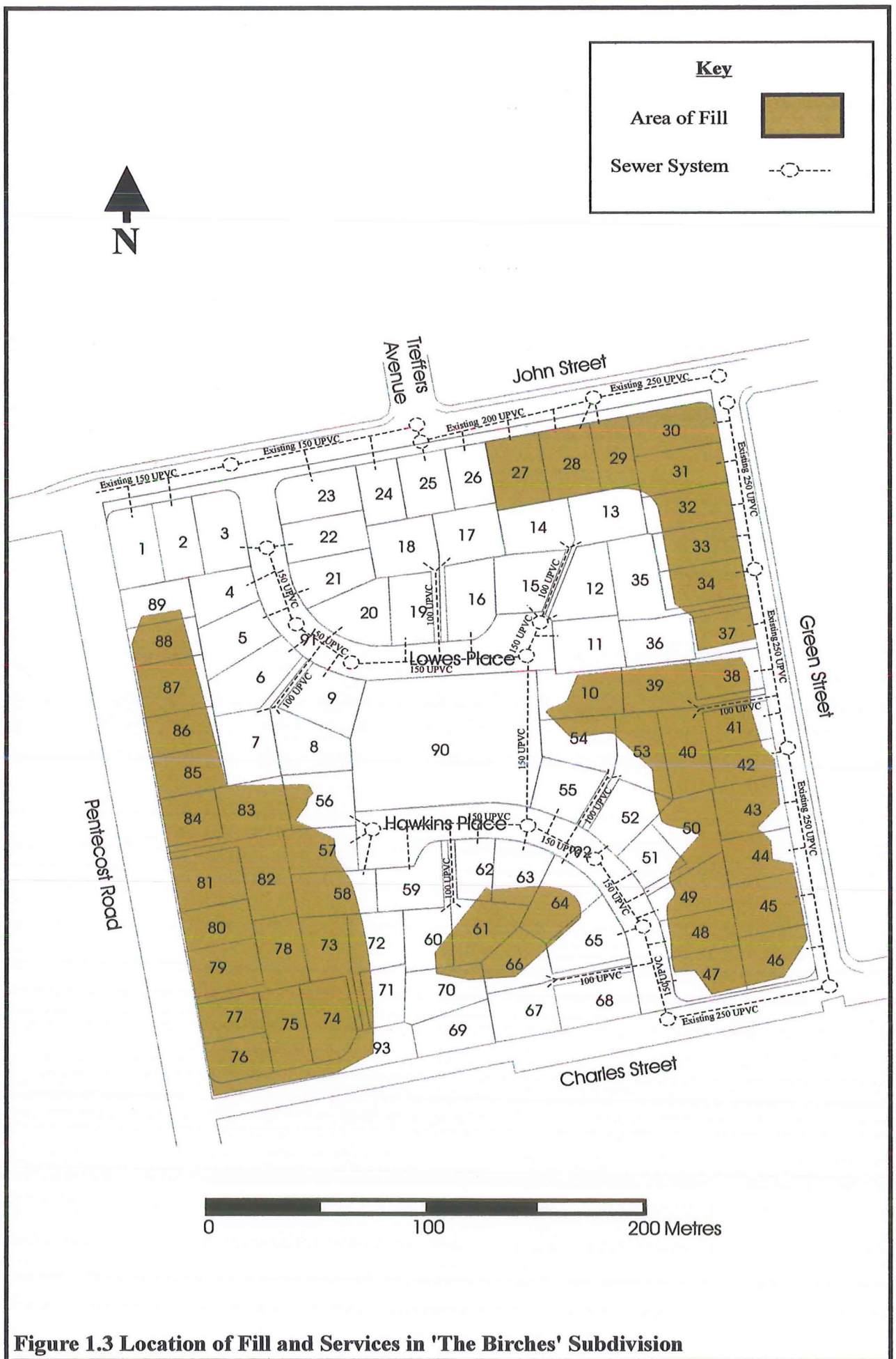
Table 1.1 Quaternary Deposits of the Ashley River Floodplain.
(adapted from McPherson, 1991 in Sisson, 1999)

1.3 Subdivision History

A general sequence of event for the installation of services and filling operations is given in Appendix B. Figure 1.3 shows the location of services and the extent of the filling operation.

1.3.1 Road and Pavement Deflections

The access road that displays a high level of deflection is known as Lowes Place. The rebound deflection of the pavement under a Benkelman Beam Test, with an axle weight of 8.2 tonnes, varied from 1.67mm to 12.76mm. Generally, values



greater than 1.5mm are regarded as high, and are indicative of a weak subgrade. Several attempts were made to reduce this deflection, but none were successful. It was sealed in early March of 1998, at the end of Stage One.

The footpath constructed in Stage One, which lifted up one to two centimetres from the kerb, is located outside Lot 27 (Figure 1.3). While the kerb was poured in late 1997, the footpath was not poured until early 1998. The soil that would eventually have the footpath lain on it was exposed to at least two months of warm, dry summer weather. This created a moisture difference between the soil beneath the footpath and the soil beneath the kerb. By the time the footpath was lain, the soil beneath the kerb had already made some progress towards equilibrium. However the soil beneath the kerb was moisture deficient from the exposure during the summer months, and started to absorb water into its structure much more rapidly. This lead to an increase in the volume of the soil beneath the footpath, and consequent uplift.

The access driveway constructed during Stage Two, which developed longitudinal cracks, runs off Hawkins Place (Figure 1.3) and provides access to Lots 66 and 67. The driveway was sealed in mid-to-late 1998, and consisted of 400mm of granular fill placed on top of the subgrade. Cracking occurred during the summer of 1998-1999. The cracks run down through the full thickness of the seal, and appear to be shrinkage cracks. It should be noted that a 100mm diameter sewer pipe (Figure 1.4) runs parallel to the cracks, although these are not the kind of cracks typically associated with poorly filled trenches. Cracks of this nature have not been found elsewhere in the subdivision. A photo of the driveway is shown in Figure 1.4.



Figure 1.4 Photo of Access Drive to Lots 67 and 66

1.3.2 House Foundations and Damage

The two houses that suffered damage were built during Stage Two. These are situated at 23 Green Street (Lot 41) and 29 Hawkins Place (Lot 50). After the topsoil was stripped, Lot 41 received 0.1-0.15m of fill. Topsoil was then laid 300mm thick over the site. After Lot 50 was stripped of its topsoil, it received 0.05-0.1m of fill on its north-eastern half. Once again, topsoil was replaced to a depth of 300mm (Eliot Sinclair and Partners Ltd Report 192295, 1999). The property at 23 Green Street had its foundations constructed early in December 1998. During the following year cracks started to appear in the wall linings. Cracks occurred at ceiling level in the living room/bedroom after a particularly wet period. Examination of the exterior of the

house found no sign of any cracking in the wall claddings. A survey was carried out on the interior floor, which showed it to be bowing up 10-15mm from the perimeter of the house to the centre. The garage perimeter level varies from 0-15mm relative to the lowest point on the perimeter (Eliot Sinclair and Partners Ltd Report 192295, 1999). This is a considerably higher variance than could be normally expected from construction error.

29 Hawkins Place had two external cracks, one in the northeast wall and one over the window in the southwest wall. The levels of topsoil around the outside of the house showed that the fill on the north-eastern half of the lot had not settled. However, while this eliminates settlement as a cause for the structural damage, it does not eliminate the possibility of swelling under the floor slab. Levels taken of the interior floor slab showed a 10-12mm rise in floor level relative to the perimeter. The two houses have since been redecorated, and no significant further damage seems to have occurred.

One other house reported cracking in March 2000, but investigation by Eliot Sinclair and Partners Ltd (Report 194115, 2000) concluded shrinkage cracking of the concrete and slab curl effects to be the cause.

Since March 2000 no further incidents of swelling or settlement have been reported, although there appears to be enough evidence to suggest the presence of a potentially expansive soil in the area. The purpose of this investigation is to locate this potentially problematic soil, and to ascertain its properties.

1.3.3 Probable Causes

The above events indicate at least three separate processes at work in 'The Birches' subdivision. First there is the high level of deflection occurring in Lowes Place, which is possibly caused by a process of initial distortion due to over-consolidation. A theoretical set of pictures demonstrating possible subgrade behaviour is shown in Figure 1.5.

Secondly, the initially high moisture content of the soil when the access drive to Lots 67 and 66 was sealed resulted in moisture gradients running parallel to the ground surface, as the asphalt acted as a impermeable membrane. This lead to either rotational failure (Figure 1.6) or crack propagation, resulting in cracking of the asphalt

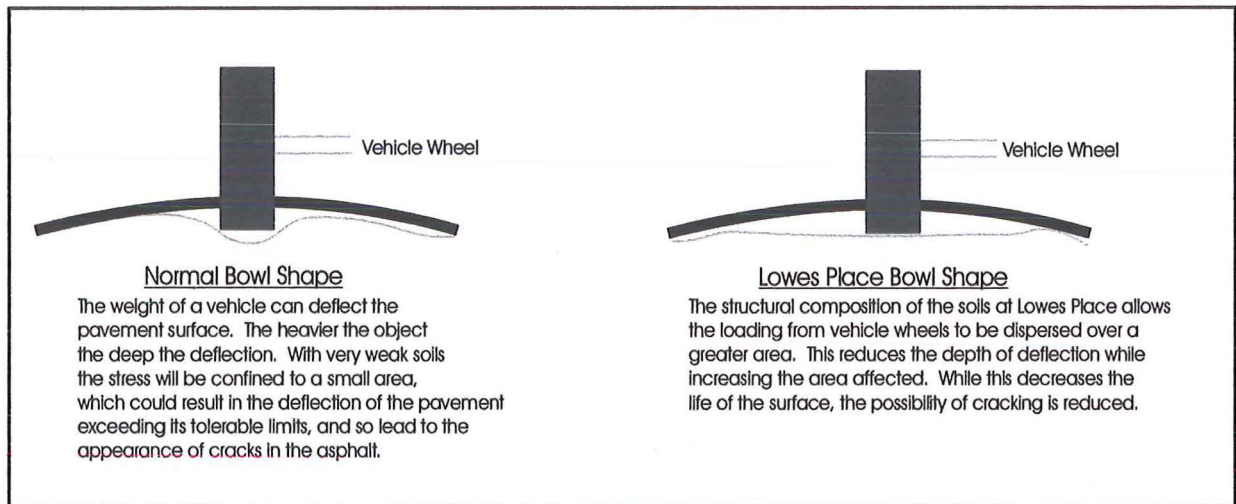


Figure 1.5 Deflection of Lowes Place in 'The Birches' Subdivision

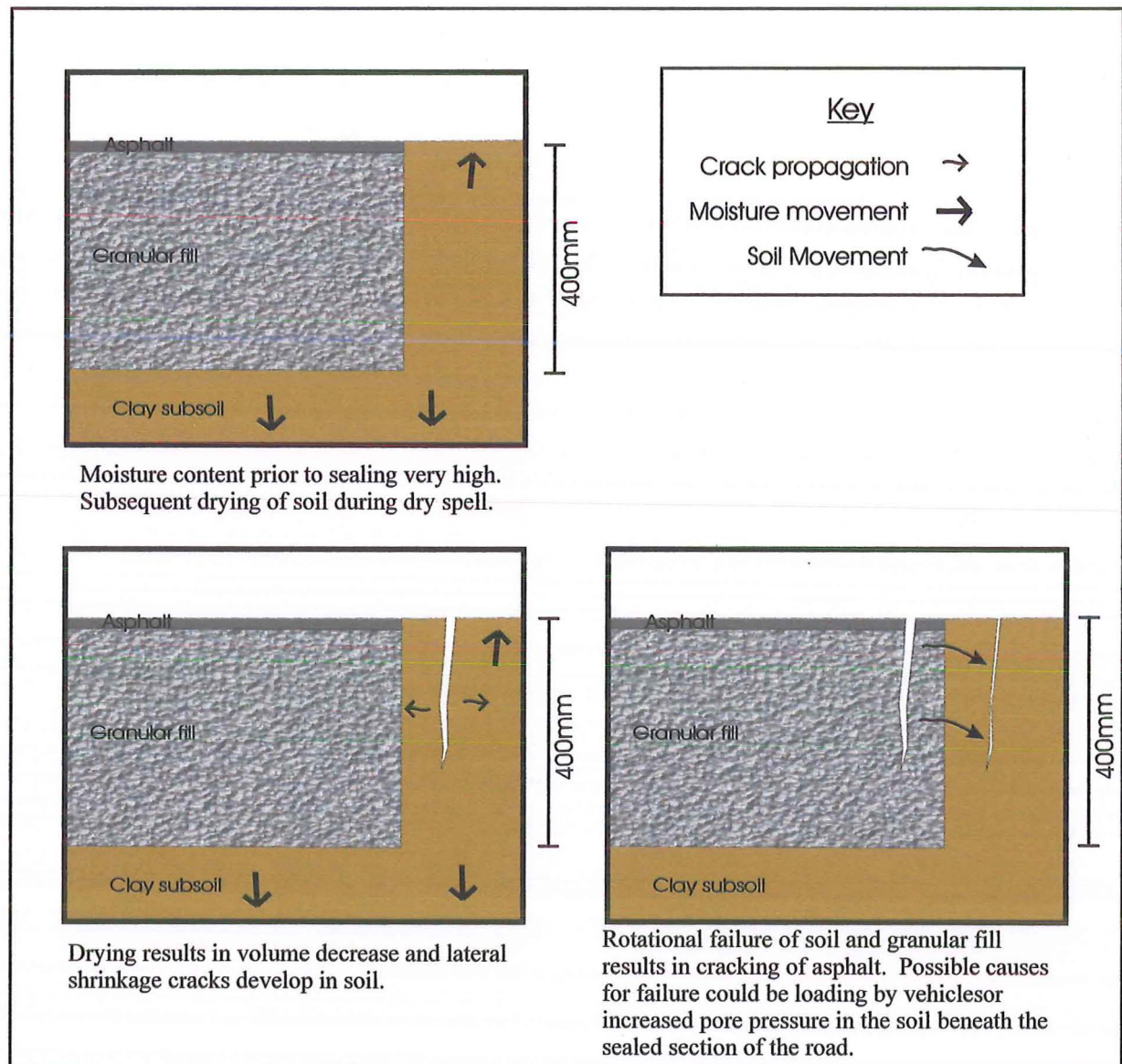


Figure 1.6 Shrinkage Cracks in 'The Birches' Subdivision

Thirdly, moisture uptake after construction of an impermeable membrane (the concrete floor slab) caused swelling of the subsoil. This resulted in differential upheaval of the floor slab, as the perimeter of the slab remained anchored to the foundation. A theoretical interaction between the foundations of the house, the soil, and ground/surface water is shown in Figure 1.7. Figures 1.5, 1.6 and 1.7 are only theoretical models of the processes occurring in 'The Birches' subdivision. Literature review, fieldwork and laboratory testing will be used to better increase the understanding of the actual processes at work.

1.4 Specific Project Objectives

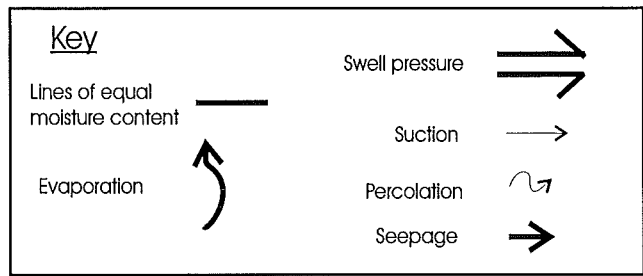
This project is concerned with the identification and evaluation of the causes of the apparent swelling soil phenomena occurring in 'The Birches' subdivision in Rangiora. It has four main objectives, as follows:

1. To locate and identify the expansive soils at the Rangiora site, and to discover the lateral and vertical extent of these soils using both field and laboratory methods.
2. To determine indicative representative geotechnical properties such as Atterberg limits, swell potential, shrinkage limits, grading curves, and density on representative undisturbed samples.
3. To establish the origins of the deposits from both the mineralogical and physical properties, together with any observed field relationships.
4. To make possible recommendations for the prevention of damage to light engineering structures if the presence of expansive soils is found to be active in this area.

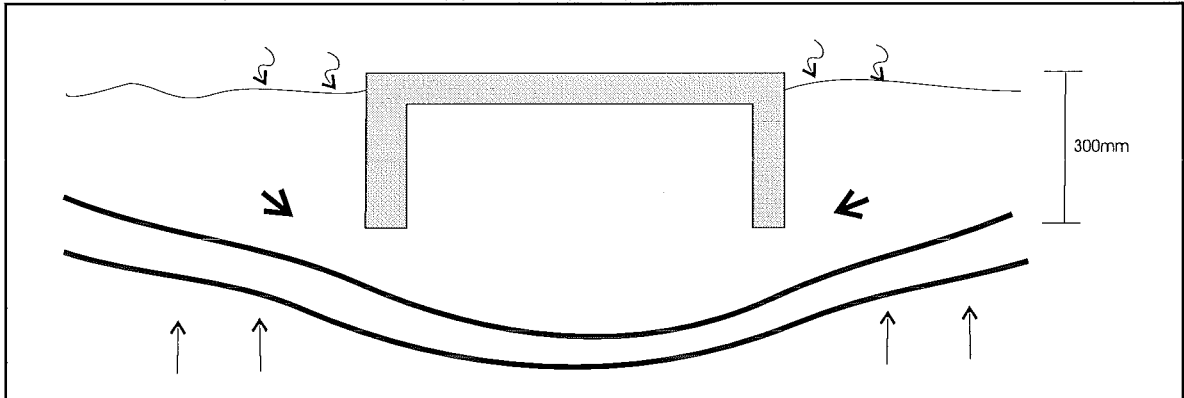
1.5 Previous Investigations

1.5.1 Expansive Soils

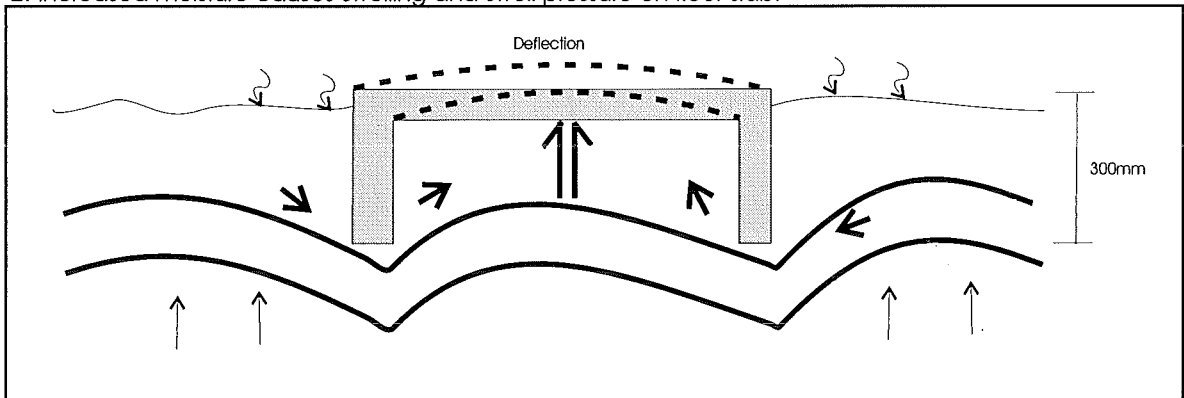
Literature is abundant on expansive soils internationally, with countries such as America, Canada, Israel, Australia and much of Europe widely suffering from expansive soil problems. (see for example Kassiff et al, 1969). Most soil mechanics textbooks have some information on expansive soils, but the major sources of information is journal articles from publications such as the *Quarterly Journal of Engineering Geology*, and proceedings from conferences on expansive soils (eg. Chen



1: House built on dry subsoil, followed by period of precipitation



2: Increased moisture causes swelling and swell pressure on floor slab.



3: Moisture reaches equilibrium under house and swell ceases.

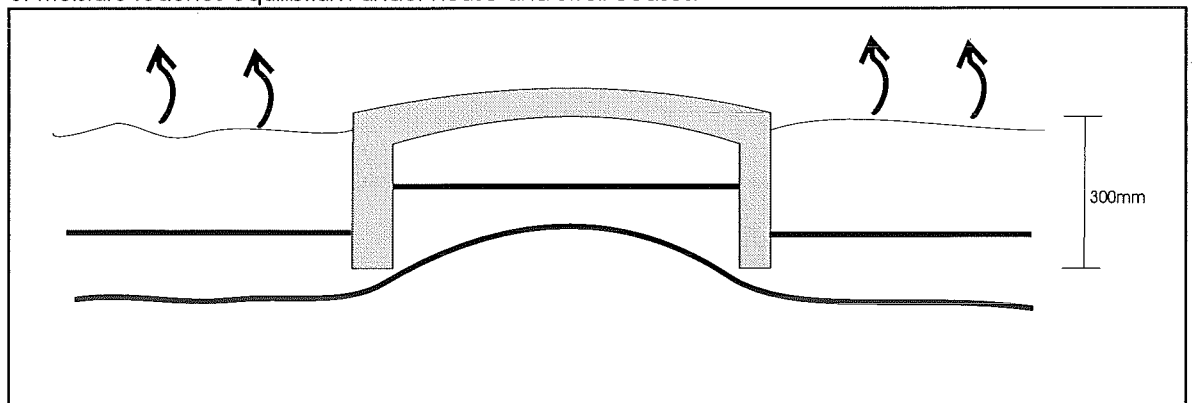


Figure 1.7 Swelling of Subsoil in 'The Birches' Subdivision

1973). The most recent source is the Internet, with companies advertising remedial techniques, and research departments posting their most recent developments. Some examples are: <http://www.ch-non-food.com/science.htm> or the *Canadian Building Digest* found at <http://www.nrc.ca/irc/cbd/cbd148e.html>.

Although there is plenty of overseas literature, there is little documented information on expansive soils in New Zealand, and no reports of expansive soils on the Canterbury Plains (with the exception of some loess deposits that display shrink/swell properties of a structural nature, as described in Section 2.4).

1.5.2 Site Specific Works

No previous work on expansive soils in the Canterbury region appears to have been done to date. After discussion with both residents of the area and some people involved with development in the Rangiora area, it appears that the settling or lifting of houses or structures is reasonably common. However, few of these events have been either reported, or linked in any way to the presence of expansive soils. Layers of peat underlie some parts of Rangiora, and these can cause settlement problems if special precautions are not taken prior to laying of the foundations.

'The Birches' subdivision is thought to be situated on overflow channels from the Ashley River. A technical investigation on the Ashley River Floodplain, carried out by the Canterbury Regional Council (Report 95(6)), showed the presence of three overflow channels running through the Rangiora Township. The report also provides excellent information on the local geomorphology and current layout of flood channels and stopbanks for the Ashley catchment area. Seismic and geological information on this area can be obtained from a number of studies, such as Cowan (1992), and Sisson (1999).

1.6 Project Format

Following this chapter, Chapter Two is a literature review focused upon the nature of swelling soils. It describes both geotechnical factors and mineralogical considerations that can affect the swell potential of a soil. This includes a discussion on the role of environmental factors in the swelling process, and also discusses the effect that the presence of objects such as trees can have on soils. Section 2.5 covers methods for identifying and then evaluating expansive soils, focusing on those

techniques available for use in my own investigation. Following that, Section 2.6 will review soil deflection under loading. These sections enabled the development of the methodology that guided my investigation of the soils in 'The Birches' subdivision. This investigation, together with its results, comprises the remainder of this project. Chapter Three covers the field investigation, and includes a literature review on the geomorphology of the Ashley Fan. It also includes a recent site history evaluation, which employs the use of aerial photos. The findings from fieldwork such as trench excavation and long term monitoring are presented in Chapter Three, and an interpretation of the data is included at the end of that chapter. Chapter Four discusses the results from laboratory testing of recovered samples. The results are discussed individually, with a synthesis at the end of the chapter to tie the data together. Chapter Five draws all the conclusions together, and presents a summary of the findings and possible recommendations for future work.

Chapter 2: Review of Soil Behaviour

2.1 Introduction

There are two classes of expansive soils, the traditional expansive soils and the swelling soils. Traditional expansive soils are soils that at some time exist in a desiccated state, and in this state can absorb additional water and swell. Expansive soils can be made up of soils ranging from clays to clayey sands, with the controlling factor being the presence of expansive clay minerals. While all clays have expansive potential to some extent, some minerals are more prone to expansion because of their structure. Swelling soils, on the other hand, are soils with a weak fabric that can also absorb water, but not into the mineral structure. They instead absorb water into the pore spaces, causing pore volume expansion. This swelling soil behaviour not only occurs in clay soils, but also in silts and sandy silts. While the swelling soils are not as unstable as expansive soils, swells of up to 25% in loess soils with only 5-10% clay have been documented. Swelling occurs mostly due to positive air pressure created during water uptake (Yetton, 1986, in Jowett, 1995). These reasons for increases in soil volume are generally classed as either mineralogical factors or geotechnical factors, and can be broken down into the following categories:

Mineralogical Factors

1. Clay mineralogy
2. Ion exchange and dielectric properties
3. Soil structure

Geotechnical Factors

4. Percentage of clay sized particles
5. Environmental conditions
6. Suction

These six parameters will control the swell potential a soil has, and are crucial in the identification and evaluation of the soil. They are the focus of this chapter and are discussed in Sections 2.3 and 2.4 respectively. The geotechnical section (Section 2.4) will also include information on swelling caused by tree roots. The process of shrinkage

introduced in Section 2.4.4 will be included in the geotechnical section due to its close relationship to swell behaviour.

Although soil volume expansion is the main concern of this project, there are other detrimental, or potentially detrimental processes at work in the 'The Birches' subdivision. This includes the process of deflection at Lowes Place that was briefly mentioned in Section 1.3.4, and which will also be discussed in depth in Section 2.6.

The aim of this chapter is to develop a basic understanding of the processes that are occurring in the 'The Birches' subdivision. This will then allow fieldwork and laboratory testing to be carried out to its full potential. The ideas picked up from this literature review will be used to develop a methodology that the rest of the project will use to evaluate the soils in question (see Section 2.7).

2.2 Field Evidence

Expansive and swelling soils predominantly cause damage to light engineering structures. Large, multiple-storey buildings and heavy engineering works are less affected as they overcome the swell pressure of the soil. Changes in moisture content are the primary reason for the volume expansion of soils, and there are four scenarios that can result from this change. (Kassiff, G. et al 1969: p2):

1. Shrinkage of the soil due to drying
2. Swelling of the soil due to wetting
3. Development of swelling pressures in soil that is confined and cannot swell
4. Decrease in strength and bearing capacity of soil as a result of swelling

Structures that fail because of volume expanding often have some very characteristic forms of damage, and recognition of the type of failure will be the first indication of a swelling or expansive soil problem. Below is a list of various structures and the corresponding possible failure types caused by the presence of expansive or swelling soils (after Jennings, 1974):

Pavements

- Distortion - resulting in an uneven appearance along a significant length of road surface

- Cracking – appearance of longitudinal cracks, normally parallel to the road axis. Transverse cracks may also develop around culverts.
- Reduced bearing capacity - localised failure of pavement with disintegration of surface (Kassiff, et al 1969)

Low rise single and double storey buildings

- Cracking in wall claddings, especially severe in rigid structures such as brickwork
- Floors distorted upwards in centre relative to perimeter

Retaining walls and support structures

- Cracking, tilting, or moving due to subjection to higher than normal lateral pressure
- Creep

Canals and Water retaining structures

- Distortion and departure from grade
- Shrinkage cracks in stop banks/canal walls may cause leakage points

Sewers and Pipes

- Pipes can crack if not flexibly constructed

Railway lines

- Distortion - requiring more line maintenance

The level of damage will depend on the amount of swell that occurs. Stable soils may have an increase in volume of only a few millimetres, while others have been known to increase to one and a half times their original volume. The smaller levels of volume increase are often not even detected, as they can occur well within the design limits of the structure. At worst, they may shorten the life of the structure affected.

2.3 Mineralogical Considerations

2.3.1 Clay Mineralogy

There are two basic units that make up the clay mineral structure, the tetrahedral and octahedral sheets. The tetrahedral sheet consists of one silicon atom surrounded by four oxygen atoms, or hydroxyls if balancing of the structure is required. These

individual units join together by sharing each oxygen atom between two tetrahedral units (Figure 2.1).

The octahedral unit also has a central atom, although this can be silicon, aluminium, magnesium or iron. This central atom is surrounded by six hydroxyl atoms, three at the top and three at the bottom, forming an octahedral shape. The octahedral units also join to form gibbsite sheets (Figure 2.1).

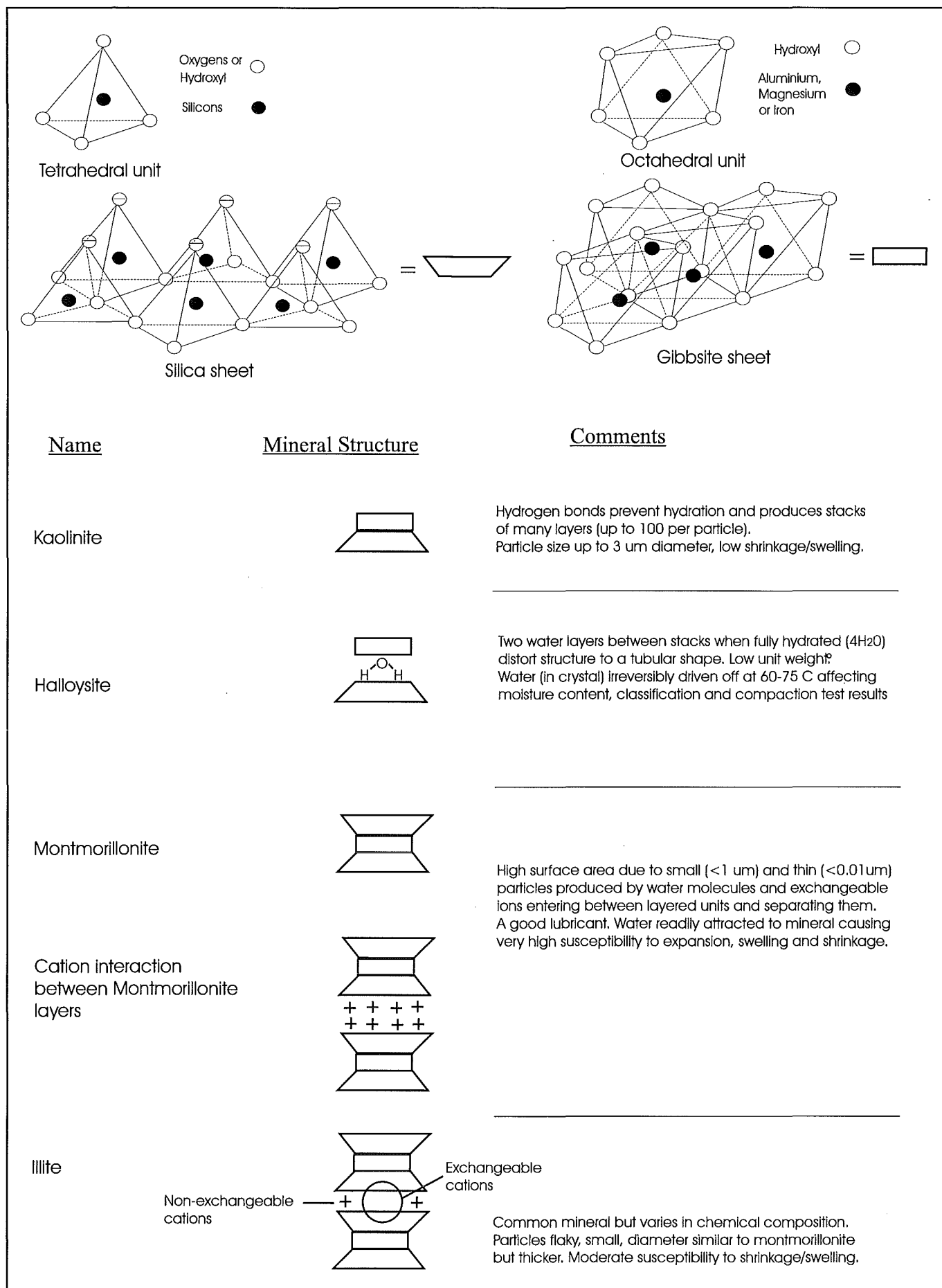
Various combinations of the octahedral and tetrahedral units results in four basic clay minerals: kaolinite, halloysite, montmorillonite and illite (Figure 2.1).

Kaolinite is made up of one gibbsite sheet with a central aluminium atom, joined to a silica sheet due to an unbalanced charge at the apex of the silica sheet.

The hydroxyl ion of the gibbsite and the oxygen ions of the silica sheet are held together by hydrogen bonds (Kassiff, G. et al 1969). Hydrogen bonds are very strong and make kaolinite very stable, as water molecules are unable to penetrate between the layers (see Section 2.3.2).

Halloysite is very similar to kaolinite, except that a layer of water is used to hold the individual layers together. If halloysite is dried sufficiently the properties of the clay will change drastically, as the process of removal of the bonded water layer is irreversible.

Montmorillonite consists of one gibbsite sheet sandwiched between two silica sheets. The gibbsite can include aluminium, iron or magnesium atoms. Structural changes called isomorphous changes can cause the aluminium atom to exchange with the silica atom and result in a negative charge on the clay mineral. This negative charge attracts cations from the soil water (such as Na^+ , Ca^{++}) that are in a continuous state of interchange. The type of cation absorbed has an effect on the activity of the clay. Sodium is the most active, with the rest decreasing in activity in the following order: lithium, potassium, calcium, magnesium and hydroxyl (Kassiff, G. 1969). The interaction between the individual units in montmorillonite and the cations is shown in Figure 2.1. Generally, the bond between these units is relatively weak, and water is easily able to penetrate between the layers. This makes montmorillonite a very active clay mineral.



Illite is similar to montmorillonite, but with aluminium ions replacing some of the silicon ions in the gibbsite sheet. This causes a high negative charge, which attracts non-exchangeable potassium ions. The attraction between the high negative charge and the potassium ions forms a strong bond. This reduces the ability of illite to absorb water. Illite is, therefore, only a moderately active clay mineral.

A summary of clay mineral characteristics is shown on Table 2.1, which includes not only the four basic clay minerals above, but several others as well.

2.3.2 Ion Exchange

Clay minerals absorb and exchange anions and cations into and out of the surface of the clay structure. All clay minerals perform this absorption and exchange to some degree, and the extent of this activity can be measured in terms of millequivalents per 100g of dry clay.

$$\text{Millequivalents (meq) per 100g} = \frac{(\text{mg/100g} \div \text{Molarweight})}{\text{Valancy}}$$

Equation 2.1

Clays will try to absorb cations or anions in order to balance any charge deficiency in the solid particles (Mitchell, J. 1993). This balance of charges can become unbalanced by changes in environmental conditions. Although environmental changes do not “...affect the structure of the clay particles it can cause changes to the physical and physiochemical properties” (Mitchell, 1993, p125). Ion exchange capacity varies from around 3-15meq for a kaolinite, up to 150meq for a montmorillonite (Table 2.1), and is dependent on the type of bonding present. There are four types of interlayer bonding in clay minerals:

1. Simple bonding of cation
2. Polar molecules, free water or hydrated cation
3. Van der Waals forces
4. Hydrogen bonding

Structural						
1. Silica Tetrahedron: Si atom at center. Tetrahedron units form hexagonal network = $\text{Si}_2\text{O}_5(\text{OH})_2$						
2. Gibbsite Sheet: Aluminum in octahedral coordination. Two-thirds of possible positions filled. $\text{Al}_2(\text{OH})_6$ —O—O = 2.60 Å.						
3. Brucite Sheet: Magnesium in octahedral coordination. All possible positions filled. $\text{Mg}_3(\text{OH})_6$ —O—O = 2.60 Å						
Type	Sub-Group and Schematic Structure	Mineral	Complete Formula/Unit Cell ^a	Octahedral Layer Cations	Tetrahedral Layer Cations	Structure Isomorphous Substitution Interlayer Bond
1:1	Allophane	Allophanes	Amorphous	—	—	—
	Kaolinite	Kaolinite	$(\text{OH})_2\text{Si}_2\text{Al}_2\text{O}_{10}$	Al_2	Si_4	Little O—OH Hydrogen Strong
		Dickite	$(\text{OH})_2\text{Si}_2\text{Al}_2\text{O}_{10}$	Al_2	Si_4	Little O—OH Hydrogen Strong
		Nacrite	$(\text{OH})_2\text{Si}_2\text{Al}_2\text{O}_{10}$	Al_2	Si_4	Little O—OH Hydrogen Strong
		Halloysite (dehydrated)	$(\text{OH})_2\text{Si}_2\text{Al}_2\text{O}_{10}$	Al_2	Si_4	Little O—OH Hydrogen Strong
		Halloysite (hydrated)	$(\text{OH})_2\text{Si}_2\text{Al}_2\text{O}_{10} \cdot 4\text{H}_2\text{O}$	Al_2	Si_4	Little O—OH Hydrogen Strong
2:1	Montmorillonite	Montmorillonite	$(\text{OH})_2\text{Si}_2(\text{Al}_{1.34}\text{Mg}_{0.66})\text{O}_{20} \cdot n\text{H}_2\text{O}$ \downarrow Na^{+}	$\text{Al}_{1.34}\text{Mg}_{0.66}$	Si_8	Mg for Al, Net charge always = 0.66/unit cell O—O Very weak expanding lattice
		Beidellite	$(\text{OH})_2(\text{Si}_{1.34}\text{Al}_{0.66})(\text{Al}_1)\text{O}_{20} \cdot n\text{H}_2\text{O}$ \downarrow Na^{+}	Al_1	$\text{Si}_{7.34}\text{Al}_{0.66}$	Al for Si, Net charge always = 0.66/unit cell O—O Very weak expanding lattice
		Nontronite	$(\text{OH})_2(\text{Si}_{1.34}\text{Al}_{0.66})\text{Fe}_{0.66}\text{O}_{20} \cdot n\text{H}_2\text{O}$ \downarrow Na^{+}	$\text{Fe}_{0.66}$	$\text{Si}_{7.34}\text{Al}_{0.66}$	Fe for Al, Al for Si, Net charge always = 0.66/unit cell O—O Very weak expanding lattice
	Saponite	Hectorite	$(\text{OH})_2\text{Si}_2(\text{Mg}_{0.34}\text{Li}_{0.66})\text{O}_{20} \cdot n\text{H}_2\text{O}$ \downarrow Na^{+}	$\text{Mg}_{0.34}\text{Li}_{0.66}$	Si_8	Mg, Li for Al, Net charge always = 0.66/unit cell O—O Very weak expanding lattice
		Saponite	$(\text{OH})_2(\text{Si}_{1.34}\text{Al}_{0.66})\text{Mg}_{0.66}\text{O}_{20} \cdot n\text{H}_2\text{O}$ \downarrow Na^{+}	Mg, Fe^{2+}	$\text{Si}_{7.34}\text{Al}_{0.66}$	Mg for Al, Al for Si, Net charge always = 0.66/unit cell O—O Very weak expanding lattice
Hydrous Mica (Illite)		Sauconite	$(\text{Si}_{1.94}\text{Al}_{0.06})\text{Al}_{0.06}\text{Fe}_{0.06}\text{Mg}_{0.34}\text{Zn}_{0.30}\text{O}_{20}(\text{OH})_2 \cdot n\text{H}_2\text{O}$ \downarrow Na^{+}	$\text{Al}_{0.06}\text{Fe}_{0.06}\text{Mg}_{0.34}\text{Zn}_{0.30}$	$\text{Si}_{6.94}\text{Al}_{0.06}$	Zn for Al O—O Very weak expanding lattice
		Illites	$(\text{K}, \text{H}_2\text{O})_2(\text{Si})_3(\text{Al}, \text{Mg}, \text{Fe})_4\text{O}_{20}(\text{OH})_2$	$(\text{Al}, \text{Mg}, \text{Fe})_{1-4}$	$(\text{Al}, \text{Si})_8$	Some Si always replaced by Al. Balanced by K between layers. K ions: strong
	Vermiculite	Vermiculite	$(\text{OH})_2(\text{Mg}, \text{Ca})_2(\text{Si}_{1.5}\text{Al}_{0.5})(\text{Mg}, \text{Fe})_4\text{O}_{20} \cdot y\text{H}_2\text{O}$ $x = 1 \text{ to } 1.4, y = 8$	$(\text{Mg}, \text{Fe})_4$	$(\text{Si}, \text{Al})_8$	Al for Si net charge of 1 to 1.4/unit cell Weak
2:1:1	Chlorite	Chlorite (Several varieties known)	$(\text{OH})_2(\text{SiAl})_2(\text{Mg}, \text{Fe})_4\text{O}_{20}$ (2:1 layer) $(\text{MgAl})_2(\text{OH})_2$ Interlayer	$(\text{Mg}, \text{Fe})_4$ (2:1 layer) $(\text{Mg}, \text{Al})_2$ Interlayer	$(\text{Si}, \text{Al})_8$	Al for Si in 2:1 layer Al for Mg in Interlayer
Chain Structure		Sepiolite	$\text{Si}_4\text{O}_{11}(\text{Mg}, \text{H}_2)_2\text{H}_2\text{O} \cdot 2(\text{H}_2\text{O})$			Fe or Al for Mg
		Attapulgite	$(\text{OH})_2(\text{Al})_2(\text{OH})_2\text{Mg}_2\text{Si}_8\text{O}_{20} \cdot 4\text{H}_2\text{O}$			Some for Al for Si Weak = chains linked by O

Structure—Continued									
Crystal Structure	Basal Spacing	Shape	Size ^b	Cation Exchange Cap. (meq/100 gm)	Specific Gravity	Specific Surface m ² /gm.	Occurrence in Soils of Engineering Interest		
		Irregular, somewhat rounded	.05–1 μ				Common		
Triclinic $a = 5.14, b = 8.93, c = 7.37$ $\alpha = 91.6^\circ, \beta = 104.8^\circ, \gamma = 89.9^\circ$	7.2 Å	6-sided flakes	$0.1\text{--}4 \mu \times \text{single}$ $.05\text{--}2 \mu$ to 3000 × 4000 (stacks)	3–15	2.60–2.68	10–20	Very Common		
Monoclinic $a = 5.15, b = 8.95, c = 14.42$ $\beta = 96^\circ 48'$	14.4 Å	Unit cell contains 2 unit layers 6-sided flakes	$1 \mu \times .025\text{--}.15 \mu$	1–30			Rare		
Almost Orthorhombic $a = 5.15, b = 8.96, c = 43$ $\beta = 90^\circ 20'$	43 Å	Unit cell contains 6 unit layers Rounded flakes	$.07 \mu \text{ O.D.}$ $.04 \mu \text{ I.D.}$ 1 μ long.	5–10	2.55–2.56		Occasional		
$a = 5.14$ in O-Plane $a = 5.05$ in OH-Plane $b = 8.93$ in O-Plane $b = 8.62$ in OH-Plane ∴ layers curve	7.2 Å 10.1 Å	Random stacking of unit cells Water layer between unit cells Tubes		5–40	2.0–2.2	35–70	Occasional		
	9.6 Å—Complete separation	Diocathedral	Flakes (Equidimensional)	>10 Å × up to 10 μ	80–150	2.35–2.7	50–120 Primary 700–840 Secondary	Very Common	
	9.6 Å—Complete separation	Diocathedral						Rare	
	9.6 Å—Complete separation	Diocathedral	Laths	Breadth = 1/5 length to several μ × unit cell	110–150	2.2–2.7		Rare	
	9.6 Å—Complete separation	Triocathedral		To 1 μ × unit cell breadth = 0.02–0.1 μ	17.5			Rare	
		Triocathedral	Similar to Mont.	Similar to Mont.	70–90	2.24–2.30		Rare	
		Triocathedral	Broad Laths	50 Å Thick				Rare	
	10 Å	Both Diocathedral and Triocathedral	Flakes	.003–.1 μ × up to 10 μ	10–40	2.6–3.0	65–100	Very Common	
$a = 5.34, b = 9.20$ $c = 28.91, \beta = 93^\circ 15'$	10.5–14	Alternating Mica and double H ₂ O layers	Similar to Illite		100–150	40–80 Primary 870 Secondary		Fairly Common	
Monoclinic (Mainly) $a = 5.3, b = 9.3$ $c = 28.52, \beta = 97^\circ 8'$	14 Å		Similar to Illite	1 μ	10–40	2.6–2.96		Common	
Monoclinic $a = 2 \times 11.6, b = 2 \times 7.86$ $c = 5.33$ $a_0 \sin \beta = 12.9, b_0 = 18$ $c_0 = 5.2$		Chain	Flakes or Fibers		20–30	2.08		Rare	
		Double Silica Chains	Laths	Max. 4–5 μ × 50–100 Å Width = 2t	20–30			Occasional	

Table 2.1 Summary of Clay Mineral Characteristics
(from Mitchell, 1993, p38,39)

The type of bond each mineral has is shown in Table 2.1.

2.3.3 Soil Structure

The aforementioned clay minerals will group together to make *clay platelets*, *clay crystals*, *clay aggregates* or *clay conglomerates*, depending on the individual clay mineral properties (Table 2.1). The arrangement of the clay structures will result in the final size, shape and expansive properties of the soil in question. The formation of the various structures will also depend on the environmental history and geology of the deposits, though this will not be discussed here.

Clay platelets are the most basic shape, having variable length and width but constant thickness. They have a sheet-like structure with a large surface area. The sheets have planar surfaces, and are surrounded by cations in order to balance the negative charge created by the individual particles.

Clay crystals consist of parallel clay platelets in a stacked unit that cannot be separated even during very drastic changes in environmental conditions. Swelling takes place between clay crystals rather than within the lattice structure.

Clay aggregates are formed when groupings of impure clay crystals are subject to high pressures (not necessarily due to geological processes) (Sankarau, et al, 1973). The crystals can occur in either parallel or random orientation. They have strong intermolecular bonds (simple bonding of cation, polar molecules, hydrogen bonding) regardless of their orientation. Expansion of clay aggregates is limited by this strong inter- and intra-molecular bonding, as the bonds will not break.

Clay conglomerates are made up of platelets, crystals and aggregates or a combination of the above. The weak intermolecular forces holding the platelets, crystals or aggregates together allow water to easily enter the structure. Stress can cause these units to break down into smaller units. Sodium montmorillonite, for example, may have five to twenty clay platelets joined in a dry clay conglomerate. Upon wetting, however, the number of platelets joined together may reduce to between three and seven (Sankarau, et al 1973).

The various clay minerals will have a variety of combinations of the above structures. The specific combination will result in a particular clay mineral having a

specific surface area. This area will closely relate to the swell potential of the clay. Some ranges for this value are given in Table 2.1.

2.4 Geotechnical Factors

These are the factors that will cause a soil to swell irrespective of the clay mineralogy. The level of swell will be controlled by the strength of the fabric and the level of interaction it has with water. It will also be strongly dependent on the environmental conditions, which will be discussed in Section 2.4.4.

2.4.1 Particle size

Clays can be defined by not only their mineralogy, but also by the size of the particle. Clay-sized particles are here defined as having a diameter of less than two microns (0.002mm). These are known as colloidal-sized particles, and have a large overall surface area, due to their small size. Having clay-sized particles present does not mean clay behaviour will occur, yet soils with some clay-sized particles and only small amounts of clay (<10%) can display clay behaviour, i.e. plasticity.

It is the small size of the particles and their relatively large surface area that allows them to attract water particles. These small clay-sized particles have a tendency to behave in an atom-like manner, as the positive charges tend towards the middle while the negative charges tend towards the edge. This encourages absorption of cations (commonly water) to balance the excess negative surface charge. This behaviour does not only apply to clays, but can also occur in silts and larger grains under the right conditions.

2.4.2 Suction

Suction is a result of negative pore pressure. This occurs when the free energy of the water in soil is less than the free energy of water under ambient air pressure. Suction plays a part in the swell behaviour of the loess soils on the Port Hills. When precipitation occurs on to a moisture deficient loess the water is quickly absorbed. The air in the spaces is then trapped, and compressed. This creates positive air pressure, resulting in

soil swelling (slaking) (Yetton, 1986). A more in depth discussion on suction and water pressure can be found in Mitchell (1993).

2.4.3 Environmental conditions

The amount of volume increase a soil will exhibit will depend on the environmental conditions or placement conditions present. There are five main environmental or placement conditions that control the swell (adapted from Chen, 1973):

1. Surcharge pressure
2. Duration of saturation or degree of saturation
3. Initial moisture content
4. Thickness of soil strata
5. Dry density
6. Vegetation

These environmental factors and their effects are summarised in Table 2.2.

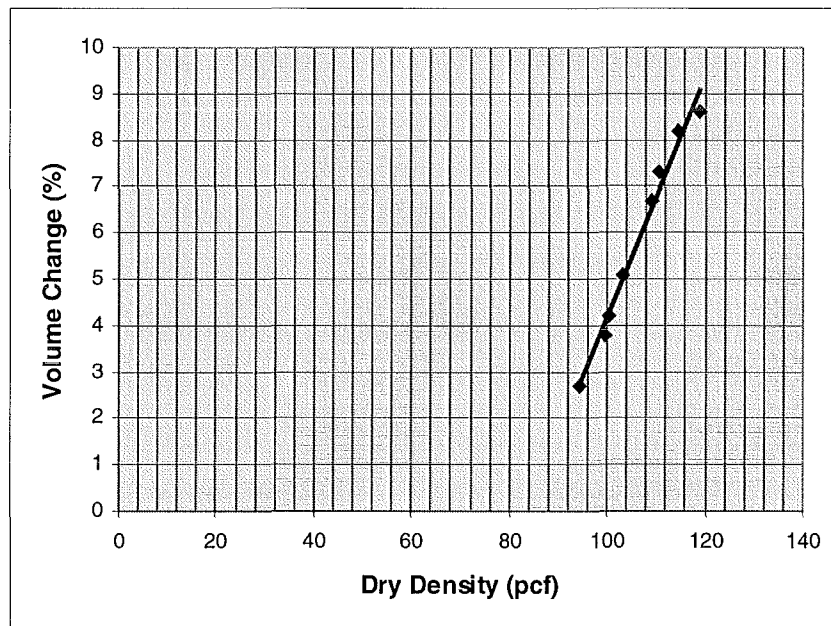


Figure 2.2, Affects of Varying Density on Volume Change for Constant Moisture Content Samples
(from Chen, 1973, p23)

Environmental Condition	Effects	Example
Surcharge Pressure	<p>Surcharge pressure, or overburden pressure, is the weight per unit area that is applied to a given surface. Swelling soils and expansive soils both exert a given amount of pressure during the absorption of water. The level of pressure exerted by the soil is related to the mineralogical or geotechnical properties of the soil, and can vary from 0kg/m^2 to 1000kg/m^2 or higher.</p> <p>When an object is placed on a swelling clay it can overcome some or all of the swell pressure. The surcharge pressure of a structure will reduce the level of swell in a soil. This allows design tolerance levels for differential movement to be reduced, which in turn reduces costs.</p>	Chen (1973) put the same soil under two different loads and measured the vertical swell. The sample under 211kg/m^2 of pressure swelled 1.6% while the sample under 42kg/m^2 swelled 5.9%.
Duration/Degree of Saturation	The same soil will swell varying amounts depending on the duration of saturation and the degree of saturation. The longer a sample has access to excess water the more likely it is to reach an equilibrium with the surrounding conditions. Some soils will have a critical value up to which swelling will occur.	Irrigation can have a large effect on the degree and duration of saturation, for example in Israel near Afula the affect of irrigation during winter resulted in moisture variation levels as high as 8-10% at a depth of two meters.
Initial Moisture Content	The lower the initial moisture content the greater the potential for swell. A common practice to control expansive soils once identified is to wet the ground before building. This allows for swelling to occur before building, and reduces the likelihood of further volume changes.	Chen (1973) compared swell to initial moisture content. The results are shown in Table 2.2. In general, it shows a reduction in swell as a percentage with increasing initial moisture content. Swell pressure is not affected.
Thickness of Soil Strata	This is a very important measurement to be aware of when designing the foundations of any civil structure. Thin ($<0.5\text{m}$) layers of swelling soil may be possible to remove. Thicker deposits ($>0.5\text{m}$), unless it is a very large structure, will require investigation and mitigation in order to avoid structural damage. In very thick layers ($>2\text{m}$) seasonal moisture changes are unlikely to affect the whole unit, though this will depend on the climate of the region. The depth of swelling activity will also be affected by tree roots.	A swell of 50% in a 10cm thick deposits will result in 5cm of uplift. 5% swell in 2 metre thick deposit will result in 10cm of uplift.
Dry Density	Dry density and swell pressure are closely related, with an increase in density resulting in an increase in swell pressure. As the density increases the void space is reduced, in turn this reducing the void space able to absorb water without increasing the soil volume. This is shown graphically in Figure 2.2	
Trees Roots	Although not an expansive or swelling soil problem this is a common cause of swelling. Tree roots can cause swelling either during dry spells when the roots extend in the search for water, or when trees are cut down, as there is a loss of the suction from the roots, so the ground expands.	Trees roots are extremely efficient at extracting moisture, and can vertically extend the active zone of swelling soils to a depth of 7 metres or more.

Table 2.2 Summary of Environmental Conditions and Affects

Initial Density (pcf)	Moisture Content		Volume Increase (%)	Swelling Pressure (psf)
	Initial	Final		
106.97	5.84	20.34	7.71	9,500
105.93	9.95	20.77	5.55	9,500
106.27	10.77	18.75	5.03	12,500
105.6	12.48	22.09	4.3	9,500
106.47	12.92	20.54	3.48	9,000
106.37	14.84	19.59	3.3	10,500
105.46	17.97	18.5	2.15	7,000
105.73	18.59	19.41	1.38	7,500
106.35	19.37	20.18	0.75	9,000
106.13		20.02		9,333

Table 2.3 Effect of Varying Moisture Content on Volume Change and Swelling Pressure for Constant Density Samples (from Chen, 1973, p21).

2.4.4 Shrinkage

Shrinkage is a result of loss of moisture from the soil due to evapotranspiration or downward percolation. Water can be broken up into four categories:

1. Chemical water - within the crystal structure
2. Absorbed water - held on the surfaces of the soil particles
3. Water held by surface tension at points of contact of the soil particles
4. Capillary water in the pores between the soil particles

(CN Non-Food Import-Export Corp, 5/23/2001)

The water of most interest is the absorbed water. It controls both the swelling and shrinking of the soil. The absorbed water forms a film surrounding the soil grains called a meniscus. If more soil moisture is removed than is stored in the pore spaces water will be drawn from the meniscus layer. When this occurs the menisci are reduced, and the grains become more negatively charged (as there are less cations with which to balance the negative charge of the colloidal sized particles). This increases the attraction that one grain has to the meniscus layer of another grain, which increases capillary stress (Figure 2.3). The result is a higher level of compaction, which reduces the volume of the soil. This leads to cracks opening up in the ground. The reversal of this process is called swelling. Shrinkage of clay soils can result in a desiccated layer at ground surface that is

over-consolidated because of the suction effect the increased attraction has caused. This is called densification.

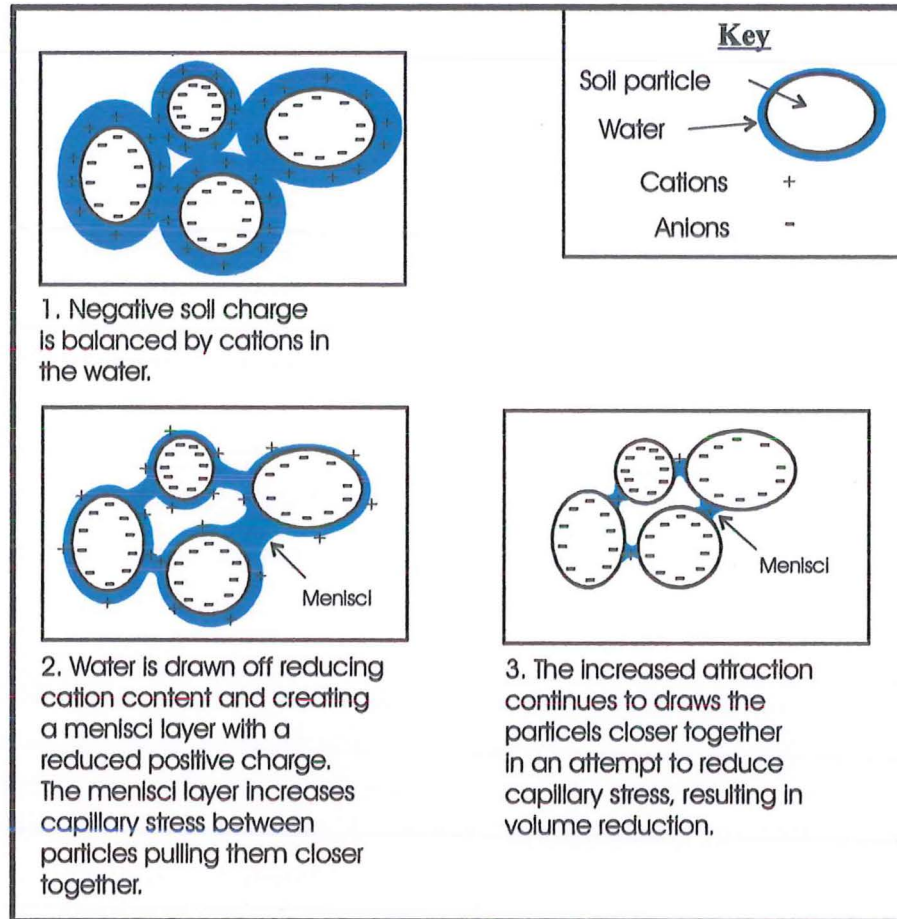


Figure 2.3 Shrinkage due to Capillary Stress

2.5 Evaluation of Shrink/Swell Behaviour

The evaluation of shrink/swell soil behaviour can be sorted into three main categories:

1. Identification and location of the problem soil, be it an expansive soil or a swelling soil
2. Evaluation of the soil
3. Evaluation of the extent of influence of environmental conditions

2.5.1 Identification and Location

Identification and location will often start with the recognition of damage caused by swelling soils (section 2.2). After initial investigation of the damaged property, a desk study may reveal much needed information about the processes at work. This will also help in developing a fieldwork program. The current practice for fieldwork is to excavate trenches, log the units present, then collect a range of samples to be used in standard engineering and mineralogical tests. These tests would identify the potentially swelling layers and provide an indication of the level of swell that could be expected. Recently, many new laboratory and field methods for the identification of expansive soils have been developed, such as the use of a field spectrometry to enable rapid identification of any swelling clay minerals (Chabrilat, 2001). Due to time and cost constraints, more traditional methods will be used for the evaluation of the soil in ‘The Birches’ subdivision.

2.5.2 Evaluation of the Soil

Once a problem has been identified and samples are collected, laboratory testing can take place. Laboratory investigations are designed to identify the cause of, and the potential for, volume expansion of the soil in the area. The following laboratory methods were used for the investigation of the soil in ‘The Birches’:

- Scanning Electron Microscope study
- Grading curves
- Atterberg limits
- Confined vertical swell tests (zero load)
- X-ray diffraction analysis
- Dry density testing

A review of each of the above methods and their ability to evaluate volume expansion in soil is included in Appendix C. Testing procedures are outlined in Chapter Four.

2.5.3 Evaluation of the Extent of Influence of Environmental Conditions

Environmental conditions will limit the amount of swell that can occur to a given soil. The most important environmental factor is rainfall, as it will result in a direct increase in the soil moisture through infiltration. The level of influence a given amount of rainfall will have can be indirectly monitored using techniques such as crack monitoring and the measuring of moisture gradients in the topsoil (both discussed in Sections 3.4.2 and 3.4.3). Rainfall levels are obtained using rainfall gauges. Using this information, a relationship between rainfall, soil moisture content and soil volume change can be calculated.

Vegetation is also a crucial environmental factor, as the roots of plants can affect the depth of active soil. The type of vegetation present will give a good indication of the depth of root penetration. An understanding of the above conditions and the role they play in volume expansion will aid in the adequate design of preventative measures. For example, if the zone of active moisture content change is known, moisture curtains (geotextiles) can be used to prevent lateral water movement, which is often the cause of cracking beneath paving.

2.6 Deflection

Lowes Place is one of two roads that access 'The Birches' subdivision (Figure 1.3). Before roads are to be sealed, they require testing to see if they have meet design standards. In the case of Lowes Place, a Benkelman Beam test was performed. Upon testing the road displayed extremely high deflection values (up to 12.76mm), suggesting either poor subgrade or poor compaction of granular fill. The soil was re-compacted and once again tested, but still showed extremely high deflection values. As these high levels of deflection did not appear to be remediable, the Rangiora District Council allowed the road to be sealed as it was. No cracking or other signs of excessive wear have as yet occurred to the road surface, or to any of the storm water culverts (usually highly susceptible to damage when movement occurs). This leaves two main questions: firstly, why such large levels of deflection are taking place, and secondly, why there is no cracking or damage of the asphalt, despite this high deflection.

The deflection that is occurring is some form of elastic behaviour, where the soil transmits the forces applied to it. Any soil, when loaded or stressed, will deform or strain (Holtz, et al, 1981, p283), but this occurs more readily in cohesive soils. Normally soils only have a small amount of elastic behaviour before permanent deformation takes place - they settle or distort (almost) immediately. In the case of 'The Birches' subdivision this instantaneous distortion is largely elastic. It is this elastic behaviour that is both the reason for the high deflection values, and for the lack of pavement damage. More detailed information on settlement and contact pressures can be found in Terzaghi, (1996), Holtz (1981) or Selvadurai (1979).

Within a soil there are two substances which can be compressed, soil and air (water is incompressible). When loading occurs there are three processes that can happen (Holtz, et al, 1981, p286):

1. Deformation of soil grains
2. Compression of air in the voids
3. Squeezing out of water and air from the voids

Although the first possibility results only in a very small change, and is usually ignored, it is impossible to differentiate between the three processes. They will therefore be treated as one.

There are many ways to mathematically analyse soil in order to ascertain its properties for evaluation, and there are many published works on the elastic properties of soil. Further reading on the subject can be found in, Holtz (1981) or Selvadurai (1979).

To evaluate the elastic behaviour of the soil, either in laboratory testing or *in situ*, deterministic methods can be used. The method mentioned below requires samples to be recovered for tri-axial testing so key soil properties such as Young's Modulus and Poisson's Ratio can be calculated.

$$\text{Young's Modulus (E)} = \frac{\sigma \frac{1}{3}}{\varepsilon_1}$$

Equation 2.2

$$\text{Poisson's Ratio (}\nu\text{)} = \frac{1}{2} \left(1 - \frac{\varepsilon_v}{\varepsilon_1} \right)$$

Equation 2.3

Where:

 ε_1 = Axial Strain ε_v = Volumetric Strain σ = Deviator Stress

Once the values E and ν have been calculated, all other elastic constants can be calculated, such as G (shear modulus). These values can then be used in halfspace surface equations like Boussinesq's Point Load Solution, or a Fourier integral equation. These equations will not be covered here; further details can be found in the aforementioned texts. From the equations mentioned above, values of vertical and horizontal displacement, and the area of effect of an applied load (the bowl shape) can be calculated. Although this does not provide the reason for the elastic behaviour of the soil, it will give parameters for future road design work and allow required depth of fill and type of pavement surface to be more adequately designed. For more detailed coverage of pavement design, see Austroads (1992).

2.7 Project Methodology

The following elements will be necessary for a through investigation:

- Desk study
- Monitoring to develop models of current environmental conditions, such as rainfall and soil moisture changes
- Trenching for the investigation of subsurface strata, as well as for sampling purposes
- Laboratory testing to evaluate the volume expansion potential of the soil

A desk study of the local geomorphology and site history (Sections 3.2 and 3.3 respectively) must take place before any physical fieldwork can be undertaken. The desk study will make use of current reports and articles relevant to the area, and include an aerial photo interpretation. The desk study should provide valuable information on the study area, and help to develop an idea of the local depositional setting, both pre- and post-European settlement.

Trenches will be used for the majority of the ground investigation as they are low cost and large samples can be obtained from the trench face. They also allow visual inspection of the subsoil for logging. Another method of investigation that will be used is the regular excavation of shallow pits for the recovery of soil moisture data. This will allow information to be gathered on soil moisture uptake and possible maximum and minimum levels for the degree of saturation. Cracks present in the topsoil will also be monitored, and measured on a regular basis. Changes in crack dimensions will possibly relate to moisture content changes, and may allow for some idea of lateral volume change.

Two types of samples will be recovered for the purposes of laboratory testing: tube samples and bulk samples. Tube samples will include recovery of samples for tri-axial testing in 38mm diameter, long (150-170mm) tubes, and the recovery of additional samples in both short (90mm) and long, 35mm diameter tubes for various other tests, such as vertical swell and soil density. Bulk samples will be used for Atterberg limits, grading curves, x-ray diffraction, and any remoulded testing that is required.

The aim of the testing will be to evaluate the soil in order to achieve the six objectives below:

1. Determine the cause of swelling - mineralogical or structural
2. Develop an understanding of the key properties/characteristics responsible for the expansive volume behaviour, such as those discussed in Section 2.5
3. Measure swell potential
4. Determine the extent and nature of the elastic behaviour of the soil
5. Determine the potential for shrinkage cracking

6. Find any relationships or critical values that will allow development on these soils to occur in a safe and damage free environment (for both remoulded and natural soils)

2.8 Synthesis

- Evidence of damage is the first clue as to the extent and nature of volume-expanding soils.
- The cause of swelling can be due to either mineralogical properties (expansive soils) or structural factors (swelling soils).
- Ion exchange and soil structure are the fundamental components influencing mineralogical swelling.
- Fundamental structural factors potentially influencing swelling are particle size and suction.
- Environmental conditions can affect the extent of volume expansion that will occur, and the zone of active soil.
- Shrinkage is closely related to suction, which is caused by increased competition for cations between soil particles.
- Evaluation of shrink/swell behaviour is a three tier process, comprising identification and location, the evaluation of soils, and the evaluation of environmental conditions.

Chapter 3: Field Investigation

3.1 Introduction

This chapter focuses on obtaining site information in order to develop a better understanding of the environmental conditions present in 'The Birches' subdivision. Site information was obtained using the following methods:

- A review of relevant literature on the field area
- Aerial photo interpretation
- Fieldwork, including long-term crack monitoring and the excavation and study of shallow moisture pits and three trenches. Rainfall data has also been acquired for comparison with the results from crack monitoring and moisture pits.

The methods for field investigation outlined in Section 2.7 have been used. A literature review and aerial photo interpretation are included in Section 3.3, and the field data gathered is presented in Section 3.4. This is followed by an interpretation of the findings in Section 3.5.

3.2 Ashley-Rangiora Fan Geomorphology

The Ashley Floodplain is divided into two major fans, the Rangiora Fan and the Ashley Fan. These are both part of the Springston Formation (Table 1.1), and they developed after the end of the last glaciation (ie, approximately within the last 14,000 years). It is difficult to differentiate between the two fan surfaces, as there are no successive down-valley outwash surfaces present (Canterbury Regional Council Report 95(6), 1995).

The Rangiora Fan deposit (Figure 3.1) is the older fan deposit, extending from east of the Ashley Gorge to just east of Rangiora. Here the fan becomes buried beneath the younger Ashley Fan deposits, but continues to extend into the sea (Figure 3.1). The Okuku Surface and the Mairaki Downs (seen in Figure 3.1) are older fan surfaces, through which modern terraces are now being formed by the Ashley River.

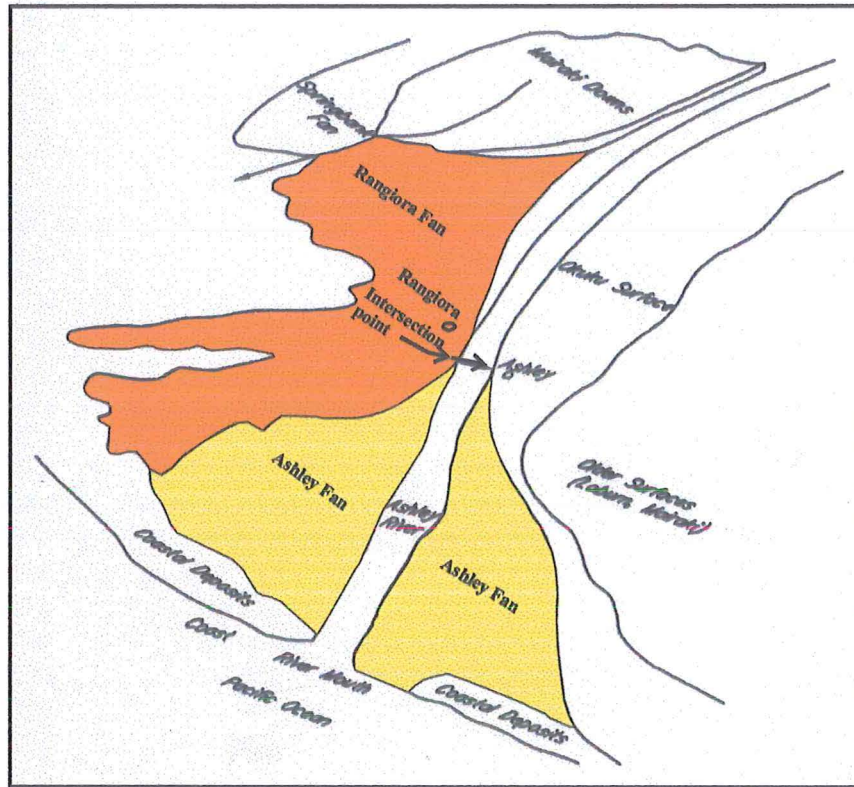
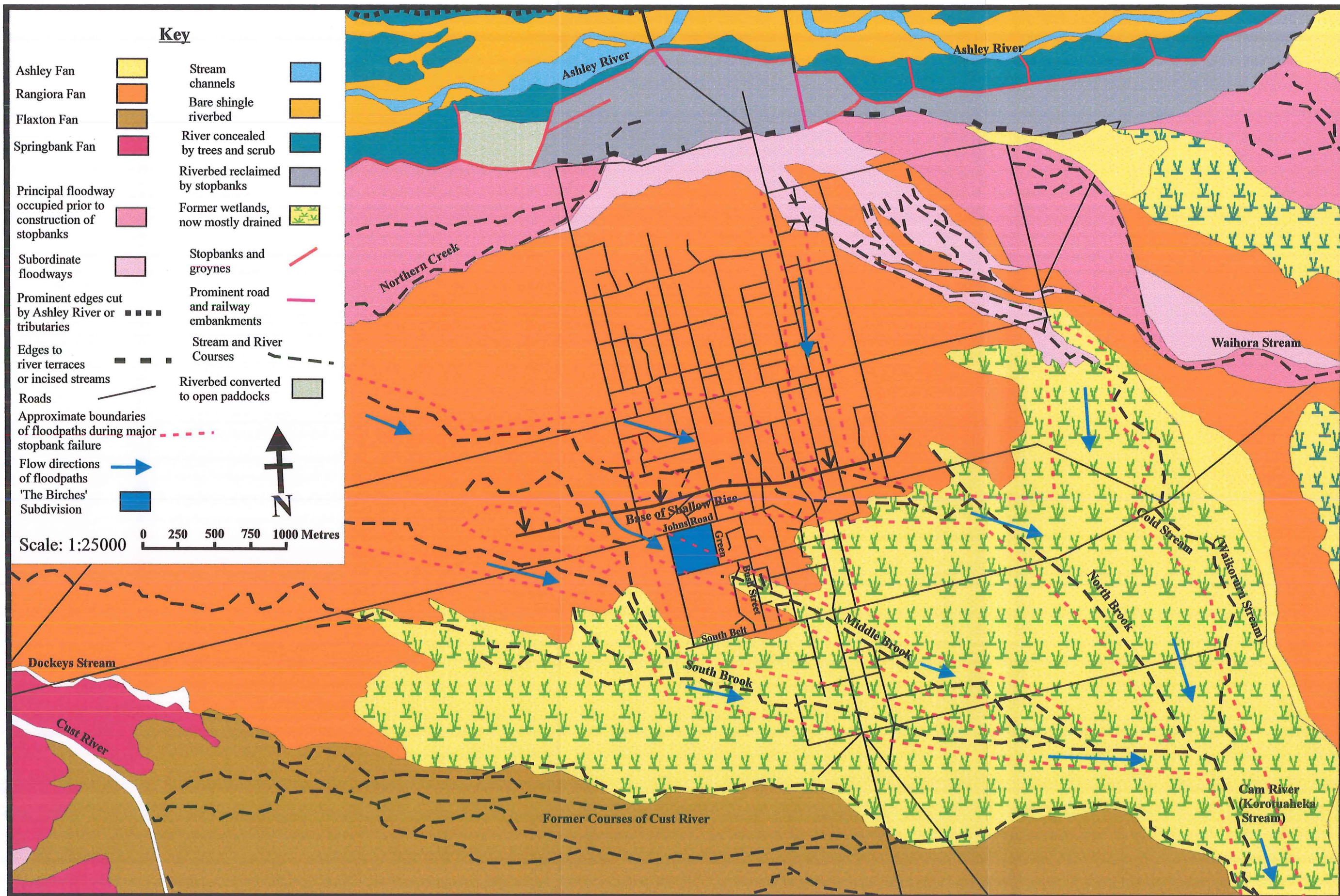


Figure 3.1 Sketch of the Rangiora and Ashley Fans.
(from Canterbury Regional Council Report 95(6), Figure 4.4, p102)

The Rangiora fan "...maintains a relatively uniform gradient of 6.3m/km east as far as Rangiora, then abruptly increases to 8.0m/km for about 2 kilometres across the built-up area of the town" (Canterbury Regional Council Report 95(6), 1995, p105). The slope decreases to 2-2.5m/km after the Rangiora township. This change in gradient is possibly a result of the Northwest Folding Belt (PPAFZ Sub-Domain 3) (see Appendix A). For the most part, on the north side of the Ashley River, the Rangiora Fan is separated from the river by an eastward-draining floodway consisting of numerous small shallow channels. To the south of the river, this fan is made up of small channels and the remnants of braiding (Canterbury Regional Council Report 95(6), 1995).

The Ashley Fan, which starts just east and south of 'The Birches' subdivision, is the youngest unit and conformably overlies the Rangiora Fan (Figure 3.2). On the south side of the Ashley River, the floodplain spreads out after the township of Ashley (Figure 3.1), and is made up of sinuous floodway channels, river loops and point-bar deposits. To the north, the Ashley Floodplain begins spreading just above the junction of the Okuku and Ashley Rivers. The floodplain area has been regularly inundated, and during the early days of European settlement was largely swampland (Canterbury Regional Council Report 95(6), 1995). Two depressions have formed on the south side of the river due to "...radial dissection, erosion



Adapted from Canterbury Regional Council Report 95(6), Map 4.27 and Map 4.3 Flood Plain Geomorphology

Figure 3.2 Geomorphic Map of the Rangiora Township and Surrounding Area

and reworking of the older fan upstream...” (Canterbury Regional Council Report 95(6), 1995: p107). The smaller depression is located to the southeast and extends down to Tuahiwi on the west, and Woodend on the east (Figure 1.1). This depression drains the lower part of the Cam River (Figure 3.2). The larger depression forms a sub-catchment to the south, and is occupied by the Cam, Waikoruru, North Brook and South Brook Rivers (Canterbury Regional Council Report 95(6), 1995). The southern half of Rangiora, which includes ‘The Birches’ subdivision, lies within this depression, and historically would have been a swampy area.

The deposits of the Ashley Fan can be further broken down into three depositional units (from Brown, 1973, in Canterbury Regional Council Report 95(6), 1995, p107). These are:

1. Relatively stone-free alluvial silt. This makes up the majority of the fan surface, and is (physically) lower than the stony silts on the Rangiora Fan “...perhaps as a result of differential compaction...” following post-European settlement draining of the land.
2. Shallow peat deposits
3. Flood sediment deposits (gravel, sand or silt) in the floodways and adjacent areas that were episodically flooded prior to construction of stopbanks

The southern border of the Ashley Fan is marked by a change in flow direction, and the area south of this is known as the Flaxton Fan (Figure 3.2)

Running through the township of Rangiora are existing flood paths. These were located in the Canterbury Regional Council Report 95(6), and are shown on Figure 3.2. These flood paths were possibly subject to regular flooding before stopbank development, and may be responsible for the deposition of much of the fine-grained material located beneath ‘The Birches’ subdivision. Floodwaters tend to carry a lot of fine-grained material in suspension, and it is likely that upon entering the depression that encompasses the southern half of Rangiora, a loss of velocity resulted in the deposition of material.

3.3 Site History

The area that the Rangiora Township now occupies has undergone some major environmental changes since Europeans first started to settle the area in 1851. Present-day Rangiora gives no indication of the sort of environmental conditions that were commonly present during the time of deposition for the Rangiora and Ashley Fan surfaces. It is for this reason that a brief site history for the Rangiora Township has been developed, using both historical documents and aerial photographs.

The first settler of the area was C.M. Torlesse, who owned what became known as Section 81. Section 81 had boundaries that coincided with John Street to the north, the South Belt to the south, Bush Street to the west, and had Green Street running through the middle of it (Hawkins, 1949). ‘The Birches’ subdivision lies on the northwest corner of this section (Figure 3.2). This section comprised mainly grassland, but also included much of the white pine and totara forest that made up Rangiora Bush. The original Rangiora homestead, located on Section 81, was built opposite the last remaining kowai stumps in King Street. This suggests that the Rangiora Township was heavily vegetated during the formation of the Rangiora and Ashley Fans.

Aerial photo interpretation was carried out on photos from 1942 (line 119/41-44). Investigation of these photos revealed the following:

- No outstanding geomorphic features could be identified in or around ‘The Birches’ subdivision.
- No vegetation other than grass can be seen, with the exception of a couple of trees located on the northwest corner (as yet undeveloped area).
- One dwelling also located in the northwest corner can be seen. This dwelling no longer exists.
- What appear to be old river channels propagate outwards from the Ashley River, but are indistinguishable by the time they reach ‘The Birches’ subdivision.

3.4 Fieldwork

3.4.1 Field Program

The field program consisted of long-term monitoring of soil conditions and trenches for stratigraphy logging and sample recovery. The location of all of the fieldwork is shown in Figure 3.3.

Long-term monitoring included crack monitoring and the regular excavation of shallow moisture pits. Crack monitoring is the regular measurement of the change in crack width to see if any seasonal trends are present. This is discussed in detail in Section 3.4.2. Shallow moisture pits (Figure 3.4) are holes dug with a spade to allow samples to be taken at close intervals at a shallow soil depth. This is the zone most affected by rainfall, and should show the most variance in moisture content levels (Section 3.4.3). The maximum depth that shows marked variance in these levels should indicate the vertical extent of the soil most susceptible to volume expansion.

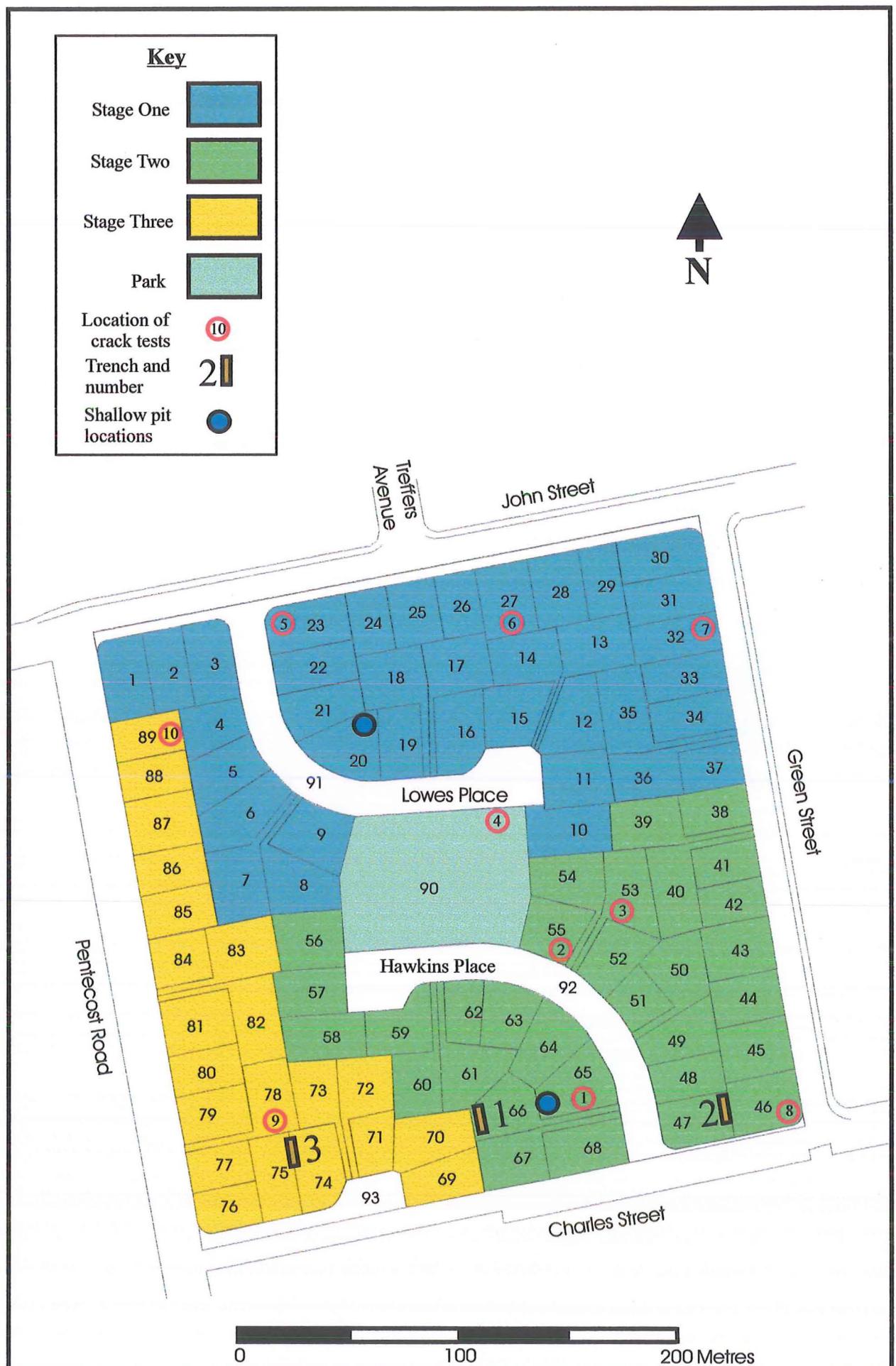


Figure 3.3 'The Birches' Subdivision Field Work Map



Figure 3.4 Shallow Moisture Pit

Three trenches (ranging from 1.95m to 2.5m deep) were excavated in order to investigate the subgrade, and to recover samples for testing (as mentioned earlier). The results from the trenches are shown in Section 3.4.4.

3.4.2 Crack Monitoring

Crack tests were set up with one nail embedded either side of a shrinkage opening in the ground (Figure 3.5). The distance to the outside of the nail heads was measured as shown in the diagram below (distance X, Figure 3.5).

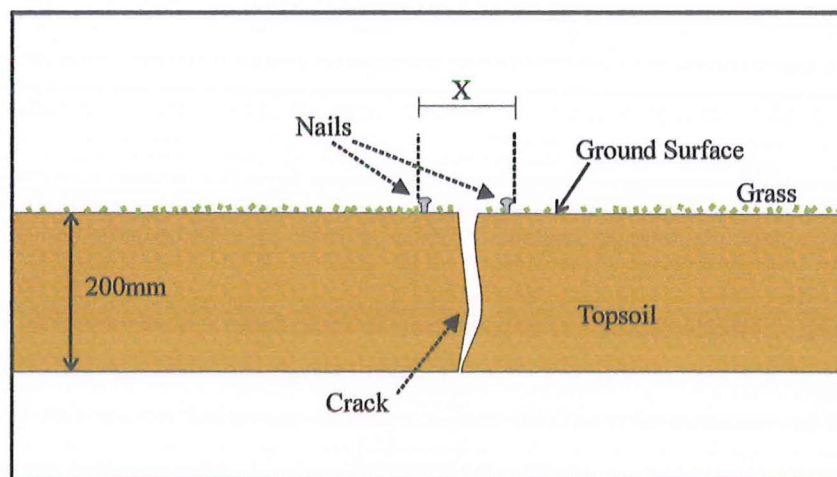


Figure 3.5 Crack Diagram

Each crack test area was then marked with green spray paint to make subsequent location easier, and measurements were collected on a fortnightly basis (with a few exceptions). Starting from the original measurement for each crack, the change in distance X (as a percentage – see Equation 3.1) is shown on the graph in Figure 3.6.

$\text{Percentage change} = \frac{X - X_o}{X_o} \times 100$ <p>Where:</p> <p>X = measured distance</p> <p>X_o = original distance</p>

Equation 3.1

The data shown on the graph only comes from Sites 4,5,7,8, and10, as they were the only sites that were not lost or destroyed during the monitoring period. Rainfall data for the same period has also been included for comparison and to help develop a rainfall/crack spacing relationship (if possible). The rainfall data was gathered by the Geography Department of the University of Canterbury, from a gauge in Rangiora (Network H32364). Crack depth measurements were also taken from Sites 4 and 8, using a stiff wire. These cracks were selected because of their greater width. Crack depth at Site 4 was $129 \pm 1\text{mm}$, while Site 8 varied from 107-200mm deep (along its 300mm length) on the 20/04/2001, to 63mm on the 8/05/2001, to closure on the 25/05/2001. Apart from Site 4, all the other cracks monitored had disappeared by the 25/5/2001 (for complete results of the crack monitoring see Appendix D). Overall an average decrease of 1.4mm in crack width occurred during the monitoring period, while the total variance was $\pm 1.3\text{mm}$ from the original value of 86.5mm

From the data obtained, several interesting trends and relationships between rainfall and crack measurements can be seen to develop over the monitoring period (12/1/2001 to 25/5/2001). These are as follows:

- After a steady climb, the trend was for gradual reduction in the nail spacing
- There is no apparent relationship between rainfall and changes in nail spacing
- Crack spacing decreases as winter progresses

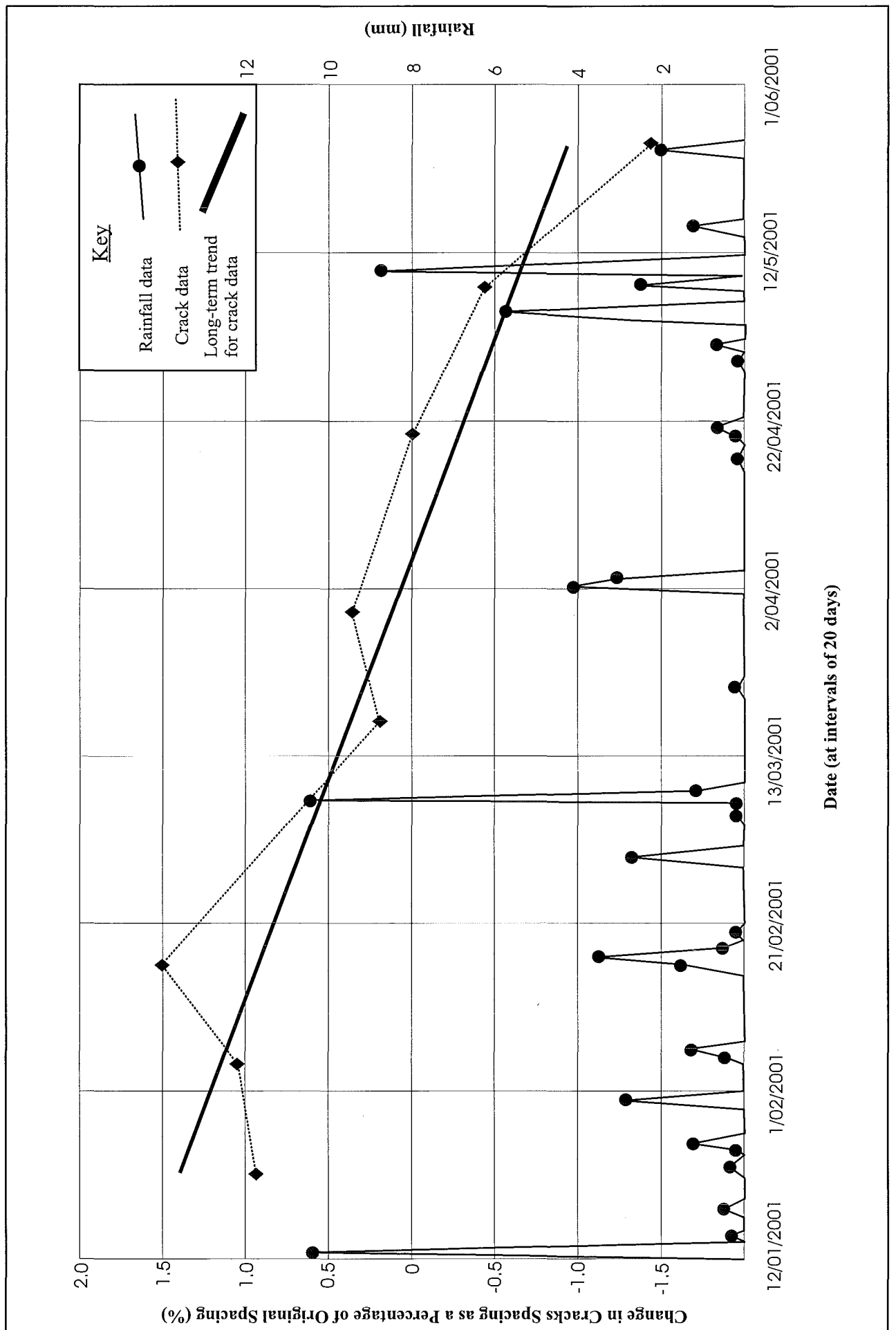


Figure 3.6 Percent Change in Spacing Between Two Nails Spanning a Surface Crack Compared with Rainfall Data

3.4.3 Shallow Pits

Shallow moisture pits (for locations, see Figure 3.3) were dug regularly, and each time soil samples were taken every 40mm, to a depth of 400mm. 400mm was chosen as the maximum moisture pit depth as difficulties were experienced digging the pit and recovering samples below this depth. The samples taken from these shallow pits were tested for moisture content in accordance with Test 2.1 of New Zealand Standards 4420, 1986.

A summary of the data collected from shallow moisture pits A, C, E, G, I, J, K, L and M can be seen in Table 3.1. The maximum and minimum values shown are the highest/lowest values recorded at the given depth at any time. The difference between these two values is the range, while the average is calculated from the sum of the holes above. A complete set of results is in Appendix D.

Depth mm	Moisture Content (%)			
	Maximum value	Minimum value	Range	Average
10	24.8	13.4	11.4	17.1
40	27.1	14.4	12.7	20.1
80	25.6	19.2	6.4	22.0
120	25.0	18.4	6.6	21.9
160	24.9	19.4	5.6	20.8
200	21.7	18.3	3.4	20.3
240	22.4	18.6	3.8	20.5
280	22.0	18.2	3.8	19.9
320	21.2	17.7	3.4	19.7
360	23.0	16.1	6.9	19.7
400	20.3	16.4	3.9	18.5

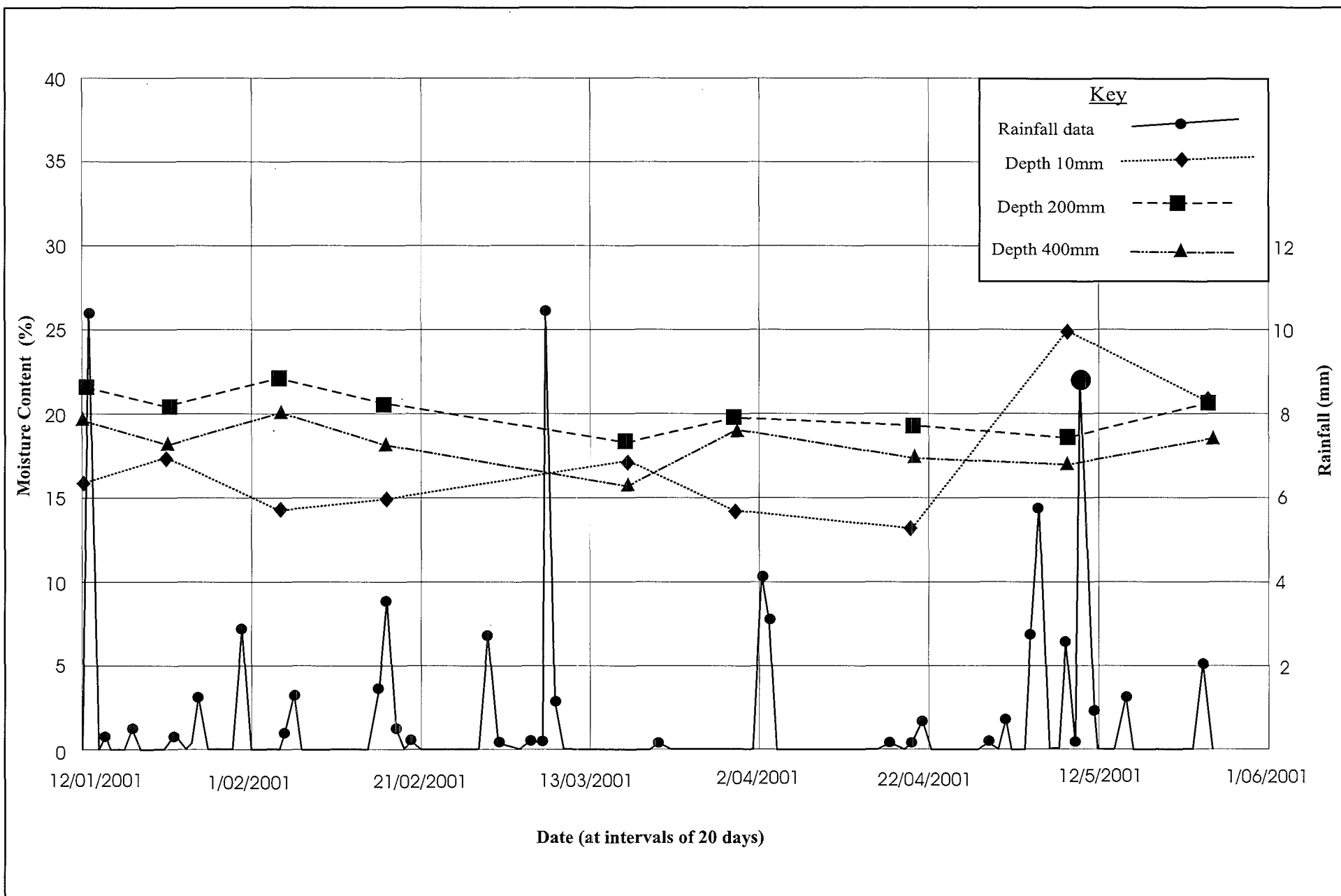
Table 3.1 Summary of Shallow Moisture Pits Data

Several key facts can be established from Table 3.1:

- Below the top 100mm of soil there is a steady decrease in the moisture content.
- With the exception of the depth of 360mm, the range of moisture contents recorded decreases with depth.
- Only the top 40mm of soil is affected by a moisture content change greater than 10%.
- The zone significantly affected by precipitation is less than 200mm thick.

The variance of the moisture content seen in the top 200mm of soil suggests rainfall-induced moisture change. Figure 3.7 plots the average moisture content for samples taken at depths of 10mm, 200mm and 400mm against time, and against the rainfall levels for the same period (Section 3.4.2).

Figure 3.7 Moisture Content versus Time for Samples taken at Varying Depths Compared with Rainfall Data



It can be seen from the graph (Figure 3.7) that very little rain fell (74.2mm) during the period 12/01/2001 to 25/05/2001. This is reflected by the low degree of variation seen at all but the shallowest level (10mm). Other points of interest from the data are:

- Little correlation between rainfall and soil moisture content (possibly due to the small amount of rainfall)
- Lack of seasonal change

3.4.4 Trenches

Three trenches were excavated on two separate occasions to allow the stratigraphy of the area to be studied, and to obtain samples for laboratory work. The first two trenches were dug on 25-1-2001, and the third was dug on 19-4-2001 (Figure 3.3).

Trenches One and Two were excavated with the expectation they would reveal river-type deposits and layered units. The purpose of these trenches was to enable the study of the subsoil to be investigated for expansive soil properties. However, upon excavation only one massive silty clay unit was found (Figure 3.8). Samples were collected at regular intervals down the entire depth of the trench using short (90mm) and long (170-190mm) tubes. Bulk samples were also collected.

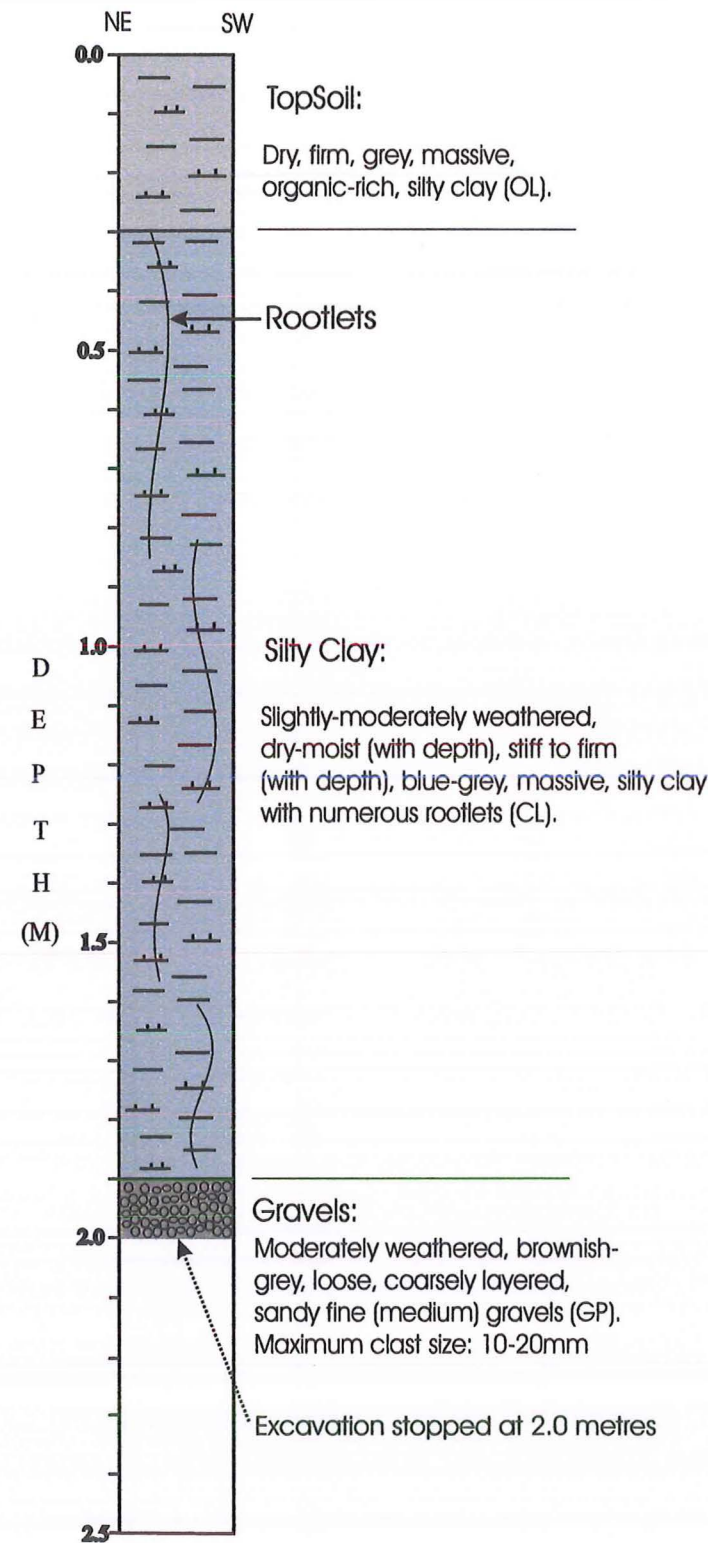
An orientated block sample was also collected from Trench One for a Scanning Electron Microscope (SEM) study, to discern if there was any microscopic layering (Section 4.1). Long tubes of 35mm diameter were used to gather samples for bulk and dry density analysis, tubes of a 38mm diameter were used to obtain samples for tri-axial testing, and short, 35mm diameter tubes were used to gather undisturbed samples for confined vertical swell testing. Bulk samples were recovered at 250mm intervals, and were later tested for moisture content, plastic limit, liquid limit, shrinkage limit, particle size distribution, and to determine the relationship between dry density and water content.

All three trenches were sampled in a similar manner, except for the additional recovery of a log of wood in Trench Two, which was sent for radiocarbon dating (Figure 3.8).

Trench Three (Figure 3.8) was dug with the aim of laterally extending the area of investigation in order to ascertain the consistency of the soil units, and gain samples for further laboratory testing. Trench Three, unlike Trenches One or Two, was excavated through an area of fill approximately 300mm deep. Below the fill was what appeared to be the original topsoil layer followed by a gravely silt clay unit of approximately 600mm. This

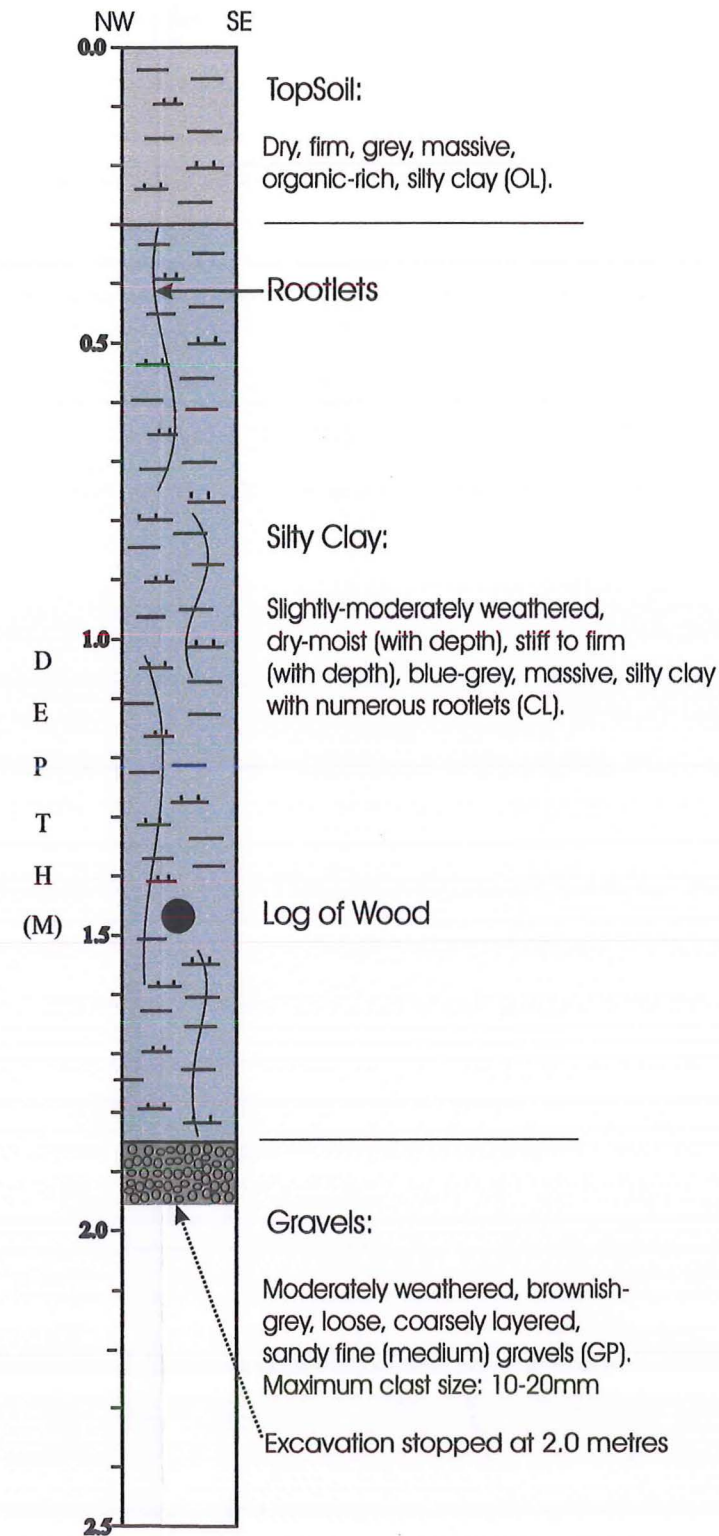
Profile of Trench One (R1)

Location: Rangiora **Date:** 25/1/01
Easting: 2476411 **Bearing:** 022° True North
Northing: 5765795



Profile of Trench Two (R2)

Location: Rangiora **Date:** 25/1/01
Easting: 2476515 **Bearing:** 348° True North
Northing: 5765798



Profile of Trench Three (R3)

Location: Rangiora **Date:** 19/4/01
Easting: 2476310 **Bearing:** 356° True North
Northing: 5765801

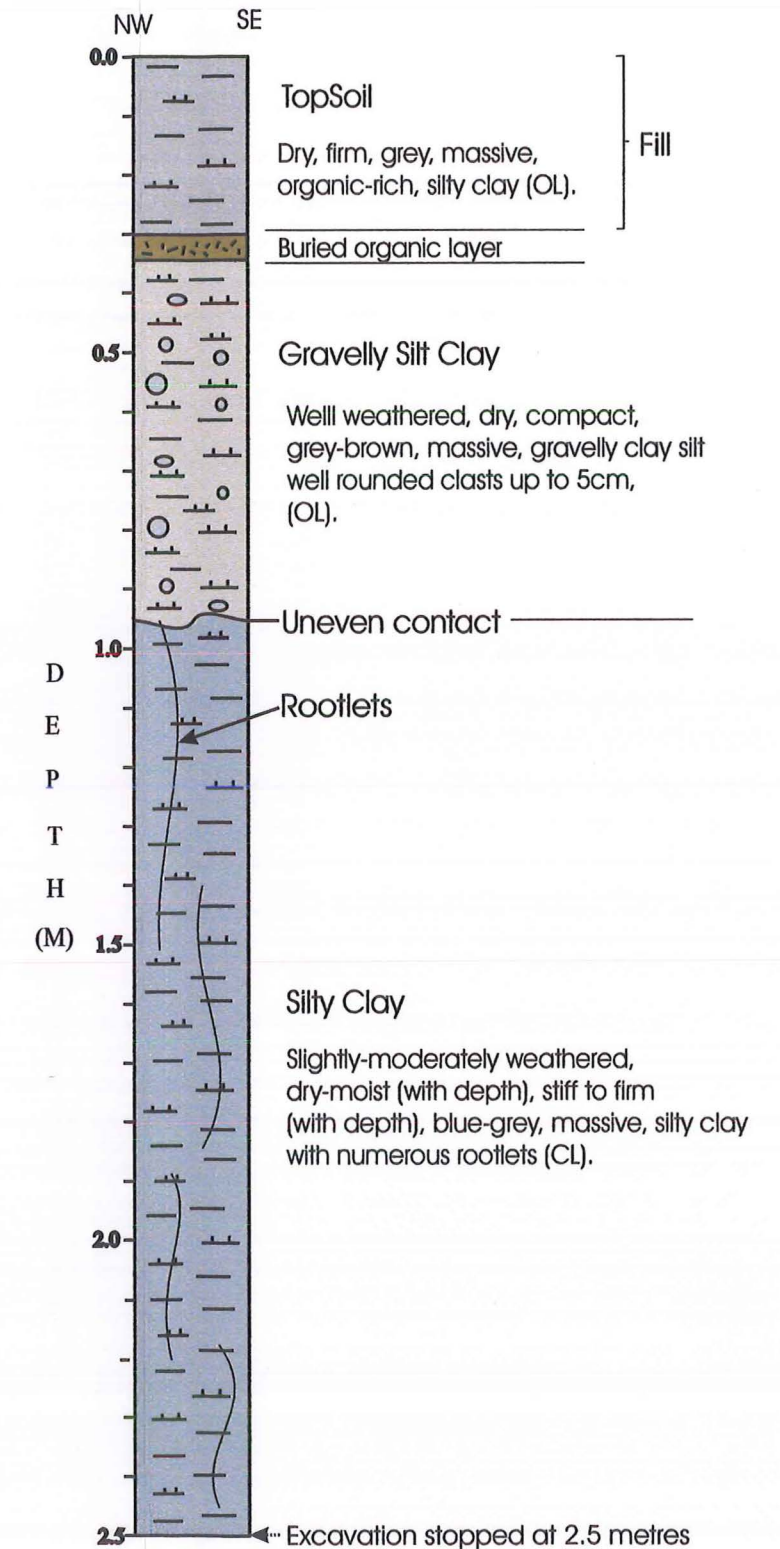


Figure 3.8 Excavation Logs

gravely silt clay layer has an uneven contact with the underlying silty clay layer, which, along with the coarser material present, suggests this is a higher-energy flood path. It is unknown if this relates to a higher-energy flood path that skirted the edge of the silty clay deposits, or if it developed through sudden channel avulsion, and passes through the unit. All three trenches had numerous rootlets present, supporting the view that this was once a well-vegetated area. Roots also cause suction, and can result in an increased level of soil density.

3.5 Data interpretation

The aerial photo interpretation revealed little development of the land since 1942. This allows the following conclusion to be made:

- Volume expansion from root decay is not an issue
- Urban development will most likely result in an increase in the soil moisture due to irrigation.

The crack monitoring, unlike the shallow moisture pits, did show a change over the monitoring period, with an average 1.4mm reduction in spacing between the nails. This was enough to eliminate the cracks at all but one site. Crack spacing did not appear to relate to the rainfall data, this could be due to the small amount of rainfall during the monitoring period. Additionally, the lack of marked rainfall events or seasonal trends makes correlation difficult. The a marked reduction in crack spacing despite there being no increase in rainfall levels, suggests either the temperature or exposure to solar radiation could play a critical role in crack formation. The reduced temperature and solar radiation during the winter months will allow for a greater level of water infiltration to occur than would during summer months. The same amount of precipitation would therefore have a greater effect on soil moisture in winter than in summer.

The shallow moisture pits revealed little in the way of long-term change in the soil moisture conditions. The lack of change in soil moisture content is not surprising, as during the monitoring period the heaviest rainfall in any 24-hour period was little over 10mm. The increased variance seen in the 10mm depth line in the later half of the fieldwork period relates closely to the rainfall graph. This implies a strong relation between soil moisture and rainfall at shallow depths, as a small amount of rainfall (23mm between the period of 22/04/2001 to 12/05/2001) can result in a soil moisture change of over 10% at a depth of 10mm. The lack of rainfall implies that the area usually exists in a desiccated state, with small amounts of water from precipitation being quickly absorbed into the soil. If the soil is

in this desiccated state prior to development, the susceptibility of the soils to volume expansion following construction will be increased.

The trenches revealed one massive silty clay unit with none of the expected bedding present. This suggests a low-energy environment with plenty of reworking of the soil by either root development or leaching. The silty clay material displays low levels of plasticity. The only unusual feature seen was a log of wood at a depth of 1.5m in Trench R2. The presence of this log suggests rare flood events may have been able to shift larger material through this area, and reduces the likelihood of the unit being a loess deposit. The numerous rootlets seen in the trenches confirms the area was previously a well-vegetated environment.

3.6 Synthesis

1. 'The Birches' subdivision is located on the Rangiora Fan, which for much of its history was a well-vegetated swampland, with trees such as the white pine, totara and kowai.
2. 'The Birches' subdivision is located within a depression that is occupied by the North Brook, South Brook and Cam Rivers and the Waikoruru Stream.
3. The land on which 'The Birches' subdivision currently lies was used for livestock grazing since at least 1942.
4. The decrease in nail spacing during monitoring period, with no corresponding increase in rainfall, suggests crack development also dependent on temperature and solar radiation exposure.
5. The natural water content of the soil at shallow depths is closely related to rainfall.
6. Only one massive silty clay unit was found, with a thickness varying between 1.5-2.0 metres
7. There appears to have been high levels of reworking of the soil due to leaching or bioturbation.
8. A small amount of rainfall (23mm) can result in large increase in soil moisture (10%) at a shallow depth

Chapter 4: Laboratory Testing

4.1 Introduction

This chapter examines the properties of the potentially expansive soils at the Rangiora site using the parameters discussed in Section 2.5. The following laboratory program (Table 4.1) outlines the desired goals as discussed in Section 2.7, and the method used to achieve each of them. Each of the test procedures will be explained in more detail in Sections 4.2 to 4.7. Following the explanation of the procedures will be the presentation of results, and a discussion.

Stage	Goal	Test Used	Comment
1	To discern if any depositional features are present, such as, bedding, bioturbation, etc. Section 4.2.	Scanning Electron Microscope	The recognition of bedding will greatly assist in the development of a geological model.
2	To establish Atterberg Limits. Section 4.3	The tests as described in New Zealand Standards 4402, tests 2.3, 2.4, 2.5, and 2.6.	These tests give a good indication of the potential of the soil for volume expansion, and allow plasticity index to be calculated. Any unusual layers should be reflected in the Atterberg Limits. This will help to focus the laboratory work at later stages.
3	To establish grading curves. Section 4.3	Pipette analysis	Grading curves allow for the distribution and content of the various grain sizes to be recognised. This aids development of geological settings and soil behaviour models.
4	To establish the dry density of the soil. Section 4.4	Measurement of large tube samples	Literature review suggests there is a direct relationship between dry density and volume expansion.
5	To discover the soil's vertical swell limits Section 4.4	Confined vertical swell test (Section 4.4)	Vertical swell testing will give a good indication as to the swell potential of the soil.
6	To ascertain the mineralogy of the soil. Section 4.5	X-ray diffraction analysis	The presence of swelling clays in the soil would clarify the source of volume expansion.
7	To discern the extent of the soil's elastic properties. Section 4.6	Triaxial	Calculating the values of Poisson's Ratio and Young's Modulus will enable displacement calculations to be made.
8	To discover the maximum dry density/ water content relationship in the soil. Section 4.7	Test 4.1 New Zealand Standards 4402	Some of 'The Birches' subdivision is built on fill. This test will discern the level of moisture content required for maximum density to be achieved. The vertical swell test (as above) will also be performed on the remoulded samples.

Table 4.1 Laboratory Program

4.2 Scanning Electron Microscope

The two trenches excavated and logged on the 25/01/2001 (R1 and R2) showed a massive unit of silty clay with no visible bedding or layering present (Section 3.4.2). This lack of bedding suggests that the deposit may not be associated with overflow deposits or flood plain deposition from the Ashley River, as originally believed. This presents several new possible depositional scenarios, including that of the soil being a loess deposit on an old fan surface. To confirm this, a Scanning Electron Microscope (SEM) was used to search for any layering on a microscopic scale.

A block of soil 200×200×200mm was cut from the bank of Trench R1 between the depths of 1400-1600mm. The block was then cut into thirds along the horizontal plain to produce three orientated slices of soil. These were placed in an oven at 40 °C, and left to dry. Once dry, the blocks were snapped in half to produce a fresh surface for study. All three samples were stuck to mounts using carbon glue and cleaned with pure nitrogen before a coating of gold-palladium was sprayed on the sample.

R. Neil Andrews prepared the samples and operated the SEM, a **Leica S440** with Oxford instruments, software and detector. The samples were studied for any visible change in texture, grain size or the presence of microscopically-sized bedding. Over three sessions, a range of magnifications from 10x to 2000x was used, and photos were taken at intervals for comparison. The photos shown in Figures 4.1, 4.2, and 4.3 are all of the same scale so a comparison between samples can be made. These photos were all taken near the centre of the photo where disturbance to the soil samples in the preparation procedure (ie, tool marks) was less likely to occur. Sample One is taken from the top slice, Sample Two from the middle, and Sample Three is the bottom slice. As well as visual inspection of the samples, an Energy Disperse Spectrum (EDS) was employed to detect any elemental banding. From the study the follow points were noted:

- No elemental banding was found.
- No layering structure of any kind was found.

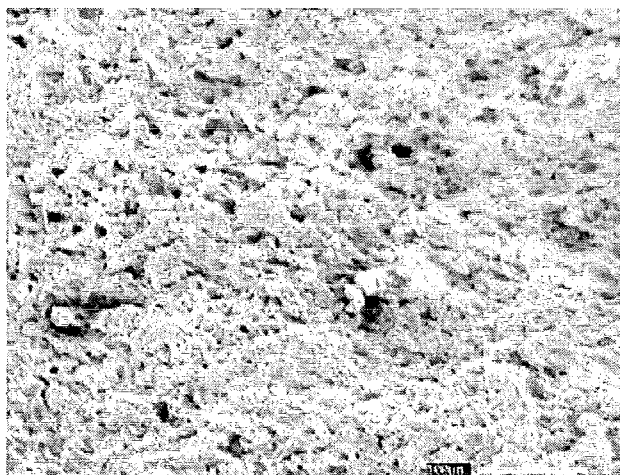


Figure 4.1 Sample 1, 200× magnification.

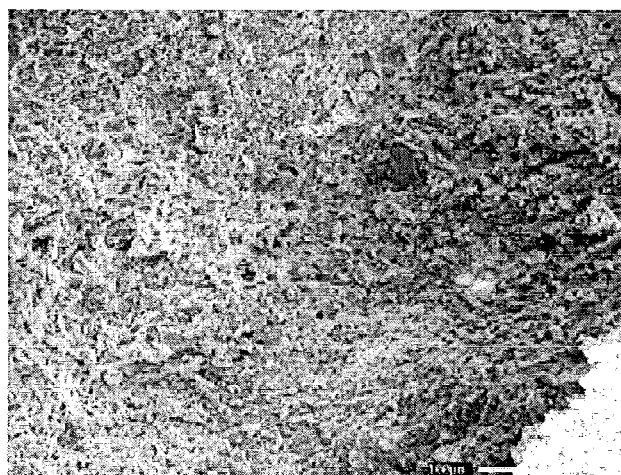


Figure 4.2 Sample 2, 200× magnifications.

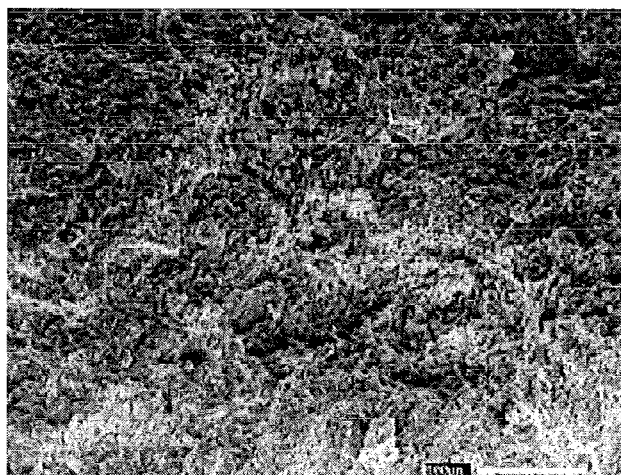


Figure 4.3 Sample 3, 200× magnification.

- There was no visible banding.
- There was no textural bonding.
- All three samples appeared highly homogeneous. This can be seen in the representative pictures from each sample in Figure 4.1, 4.2 and 4.3.
- There appears to be some swirling on the sample in Figure 4.3, which could be bioturbation.

These results indicate the soil could be either a well-reworked sample (due to bioturbation or leaching), or a loess type deposit.

4.3 Atterberg Limits and Grading Curves

4.3.1 Methods

All testing done to determine Atterberg Limits used the methods outlined in New Zealand Standard 4402: 1986. The following tests were performed:

- 1.** Plastic Limit (Test 2.3)
- 2.** Liquid Limit (Test 2.5, Cone Penetration Limit)
- 3.** Linear Shrinkage (Test 2.6)
- 4.** Plasticity Index (Test 2.4)

Grading curves were obtained from pipette analysis of a minus 4 ϕ fraction (<0.0625mm) to gain information on the distribution of the clay- and silt-sized particles. The method used for pipette analysis is described in Lewis (1981, 93-95).

4.3.2 Results and Discussion

Table 4.2 contains the Atterberg Limits and clay-sized fraction data for all three trenches. The table also shows the depth from which each sample was taken. A plot of the liquid limit against plasticity index is shown in Figure 4.4. A selection of grading curve results are shown on Figure 4.5, and a complete set of grading curves is given in Appendix F.

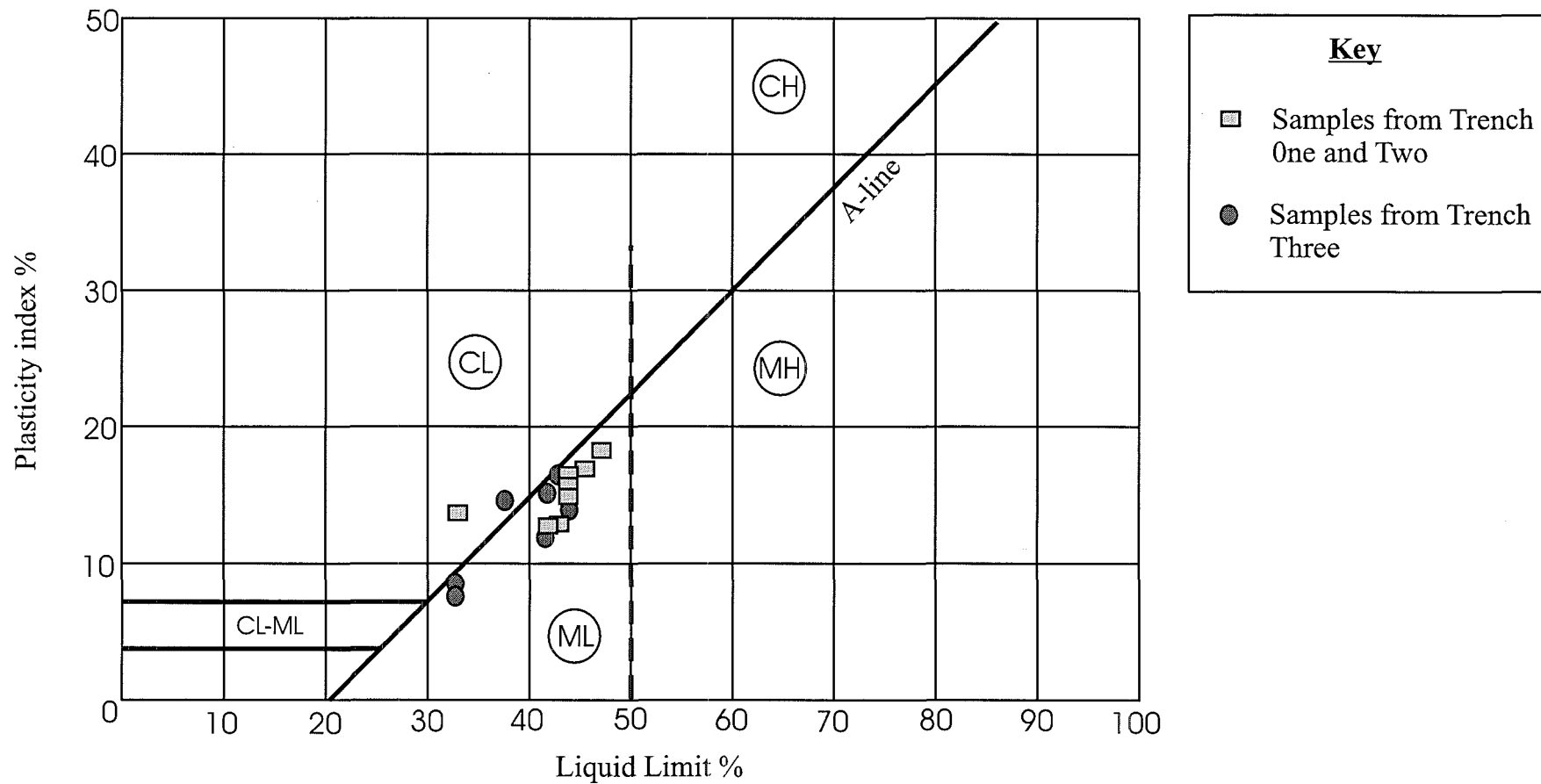


Figure 4.4 Casagrande Plot with Unified Soil Classification System (USCS) Categories for Soil from the 'The Birches' Subdivision. Fine grained soils are distinguished on the basis of being predominantly clays (C) or silts (M). Organic soils usually lie below the A-line and are marked as "O" (not represented here).

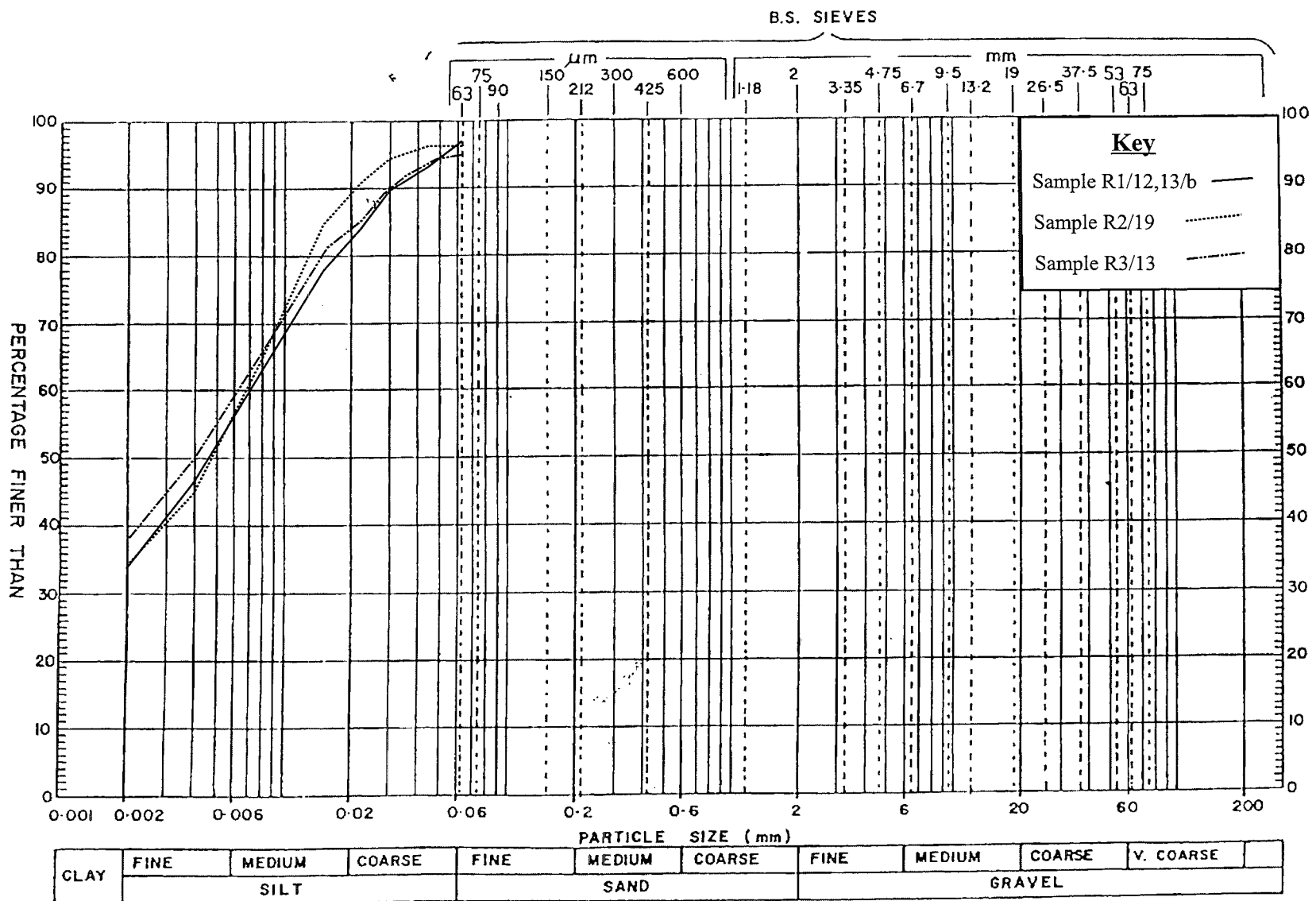


Figure 4.5 Determination of the Particle Size Distribution for the < 0.063mm Material

Sample No.	Depth (mm)	Linear Shrinkage	Plastic Limit ± 2	Liquid Limit ± 2	Plasticity Index	% Clay Fraction	Colloidal Activity
R1/12,13/A	1500	7	28	44	16	34.9	0.4
R1/12,13/B	1500	7	28	44	16	34.2	0.5
R2/3	500	11	29	47	18	31.5	0.6
R2/7	750	10	29	44	15	45.9	0.3
R2/11	1000	11	29	46	17	41.4	0.4
R2/15	1250	10	29	43	13	39.2	0.3
R2/19	1500	11	30	43	13	34.6	0.4
R2/23	1750	9	19	33	14	34.0	0.4
R3/2	500	11	27	44	16	-	-
R3/4	1000	11	29	42	12	43.4	0.3
R3/5	1250	9	27	42	15	-	-
R3/11	1500	10	23	38	15	-	-
R3/13	1750	11	30	44	15	38.6	0.4
R3/16	2000	10	25	33	8	-	-
R3/19	2250	8	24	33	9	-	-

Table 4.2 Atterberg Limits and Clay Size Fractions (R1=Trench One, R2=Trench Two, R3=Trench Three)

From Figure 4.4 it can be seen that the soil generally appears to be a low liquid limit, low plasticity silt or clayey silt (ML). This is in agreement with the grading curves from the pipette analysis, which show a greater than 50% content of silt. This is contrary to the CL classification given during fieldwork (Section 3.4.4), although this classification is understandable due to the clayey appearance of the soil, and the close proximity to the A-line of most of the plotted samples. For the above reasons it is appropriate to classify the soils as a CL-ML. Linear shrinkage ranges from 7-11. Activity ranges from 0.3 to 0.6, which is indicative of stable clay mineralogy, possibly kaolinite (Appendix C-2).

The results from Table 4.2, and Figures 4.4 and 4.5 display very little variance through the depth of the silty clay unit, and are also laterally consistent between Trenches R1, R2 and R3. The exception is the gravelly silt clay unit seen in Trench R3 between the depths of 0.35 – 0.95 metres (Figure 3.8). This largely consistent behaviour supports the field observations that this is a massive deposit resulting from bioturbation or leaching. Because of the soil's high clay content, it is more likely that the massive appearance of the unit is due to one or both of these processes, rather than it being a loess-type deposit. Loess deposits in the Christchurch area tend to have clay contents

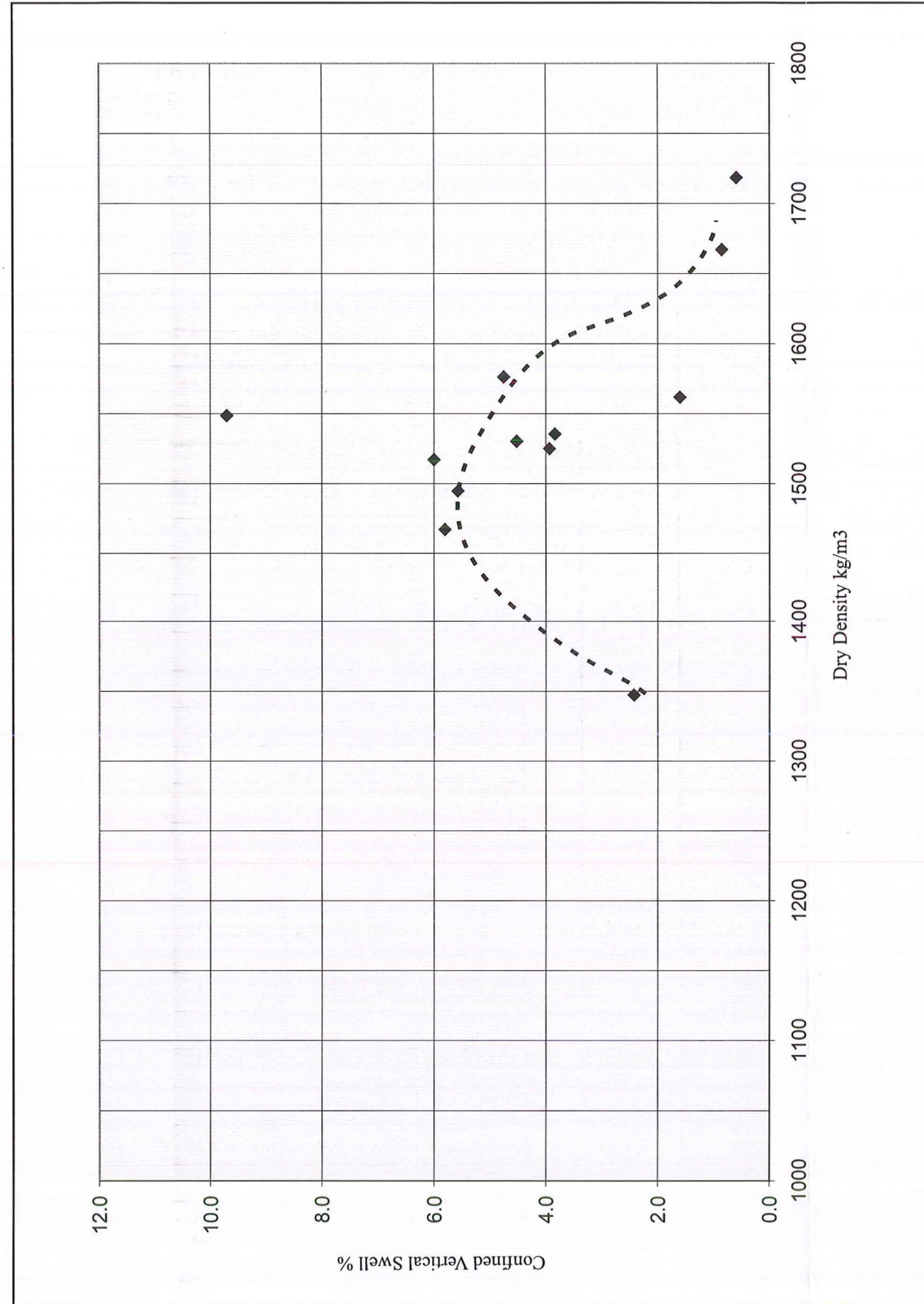


Figure 4.6 Dry Density Versus Confined Vertical Swell for Natural Samples

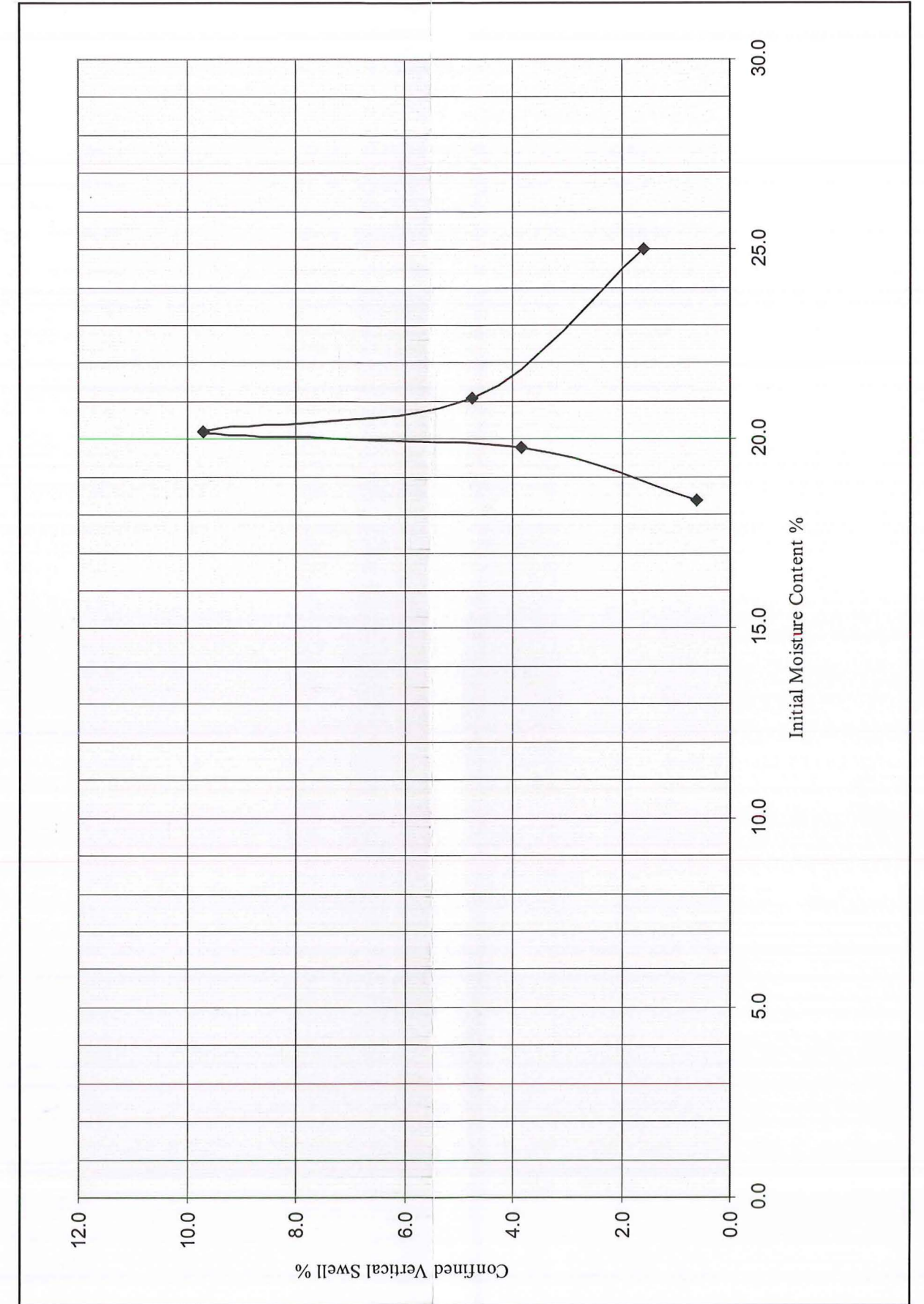


Figure 4.7 Confined Vertical Swell Versus Initial Moisture Content for Natural Samples

Short Tube Samples (90mm)

Sample No.	Depth (mm)	Dry Density kg/m^3	Bulk Density kg/m^3	Initial Moisture Content%	Confined Vertical Swell %
R1/10	1500	1790	-	-	-
R1/11	1500	1656	-	-	-
R1/6	1500	1468	1802	0	6.4
R1/7	1500	1654	1772	0	7.4
R1/9	1500	1667	1828	0	5.6

Long Tube Samples (150-170mm)

Samples	Depth (mm)	Dry Density (kg/m^3)	Partial Saturation Density (kg/m^3)
R2/4	500	-	-
R2/10	750	1698	2033
R2/14	1000	1707	2110
R2/18	1250	1663	2007
R2/22	1500	1504	1929
R2/24	1750	1661	1975
Average Dry Density		1647	

Table 4.3 Result of Dry/Bulk Densities and Vertical Swell

Vertical swell levels appear to peak around a dry density of 1530kg/m^3 . After this they decline sharply. Most swelling never exceeds 6%, although there is a large degree of scatter associated with the data.

The relationship between moisture content and vertical swell, plotted in Figure 4.7, displays a similar shape to that in Figure 4.6. It demonstrates a close relationship between initial moisture content and confined vertical swell, with the maximum swell occurring at a soil water content of just above 20%. Laterally-confined vertical swell is low, with 9.7% the highest value recorded. This is largely what was indicated from earlier site investigations.

Three key points can be taken from the dry density and confined vertical swell data:

- Vertical swell appears to be related to both dry density and moisture content, with maximum of 9.7% swell achieved at a density 1550kg/m^3 , and a water content of 20%.
- The results for the laterally-confined vertical swell tests are lower than would normally be expected for soils displaying expansive/swell behaviour.

- The dry density/confined vertical swell relationship is represented by a bell-shaped curve, with a large amount of scatter.
- The greatest fluctuations in soil volume occur in soils with an initial moisture content of 18 – 25%.

4.5 X-Ray Diffraction Analysis

4.5.1 Method

X-Ray Diffraction (XRD) analysis of the soil was undertaken in order to determine its mineralogy. Stephen Brown (Geochemistry Technician, Department of Geological Sciences, University of Canterbury) performed the XRD analysis on both bulk samples and clay size fractions. The procedure is outlined in Appendix E. A complete set of the diffractograms is also included there.

4.5.2 Results

The main goal of the XRD analysis was to identify swelling clay minerals. However, on average the results reveal a mineralogical make-up of 20% kaolinite and 80% muscovite (Table 4.4). Kaolinite is known to be a reasonably stable clay mineral, and showed no shift of peaks when glycolated (Appendix E). The presence of kaolinite was further confirmed when it was destroyed after firing at 500 °C.

Muscovite is a non-clay mineral, and, like kaolinite, possesses a very stable lattice structure. The lack of shift in the peaks of either mineral when samples were glycolated suggests there are no swelling minerals present in the soil. This complete lack of swelling clay minerals indicates that volume expansion must be occurring because of geotechnical properties (as described in Section 2.4). It is most likely the swelling is a result of a reduction in suction in the soil during periods of rainfall. This suction is caused by the downwards percolation of water into the underlying gravels and the near-constant moisture-deficient state of the soil. The implications of the presence of a structurally swelling soil include:

- These swelling soils cannot be categorised by their mineralogy.

- The structural framework responsible for soil swelling could also be responsible for the high deflections of the road surfaces.

Table 4.4 XRD Results

Bulk Sample	Depth (mm)	Mineral $\pm 5\%$			
		Quartz	Albite	Muscovite	Kaolinite
R1/12,13/A	1500	60	25	5	10
R1/21	500	70	30	Trace	Trace
Clay-sized Samples					
R2/3	500	-	-	80	20
R2/7	750	-	-	85	15
R2/11	1000	-	-	80	20
R2/23	1750	-	-	75	25
R1/12,13/A	1500	-	-	80	20
R1/21	500	-	-	80	20

Kaolinite is a product of acid weathering and only develops in soils under certain conditions. These conditions are:

1. A low pH environment.
2. Levels of precipitation greater than the rate of evaporation; i.e. excess soil moisture available.
3. Prolonged leaching of the soil, without the presence of stagnant water
4. The presence of a silicic parent rock/mineral for the kaolinite to form from

Kaolinite formation is also helped by a covering of peat over the soil, through which leaching occurs. This reduces the pH levels and oxygen content of the soil, and in turn increases the reaction rate for the kaolinite formation. Flushing abundant amounts of organics through the water responsible for leaching can have the same effect, without requiring the peat layer. A well-vegetated floodplain, such as the Rangiora Bush, could provide the organic material. All of these conditions suggest a depositional environment near an organically-rich source (for example, a swamp). Combined with field investigation, this indicates the depositional setting was a backwater swamp deposit.

The bioturbation/leaching seen in the SEM photographs, and in the well-reworked silty clay unit logged during excavation supports the theory of the depositional setting.

The massive homogenous unit, with its high clay and silt content, suggests a low-energy environment, while the gravelly silt clay unit could have been a channel leading into the swamp. The relative commonness of peat deposits in the Rangiora area also suggests the area surrounding the investigated site was once swampland, and the abundance of rootlets present in the soil indicates that, at some stage, there was abundant vegetation there. Together with the precedent for peat deposits in the Rangiora area, implying the close presence of a swamp, and the rootlets indicating plenty of vegetation growth. This all points towards a depositional area close to, but not within, the boundaries of a swamp.

The proposed scenario for the depositional setting is the transitional area between flood channel and swamp, where there is a build up of organic material, but where regular flushing of the water prevents peat formation and water stagnation. This flushing also allows for the soil to be in a moisture-rich state most of the time, which promotes leaching. This constant leaching, and the bioturbation (anaerobic conditions not yet being developed this far from the swamp) caused by roots, not only leads to unevenness of the soil structure, but also to the removal of bedding layers. A sketch of this geological model is shown in Figure 4.8.

4.6 Triaxial Test

Two sets of four triaxial amples were collected in 38mm diameter tubes, from a depth of 1.5m. One set was taken from Trench R1, and the other from Trench R2. Additionally, an undrained triaxial test (as prescribed in New Zealand Standards 4402:1986, Test 6.2.1) was performed on four samples recovered from Trench R3. The results of these tests are collected in Figure 4.9. These results indicate there may be a degree of cohesion in the soil, possible due to its kaolinite content.

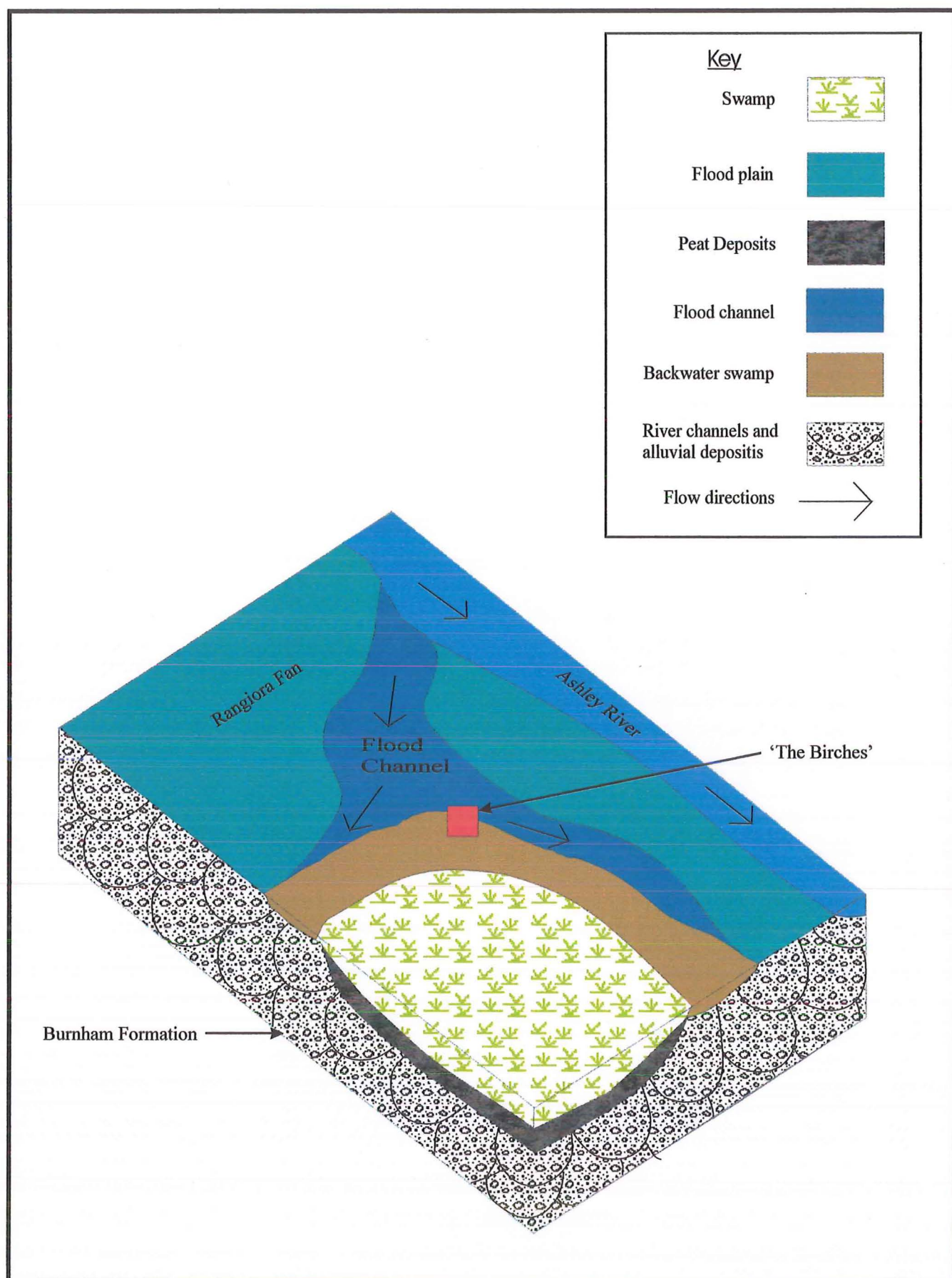


Figure 4.6 Block Diagram of the Geological Setting During Deposition of the Silty Clay Unit Beneath 'The Birches' Subdivision

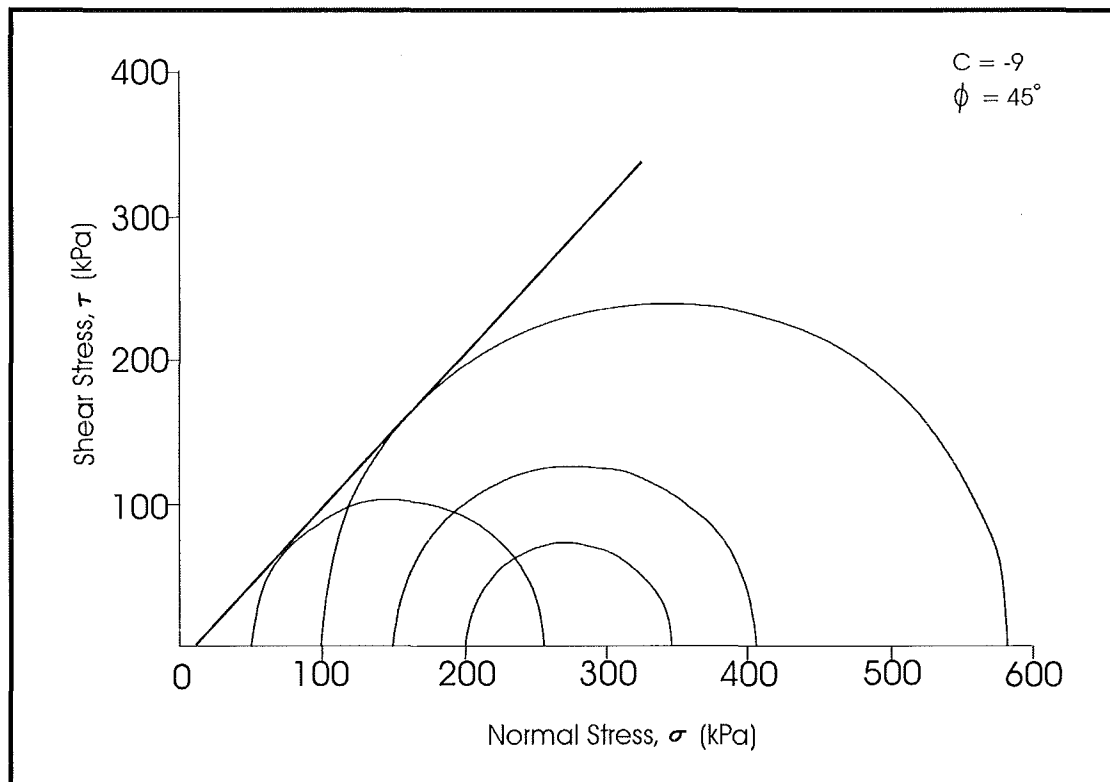


Figure 4.9 Undrained Triaxial Shear Stress versus Normal Stress for Soils Recovered from Trench R3, 'The Birches' Subdivision

4.7 Swell Tests on Recompacted Samples

4.7.1 Method

A compaction test was performed on a combination of several samples (R1/12 and 13, R2/3, 7 and 15 and R3/4 and 13). This test was performed as prescribed by the New Zealand Standards 4402 (1986) Test 4.1, with the additional testing of remoulded samples for vertical swell limits. To test the samples, a tube was first pushed into the soil mass following completion of compaction, but prior to extrusion of the mass from the mould. Once the compacted mass is extruded, a sample is taken for moisture content sampling (as stated in the standard test procedure). The tube with the sample inside is then broken out of the compacted mass, trimmed as necessary, and placed in the vertical swell apparatus for testing (as discussed in Section 4.4).

4.7.2 Results and Discussion

The following property values are averages produced from two samples taken from the combined sample (used for the compaction and remoulded vertical swell tests).

- Plastic Limit: 28 ± 2
- Liquid Limit: 47 ± 2
- Plasticity Index: 19 ± 4

The results from the compaction test are shown in Figure 4.10, while Figure 4.11 shows the confined vertical swell of the re-compacted samples versus their initial moisture content. The plot of confined vertical swell versus moisture content for natural samples (as seen in Figure 4.7) has also been superimposed on Figure 4.11 so comparisons between natural and re-compacted samples can be made.

Figure 4.10 shows maximum dry density is achieved at a moisture content of 24.4%, with a corresponding dry density of 1565 kg/m^3 . Although this is similar to the values seen in Figure 4.6, it is a much lower dry density value than those obtained from the long tube samples (as seen in Table 4.3). Figure 4.10 shows the results of the confined vertical swell of the re-compacted sample. It has a similarly-shaped curve to that seen in Figure 4.9, although maximum swell is achieved here at 19% water content, as opposed to the 24.4% water content for the natural soil samples. This information suggests that dry density has a direct affect on the swell potential. This is explained by the following points:

1. Initial water content is not the primary controlling factor, as the rapid drop in the levels of vertical swell prior to the point of void saturation indicates control of swell potential is largely due to other properties.
2. At the point of critical density the inter-grain spacing is reduced to a point where menisci layer formation (Figure 2.3) cannot fully develop between particles. This results in a reduced level of suction, and a negative linear relationship.
3. Water has a controlling influence on confined vertical swell once the water content exceeds the optimum water content value associated with maximum dry density.
4. The increased confined vertical swell results of the re-compacted samples show greater extents of vertical swell than the natural samples (Figure 4.10). This

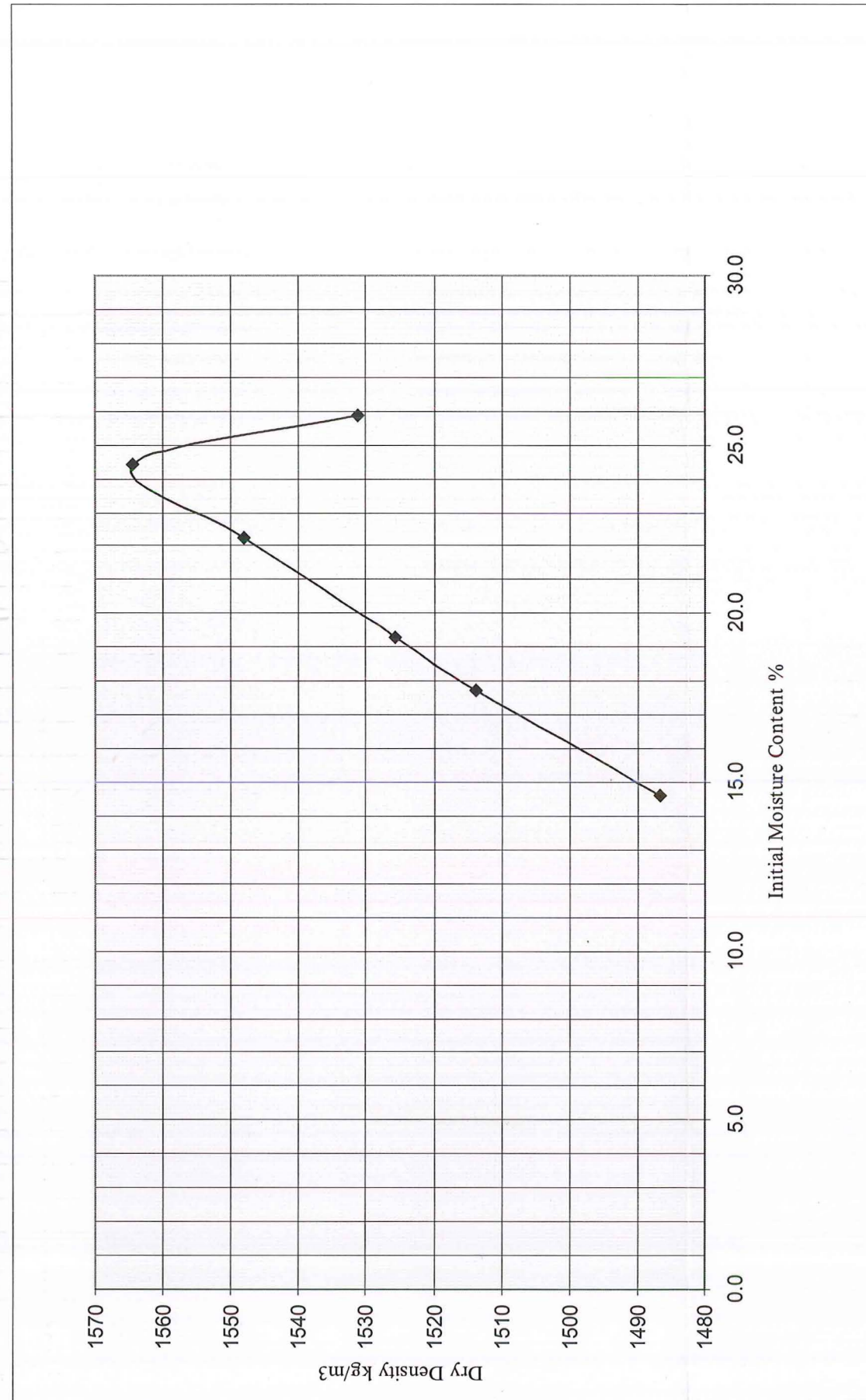


Figure 4.10 Determination of the Dry Density/Water Content Relationship, Combined Sample

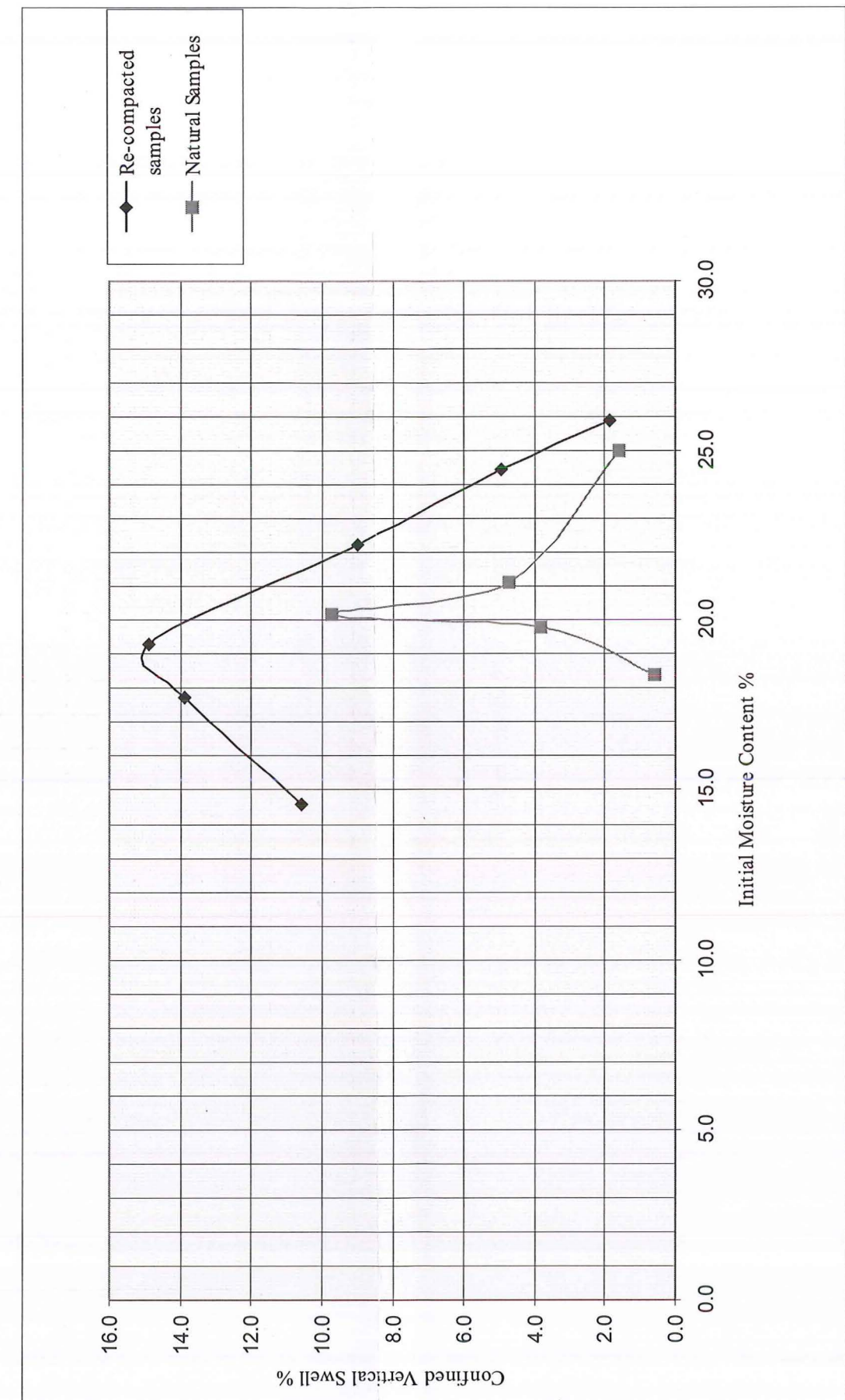


Figure 4.11 Confined Vertical Swell on Re-compacted Samples Versus Natural Samples

suggests reworked material is more susceptible to swelling. It is likely that soils probably become more stable with time as shrink/swell cycles are repeated. Reworking will destroy the more stable structures developed through densification cycles, and start the process all over again.

4.8 Synthesis

The following is a list of the key points and relationships discovered through the laboratory testing.

1. SEM study revealed the absence of layering, and showed minor evidence of bioturbation or leaching of the soil.
2. The high clay content of the soil suggests it is not a loess-type deposit.
3. A low activity index and typical clay linear shrinkage values indicate a stable clay mineral composition.
4. The silty clay unit is a homogenous structure displaying high levels of both vertical and lateral consistency.
5. XRD analysis revealed there are no swelling clay minerals present in the soil. This suggests the reasons for volume expansion are structural.
6. Moisture deficiency in the soil results in densification and forces of suction. When moisture levels are increased, suction is reduced and volume expansion occurs.
7. The presence of kaolinite suggests that deposition took place in an acidic, leaching environment, such as near a swamp.
8. Remoulded material is more susceptible to vertical swelling, with both an increase in maximum potential swell, and in the range of moisture contents over which the soils will display swelling behaviour. This is possibly because reworking destroys the stability of the lattice structure, which was achieved through the repetition of shrink/swell cycles.

Chapter 5 Conclusions

From the literature review, fieldwork and laboratory testing, the following conclusions have been drawn:

- ‘The Birches’ subdivision is located on the Rangiora Fan, which for much of its history was a well-vegetated swampland, with tree species including white pine, totara and kowai.
- ‘The Birches’ subdivision is located within a large depression that forms a subcatchment located on the Rangiora Fan. This depression is occupied by the North Brook, South Brook and Cam Rivers, and the Waikoruru Stream.
- The soils were originally thought to be expansive, as they displayed characteristics common to these types of soils.
- Due to the potential presence of swelling clay minerals, the primary focus of this project was to undertake laboratory testing in order to gain information about the mineral structure of the soil, and its potential to swell. This testing included dry density tests, the plotting of grading curves, confined vertical swell tests, and scanning electron microscope studies.
- As the decrease in nail spacing during the monitoring period of 12/01/2001 to 25/05/2001, did not correspond with an increase in rainfall, it is suggested that crack formation/development is also dependent on temperature and solar radiation exposure.
- The natural water content of the soil at shallow depths (less than 160 mm) is closely related to rainfall, while only the top 40 mm of soil is subject to moisture content changes greater than 10%.
- Upon excavation, only one massive, homogenous, silty clay unit was found, overlying oxidised fan gravels (in which the water table was approximately level

with the base of the silty clay unit). It has a varying thickness of between 1.5-2.0 metres.

- A SEM study of the silty clay samples indicated that no layering or bedding is present, but showed some evidence of bioturbation and/or leaching.
- The high clay content of the soil (31.5-45.9%), and the presence of a log of wood at a depth of 1.5 metres, suggests the silty clay unit is not a loess-type deposit.
- XRD analysis revealed that no swelling clay minerals are present in the soil. The average mineral makeup of the clay-size fraction (less than 0.002mm) is 20% kaolinite and 80% muscovite. As these are stable minerals, this indicates that the causes of volume expansion in this soil are structural.
- Kaolinite is a product of acid leaching. This further suggests that deposition took place in an acidic, leaching environment, such as a swamp margin.
- The average soil moisture varied from 17.1 to 22.0% (for the top 400mm of soil). This moisture deficiency in the soil results in suction and densification. Upon wetting of the soil, suction is reduced and volume expansion of the soil occurs.
- Remoulded material is more susceptible to vertical swelling, with both an increase in the maximum swell potential, and in the range of moisture contents over which the soils will display swelling behaviour. The maximum laterally-confined vertical swell for re-compacted samples was 14.9%, compared with 9.7% for a natural sample. This is possibly because reworking destroys the stability of the lattice structure, which is formed through repeated shrink/swell cycles

In summary, it has been found that the soils of 'The Birches' subdivision are swelling soils, owing to their weak structural fabric. They generally have a low potential for swell, but reworking of the soil can destroy the stability of the lattice structure, which in turn can result in an increase of the swell potential of the soil.

The following are recommendations for further fieldwork in the area:

1. Mapping of the extent of the deposits and the flood channels that fed the old swamp. This would allow for the location and zoning of areas potentially susceptible to soil volume expansion.
2. Laboratory work to distinguish whether the swelling is caused by positive air pressure, or by the relaxation of the mineral structure during periods of reduced suction. This would allow for the further formulation of possible methods for remediation.

References:

- Akroyd, T.N.W. *Laboratory Testing in Soil Engineering*. Marshal Press Ltd, London. 1958.
- Alexander, W.S., Maxwell, J. *Controlling Shrinkage Cracking From Expansive Clay Sub-Grades*. Proceedings of the Third International RILEM Conference. 1996.
- Austrroads. *Pavement Design, A guide to the Structural Design of Road Pavements*. Sydney 1992.
- Barnes, G.E. *Soil Mechanics Principles and Practice*. MacMillan Press Ltd, London. 1995.
- Bolton, M. *A Guide to Soil Mechanics*. Macmillan Press Ltd. London. 1979.
- Browne, G.H. Thrasher, G.P. *Stratal patterns and sedimentology of low stand deposits of mid-Canterbury, New Zealand*. Geological and Nuclear Sciences, New Zealand, 1996.
- Canadian Building Digest-84, 'CBD-84. Swelling and Shrinking Subsoil's', <http://www.nrc.ca/irc/cbd/cbd148e.html>, 5/23/2001.
- Canterbury Regional Council, *Ashley River Floodplain Management Regional Plan, Technical Investigation*. Report 95(6), May 1995.
- Chabrillat, S. Goetz, A.F.H. Olsen, H.W. Krosly, L. Noe, D.C. *Identification and Mapping of Expansive Clay Soils in the Western U.S Using Field Spectrometry and AVIRIS Data*. http://cries.colorado.edu/cses/research/swelling_soils.html, 5/23/2001.
- Chen, F.H. 'The Basic Physical Property of Expansive Soils'. *Proceedings of the Third International Conference on Expansive Soils, July 30-August 1, 1973, volume 1*. Haifa, Israel: Jerusalem Academic Press. 1973. p17-25.
- Chen, Wai-Fah. *Limit Analysis and Soil Plasticity*. Elsevier Scientific Publishing Company, Amsterdam. 1975.
- CN Non-Food Import-Export Corp. *Road Construction With RRP-Special*. <http://www.ch-non-food.com/science.htm>, 5/23/2001.
- Cowan, H.A. *Structure, Seismicity & Tectonics of the Porter's Pass – Amberley Fault Zone, North Canterbury, New Zealand – Geology*. University of Canterbury, New Zealand. 1992.
- Dixon, J.B. Weed, S.B. *Minerals in soil Environments*. Soil Science Society of America, Inc, U.S.A. 1977.
- Douglas, W.L. David, M. *Practical Sedimentology*. Chapman & Hall, New York. 1994.
- Ethridge, F.G. Flores, R.M. Harvey, M.D. *Recent Developments in Fluvial Sedimentology, Contributions from the Third International Fluvial Sedimentology Conference*. Tulsa Oklahoma, U.S.A: Society of Economic Palaeontologists and Mineralogists. Special Publication no.39. 1987. p111-120.
- Fredlund, D.G. *Engineering Properties of expansive Clays*. The Publication Series of the University of Saskatchewan Transportation and Geotechnical Group. 1975.

- Grim, R.E. *Applied Clay Mineralogy*. McGraw-Hill Book Company Inc. New York. 1962.
- Grim, R.E. *Clay Mineralogy*. McGraw-Hill Book Company. New York. 1968.
- Hawkins, D.N. *Rangiora - The Story of a Rural Community - History*. Honours Thesis at the University of New Zealand. 1949.
- Herzer, R.H. Bradshaw, J.D. 'The Motunau Fault and other Structures at the Southern Edge of the Australian-Pacific Plate Boundary, Offshore Marlborough, New Zealand – Discussion', *Tectonophysics*, 115. 1985. p161-166.
- Holtz, D.R. Kovacs, W.D. *An Introduction to Geotechnical Engineering*. Englewood Cliffs, New Jersey: Prentice-Hall, Inc. 1981.
- Jennings, J.E. 'The Engineering Significance of Constructions on Dry Subsoils'. *Proceedings of the Third International Conference on Expansive Soils, July 30-August 1, 1973, volume 2*. Haifa, Israel: Jerusalem Academic Press. 1974. p27-32.
- Jowett, T.W.D. *Structure, An Investigation of the Geotechnical Properties of Loess from Canterbury and Marlborough-Engineering Geology*. University of Canterbury, New Zealand. 1995.
- Kassiff, G. Livneh, M. Wiseman, G. *Pavements on Expansive Clays*. Faculty of Civil Engineering, Israel-Institute of Technology. Jerusalem Academic Press. 1969.
- Lewis, D.W. *Practical Sedimentology*. University of Canterbury (D.W. Lewis, 1981).
- Mitchell, J.K. *Fundamentals of Soil Behaviour, second edition*. University of California, Berkeley, John Wiley & Sons, New York, 1993.
- NZS 4402: 1986 'Methods of Testing Soils for Civil Engineering Purposes' Standards Association of New Zealand (1986).
- NZS 4431: 1989 'Code of Practice for Earth fill for Residential Development' Standards Association of New Zealand (1989).
- NZS 3604: 1990 'Code of Practice for Light Timber Framed Buildings Not Requiring Specific Design' Standards Association of New Zealand (1990).
- Pettinga, J.R. Christopher, G.C. Yetton, M.D. Van Dissen, R.J. Downes, G. *Earthquake Source Identification and Characterisation*. Canterbury Regional Council, 1998.
- Sankaran, K.S. Venkateshwar, D. 'A Microscopic Model of Expansive Clay'. *Proceedings of the Third International Conference on Expansive Soils, July 30-August 1, 1973, volume 1*. Haifa, Israel: Jerusalem Academic Press. 1973. p65-71.
- Selvadurai, A.P.S. *Elastic Analysis of Soil-Foundation Interaction*. Development in Geotechnical Engineering vol. 17. Elsevier Scientific Publishing Company, New York. 1979.

- Sinclair, M. 'Klondyke Development Ltd – “The Birches”, Rangiora. Filling Operation – Inspecting Engineers Report'. Christchurch: Eliot Sinclair and Partners Limited. 10 April 1997. Ref: 142263
- Sinclair, M. 'Klondyke Development Ltd – “The Birches” Subdivision, John Street, Rangiora. Filling Operation Stages 2 and 3 – NZS 4431 Certificates'. Christchurch: Eliot Sinclair and Partners Limited. 16 July 1998. Ref: 154229
- Sinclair, M. *Re: Structural movement in Houses at 23 Green Street and 29 Hawkins Place. Rangiora.* Christchurch: Eliot Sinclair and Partners Limited. 21 December 1999. Ref: 192295
- Sinclair, M. *Re: Concrete Floor Slab and Driveway at 31 Hawkins Place.* Christchurch: Eliot Sinclair and Partners Limited. 2 March 2000. Ref: 194115
- Sisson, R.J. *Paleoseismic Investigation of the Ashley Fault, North Canterbury, New Zealand.* Honours Thesis at the University of Christchurch, July 1999.
- Soons, J.M. Selby, M.J. *Landforms of New Zealand.* Longman Paul, Hong Kong, 1992.
- Sridharan, A. Rao, S.M. Murthy, N.S. *A Rapid Method to Identify Clay Type in Soils by the Free-Swell Technique.* Geotechnical Testing Journal. GTJODJ, vol. 9, No 4. Dec. 1986, p198-203.
- Suggate, R.P. *Late Pleistocene Geology of the Northern Part of the South Island, New Zealand.* New Zealand Geological Survey Bulletin No. 77. 1965.
- Suggate, R.P. Stevens, G.R. Te Punga, M.T. *The geology of New Zealand, Vol. 1.* New Zealand Geological Survey, Government Printer, Wellington. 1978
- Terzaghi, K. Peck, R.B. Mesri, G. *Soil Mechanics in Engineering Practice, Third Edition.* John Wiley & Sons, Inc. Illinois, 1996.
- Watt, J.P.C. *Loess Soils and Problems of Land Use on the Downlands of the South Island, New Zealand.* Otago Catchment Board Publication No. 4. 1971.
- Ward, S.J. *The Physical, Chemical and Mineralogical Properties of a Fault Zone. The Hope Fault, East Hanmer Basin, New Zealand.* University of Canterbury, New Zealand, 2000.
- Yong, R.N., Warkenton, B.P. *Soil Properties and Behaviour.* Elsevier Scientific Publishing Company. 1975.
- Yetton, M. 1986 *Investigation and Remedial Methods For Subsurface Erosion Control in Banks Peninsula Loess.* University of Canterbury, New Zealand, 1986.

Appendix – A

Tectonic Setting

Ashley Fault

Only a brief summary of the active tectonics of the North Canterbury region is described here, for a more extensive report refer to R.J. Sisson's 1999 thesis, *Paleoseismic Investigation of the Ashley Fault, North Canterbury, New Zealand*.

The Porters Pass-Amberley Fault Zone (PPAFZ) has the most effect upon the formation of units on the Ashley Floodplain (Pettinga, et al, 1998). The strike runs sub-parallel to the present-day plate activity, and is represented by a disseminated zone of shearing (Herzer & Bradshaw 1985). Herzer and Bradshaw (1985) inferred the possible continuation of the Porters Pass Fault south of Oxford across the Canterbury Plains and into the Ashley River at Mairaki Downs, where it is thought to become the Ashley Fault (Figure 1.2). The PPAFZ is a juvenile fault system, and represents the latest phase of plate boundary zone widening in the late Pleistocene (Pettinga et al, 1998: p18). The PPAFZ displays the presence of three types of sub-domains, which are discussed in H. Cowan's, 1992 thesis, *Structure, seismicity and tectonics of the Porter's Pass-Amberley Fault Zone, North Canterbury, New Zealand*. These subdomains were originally referred to as separate domains prior to the regional nomenclature system proposed by Pettinga et al (1998). They should now be viewed as subdomains.

The PPAFZ is responsible for the uplift in the eastern half of the basin. This causes the numerous folds and faults that the Ashley River crosses from the Loburn Basin down to the Ashley Floodplain. Uplifting occurring during the late Quaternary up until the present could be as rapid as 0.5 metres per thousand years (Canterbury Regional Council Report 95(6). 1995: p91). Many of the anticlines and synclines, such as the Bullock Creek Anticline that is located on the Northwest side of the Loburn basin (Figure 1.2), are a result of movement in the PPAFZ.

Appendix – B

Subdivision History

General Sequence

“The Birches” subdivision is located in the south west of Rangiora (Figure 1.1) and is enclosed by Pentecost Road, Green Street, Johns Street and Charles Street (Figure 1.3). The development was carried out in three stages, as follows:

- Stage one included lots 1-37, 90, 91 and associated services.
- Stage two was lots 38-68, 92 and the associated services. The filling operation for stage three lots, which includes 69-89 and 93, was also completed at this point.
- Stage three will be the individual development of lots 69-89 and 93.

All three stages involve of the construction of the four basic services: a sewer system, storm water drains, telephone lines and power lines. The sewers are made up of either 100 or 250mm UPVC pipes (Figure 1.3). The storm water service includes the construction of gutters, sumps, and 100/150 or 250mm UPVC pipe. Telephone and power lines were laid in the same trenches as the sewer system (Figure 1.3).

Following installation of the four basic services, a filling operation took place to encourage drainage. This was achieved by both the cutting down of some areas, such as Lowes Place, and the rasing up of some areas of land, using the excavated material, which was silty clay with some rarefied gravels.

The areas filled in stage one (early 1997), lots 27-34 and 37, were first stripped of 300mm of topsoil. Then 200-300mm of clean silty clay was placed and compacted with the use of a smooth wheeled vibrating roller. Soil testing following compaction showed that a density of 90-106% of the maximum dry density (1750Kg/m^3) was achieved. Testing of the fill used a nuclear density gauge by Fulton Hogan Canterbury Limited, Telrac laboratory (Eliot Sinclair and Partners Ltd Report 142263, 1997). The exception to this was lot 37 which had a slightly lower standard of compaction. It was recommended that foundations on lot 37 be constructed to a depth of 400mm so as to bear on the natural silt material (Eliot Sinclair and Partners Ltd Report 142263, 1997).

Stage two started in early 1998, and the filling operation for both stages two and three was done at this time (Figure 1.3). The filling operation was carried out in a similar fashion to that of stage one. Approximately 300mm of topsoil was removed, revealing the underlying natural silts, and this was replaced with 200-400mm of clean silt combined with rare gravel that was compacted with a smooth wheeled vibrating roller. Post compaction soil testing

revealed that density of 90-115% of the maximum dry density (1700kg/m^3) was achieved (Eliot Sinclair and Partners Ltd Report 154229, 1998). The maximum dry density for stage two was calculated using New Zealand Standard Compaction Test 4.1: 1986, as apposed to the nuclear density gauge used for stage one.

Appendix – C

Test Method Review

Scanning Electron Microscope

Identification of the mineral composition will help in the development of geological models and the identification of the cause of swelling (structural or mineralogical). XRD analysis is commonly used as it can differentiate between swelling clay minerals (illite) and non-swelling clay minerals (muscovite). This is done using the diffractograms from the glycolated and fired samples (section 4.5). This will be the key method for the determination of the cause of the volume expansion.

Grading curves

Grading curves are used to show the distribution of the soil particles in a given sample. Methods that rely on grain size alone are generally insufficient to properly analysis the soil behaviour. But when combined with Atterberg limits and mineralogy tests they provide an important piece of the puzzle. They also provide information on the clay size fraction which is important for the analysis of expansive soils. Combined with plasticity index they produce a value known as activity index. This evaluates the extent the clay sized fraction has control over the soil (see below).

Atterberg limits

Atterberg limits are widely used for the identification description and classification of soils. They can be broken up into four main categories plasticity limit, liquid limit, linear shrinkage and the plasticity index. The plasticity limit is the lower limit of the plastic state, or the point when the moisture content becomes to low for the clay to behave cohesively. The liquid limit is the upper limit of plastic state after which the soil will lose all shear strength. The linear shrinkage is the amount of volume change that can occur from a liquid limit state to dry state. The plasticity index is the range of moisture content where the soil will behave in a plastic manner. All the Atterberg limits are arbitrary but very important in describing the engineering properties of clay soils. The test procedures used for Atterberg limits are described in Section 4.3.

Colloidal activity, because it is the ratio of plasticity index to the percent of particles less than two microns has been included with the Atterberg limits. There are three degrees of activity:

Activity less than 0.75 -inactive clay (kaolinite)

Activity 0.75-1.25 -normal clay (illite)

Activity greater than 1.25 -active clay (montmorillonite)

(from Kassiff et al, 1969).

This will give a good indication as to the stability of the mineral lattice with out the added information of mineralogical tests.

Vertical swell under zero load (laterally confined)

Vertical swell under zero load (confined laterally) gives a direct measurement of the volume expansion potential of the soil. This is a crucial test if designing for flexible foundations, though it does not measure the swell pressure. This will make gauging the extent of the influence under surcharge pressures difficult.

X-ray Diffraction (XRD) Analysis

Mineralogy will be studied using x-ray diffraction. This test method allows for the study of the clay size fraction as well as the bulk fraction. It also has the ability to differentiate between swelling clay minerals and non-swelling clay minerals, through the analysis of glycolated and fired samples. This will allow the soil to be classified as either an expansive soil or a swelling soil.

Dry Density

Dry density has a direct relationship with volume expansion as shown in section 2.4.4. Dry density is easily calculated from both *in situ* tube samples, through drying and weighing and remoulded samples using the compaction test. Dry density is simply the weight of the soil particles plus the weight of water over a volume of area.

Appendix – D

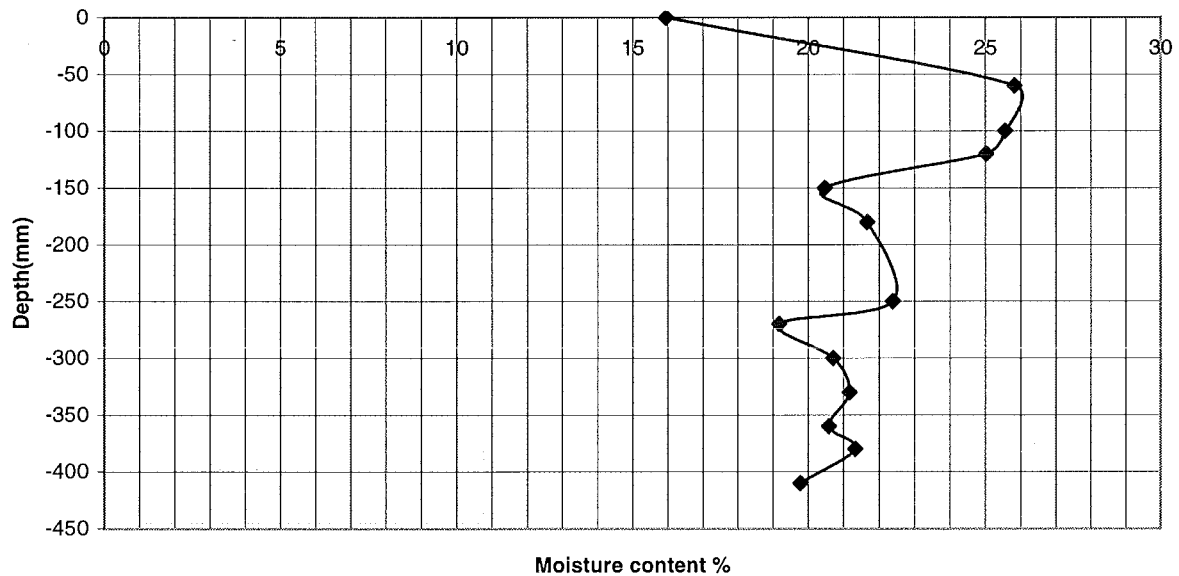
Fieldwork

Date	site 1	site 2	site 3	site 4	site 5	site 6	site 7	site 8	site 9	site 10
12/1/2001	41.52	57.57	65.73	132.4	56.99	61.03	70.43	99.91	86.75	72.98
22/1/2001	40.64	58.39	66.13	133.1	57.2	61.69	70.96	102.51	88.73	73.29
4/2/2001	41.7	58.54	66.09	133.69	56.94	-	70.82	103.58	88.87	73.07
16/2/2001	41.76	58.31	66.03	134.65	56.74	-	71.44	104.71	90.01	72.98
17/3/2001	41.29	-	-	134.09	56.43	-	69.79	101.23	-	73.2
30/3/2001	-	-	-	134.61	55.84	-	70.06	102.43	-	73.1
20/4/2001	-	-	-	133.58	56.14	-	69.47	101.77	-	73.07
8/5/2001	-	-	-	132.08	56.22	-	69.39	99.62	-	73.82
25/5/2001	-	-	-	129.24	56.31	-	68.63	97.64	-	73.85

Crack Monitoring Data

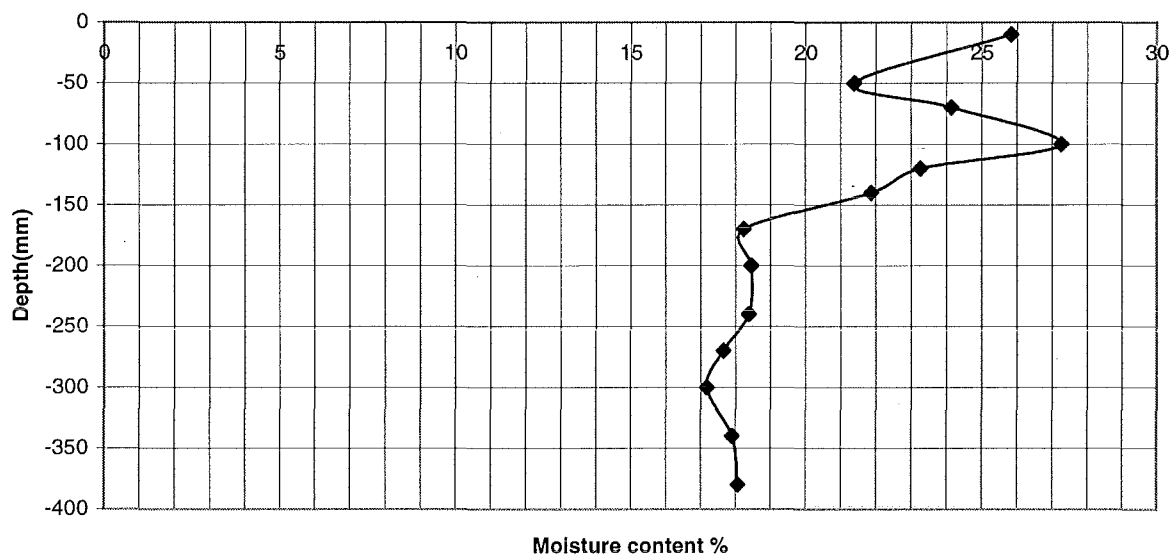
Hole A		12/1/2001				
Depth (mm)	Moisture content %	Tin + wet soil (g)	Tin + dry soil (g)	Mass of Moisture (g)	Mass of dry soil(g)	Weight of tin (g)
0	15.94829	84.54	74.831	9.709	60.878	13.953
-60	25.82213	50.914	43.423	7.491	29.01	14.413
-100	25.56557	59.207	49.963	9.244	36.158	13.805
-120	25.03012	68.946	57.934	11.012	43.995	13.939
-150	20.47025	60.964	52.876	8.088	39.511	13.365
-180	21.6686	65.241	56.091	9.15	42.227	13.864
-250	22.38959	75.679	64.293	11.386	50.854	13.439
-270	19.17923	70.456	61.296	9.16	47.76	13.536
-300	20.71007	69.604	60.02	9.584	46.277	13.743
-330	21.16516	74.191	63.648	10.543	49.813	13.835
-360	20.5899	77.04	66.143	10.897	52.924	13.219
-380	21.33559	76.217	65.137	11.08	51.932	13.205
-410	19.7855	77.451	66.862	10.589	53.519	13.343

Moisture Gradient, hole A



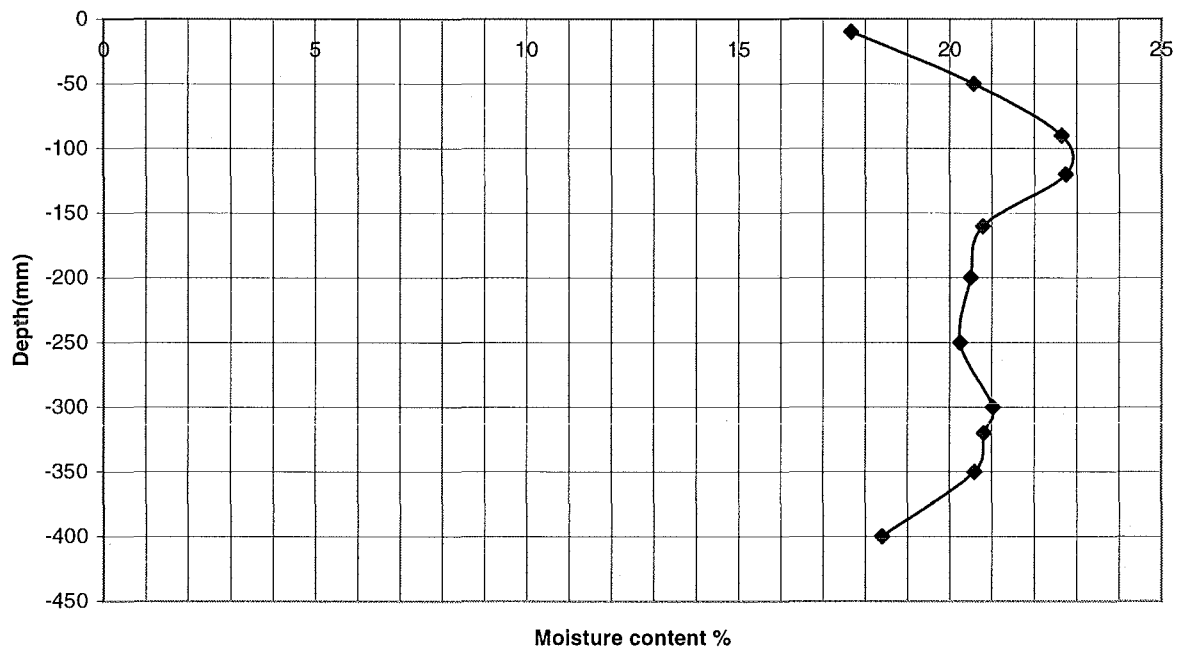
Hole B		12/1/2001				
Depth (mm)	Moisture content %	Tin + wet soil (g)	Tin + dry soil (g)	Mass of Moisture (g)	Mass of dry soil(g)	Weight of tin (g)
-10	25.8309	54.865	46.448	8.417	32.585	13.863
-50	21.38342	64.933	55.968	8.965	41.925	14.043
-70	24.15338	57.402	48.936	8.466	35.051	13.885
-100	27.26412	59.326	49.539	9.787	35.897	13.642
-120	23.26678	72.501	61.547	10.954	47.08	14.467
-140	21.87116	71.731	61.41	10.321	47.19	14.22
-170	18.23881	73.847	64.566	9.281	50.886	13.68
-200	18.45323	74.478	64.984	9.494	51.449	13.535
-240	18.38355	77.741	67.833	9.908	53.896	13.937
-270	17.64853	79.653	69.755	9.898	56.084	13.671
-300	17.16822	72.532	63.963	8.569	49.912	14.051
-340	17.90682	76.296	66.86	9.436	52.695	14.165
-380	18.06691	74.837	65.646	9.191	50.872	14.774
-400	17.98259	80.134	70.033	10.101	56.171	13.862

Moisture Gradient, hole B



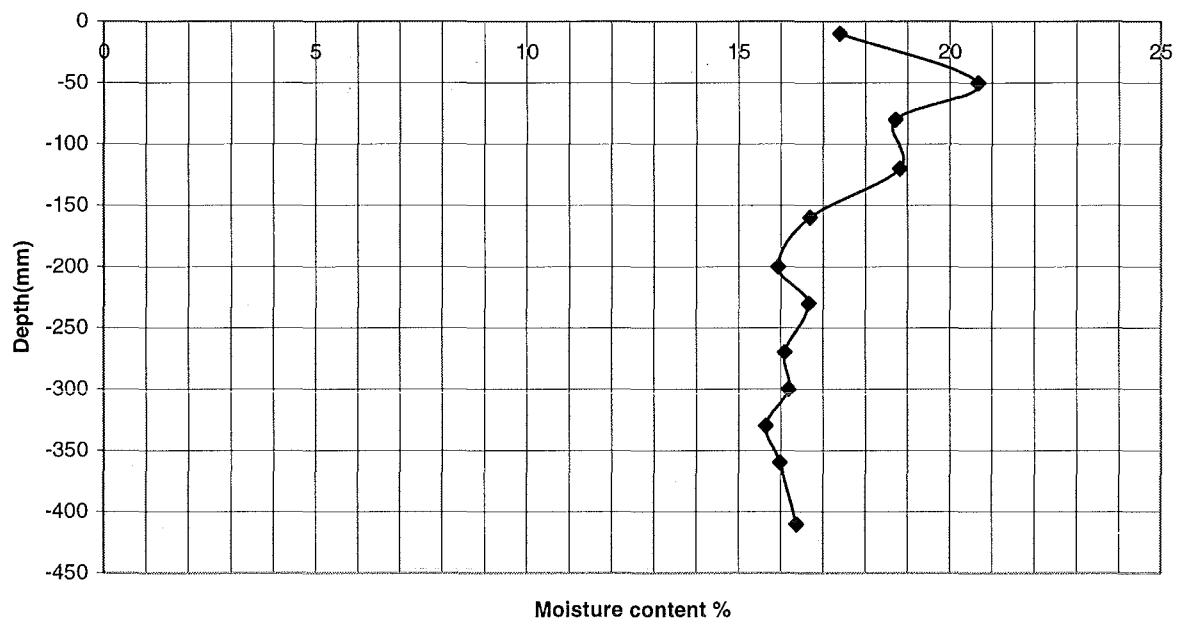
Hole C		22/1/2001				
Depth (mm)	Moisture content %	Tin + wet soil (g)	Tin + dry soil (g)	Mass of Moisture (g)	Mass of dry soil(g)	Weight of tin (g)
-10	17.66914	66.978	59.916	7.062	39.968	19.948
-50	20.57309	63.266	55.835	7.431	36.12	19.715
-90	22.64425	55.163	48.778	6.385	28.197	20.581
-120	22.74569	67.345	58.645	8.7	38.249	20.396
-160	20.78527	60.996	54.04	6.956	33.466	20.574
-200	20.50091	70.155	61.634	8.521	41.564	20.07
-250	20.25304	68.026	59.894	8.132	40.152	19.742
-300	21.02407	63.46	55.905	7.555	35.935	19.97
-320	20.81474	78.531	68.547	9.984	47.966	20.581
-350	20.6006	77.739	67.936	9.803	47.586	20.35
-400	18.39861	83.687	73.935	9.752	53.004	20.931

Moisture Gradient, hole C



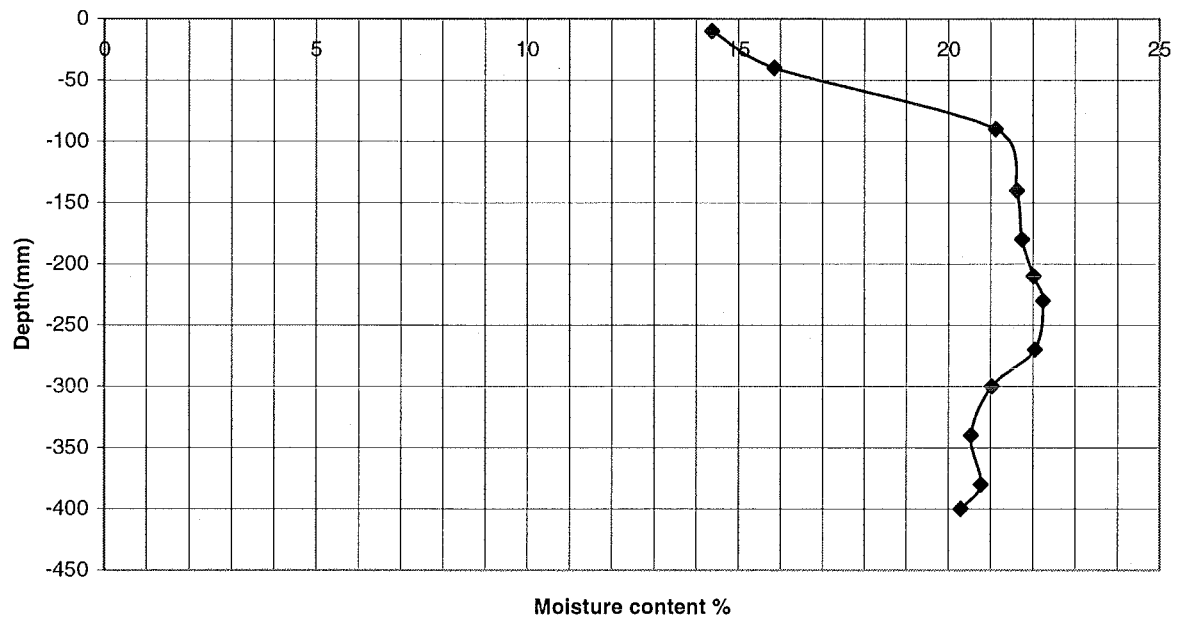
Hole D		22/1/2001				
Depth (mm)	Moisture content %	Tin + wet soil (g)	Tin + dry soil (g)	Mass of Moisture (g)	Mass of dry soil(g)	Weight of tin (g)
-10	17.39703	58.76	53.075	5.685	32.678	20.397
-50	20.67089	66.654	58.754	7.9	38.218	20.536
-80	18.71296	55.393	49.804	5.589	29.867	19.937
-120	18.82474	71.121	63.077	8.044	42.731	20.346
-160	16.69089	71.228	63.877	7.351	44.042	19.835
-200	15.92717	73.397	66.189	7.208	45.256	20.933
-230	16.65452	71.603	64.289	7.314	43.916	20.373
-270	16.09422	71.24	64.23	7.01	43.556	20.674
-300	16.1898	72.318	65.064	7.254	44.806	20.258
-330	15.64299	66.972	60.694	6.278	40.133	20.561
-360	15.97877	70.604	63.678	6.926	43.345	20.333
-410	16.37179	70.953	63.8	7.153	43.691	20.109

Moisture Gradient, hole D



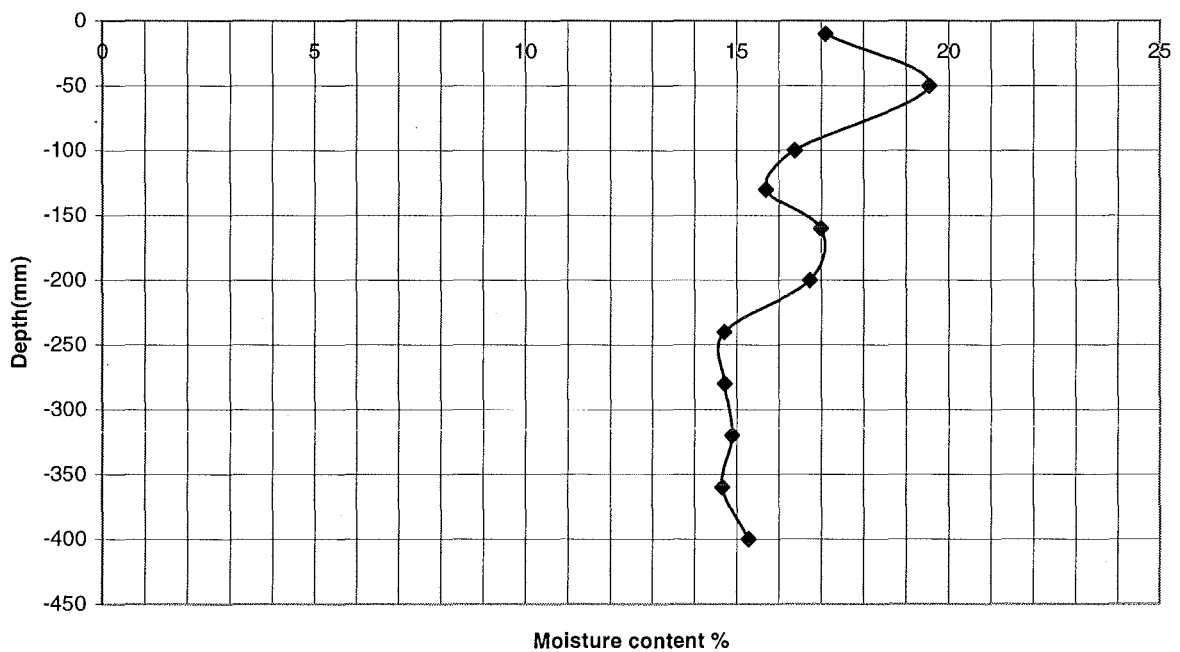
Hole E		4/2/2001				
Depth (mm)	Moisture content %	Tin + wet soil (g)	Tin + dry soil (g)	Mass of Moisture (g)	Mass of dry soil(g)	Weight of tin (g)
-10	14.38022	73.809	67.027	6.782	47.162	19.865
-40	15.84977	60.025	54.56	5.465	34.48	20.08
-90	21.11908	58.022	51.364	6.658	31.526	19.838
-140	21.62421	59.45	52.455	6.995	32.348	20.107
-180	21.73952	61.148	53.837	7.311	33.63	20.207
-210	22.01541	59.011	52.009	7.002	31.805	20.204
-230	22.23622	55.532	49.003	6.529	29.362	19.641
-270	22.04417	70.355	61.262	9.093	41.249	20.013
-300	21.02849	68.044	59.837	8.207	39.028	20.809
-340	20.54208	60.993	53.99	7.003	34.091	19.899
-380	20.77315	54.321	48.496	5.825	28.041	20.455
-400	20.29635	70.662	62.197	8.465	41.707	20.49

Moisture Gradient, hole E



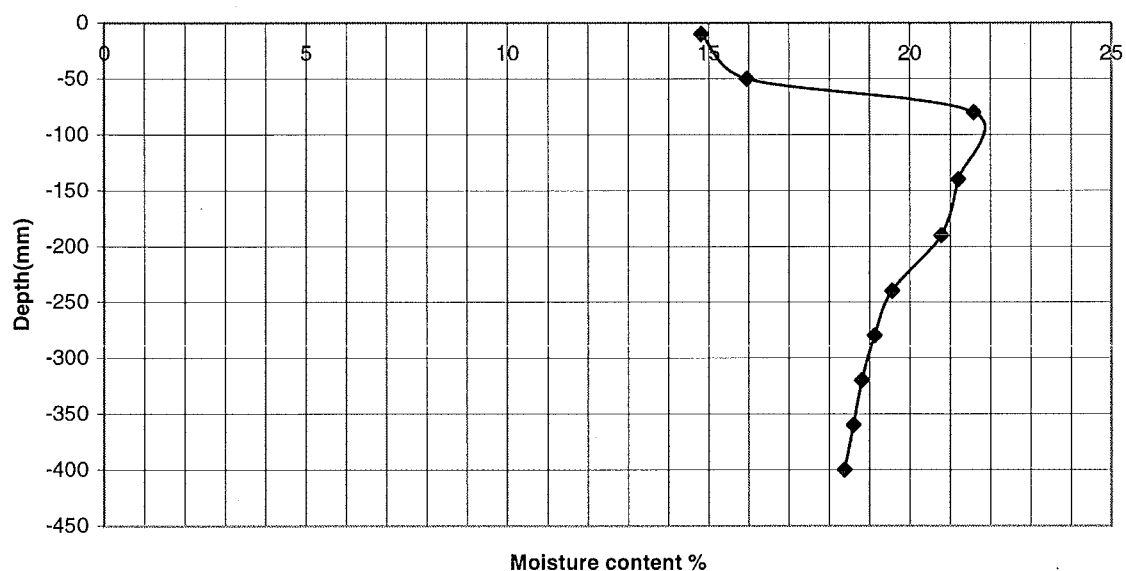
Hole F		4/2/2001				
Depth (mm)	Moisture content %	Tin + wet soil (g)	Tin + dry soil (g)	Mass of Moisture (g)	Mass of dry soil(g)	Weight of tin (g)
-10	17.10284	43.033	39.687	3.346	19.564	20.123
-50	19.5306	56.925	50.867	6.058	31.018	19.849
-100	16.37725	65.993	59.561	6.432	39.274	20.287
-130	15.69052	66.641	60.34	6.301	40.158	20.182
-160	16.99183	50.605	46.259	4.346	25.577	20.682
-200	16.73748	52.554	47.945	4.609	27.537	20.408
-240	14.70612	63.817	58.265	5.552	37.753	20.512
-280	14.72476	56.615	51.958	4.657	31.627	20.331
-320	14.8884	64.197	58.494	5.703	38.305	20.189
-360	14.66191	61.523	56.267	5.256	35.848	20.419
-400	15.2809	67.444	61.256	6.188	40.495	20.761

Moisture Gradient, hole F



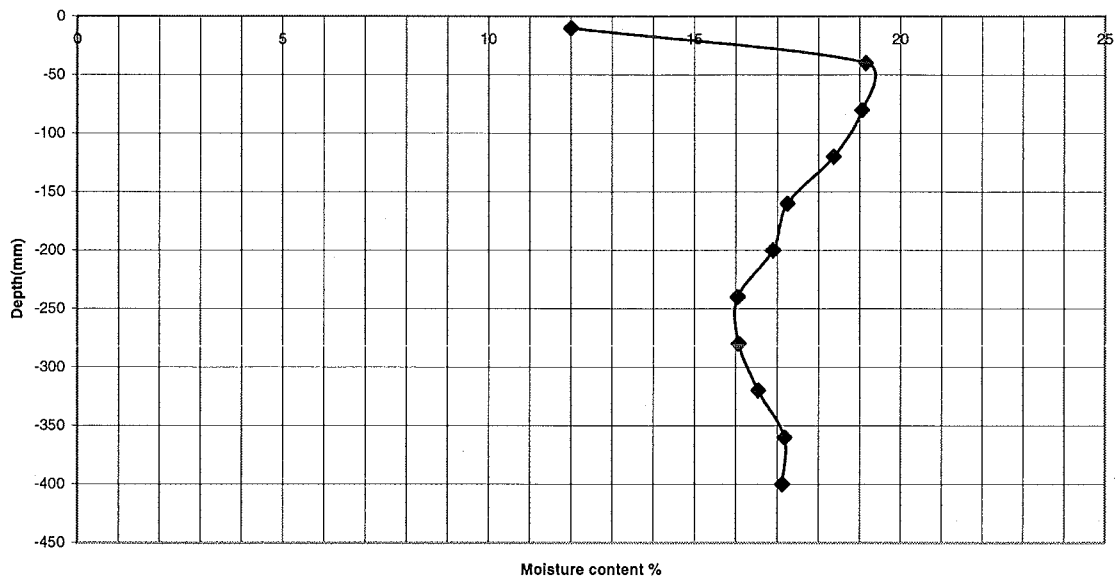
Hole G		16/2/2001				
Depth (mm)	Moisture content %	Tin + wet soil (g)	Tin + dry soil (g)	Mass of Moisture (g)	Mass of dry soil(g)	Weight of tin (g)
-10	14.81549	45.32	42.052	3.268	22.058	19.994
-50	15.94801	41.232	38.336	2.896	18.159	20.177
-80	21.58709	54.569	48.47	6.099	28.253	20.217
-140	21.19796	49.463	44.473	4.99	23.54	20.933
-190	20.7842	57.092	50.853	6.239	30.018	20.835
-240	19.55954	50.766	45.677	5.089	26.018	19.659
-280	19.12218	62.529	55.898	6.631	34.677	21.221
-320	18.80596	50.957	46.147	4.81	25.577	20.57
-360	18.59979	64.01	57.161	6.849	36.823	20.338
-400	18.38274	67.37	60.084	7.286	39.635	20.449

Moisture Gradient, hole G



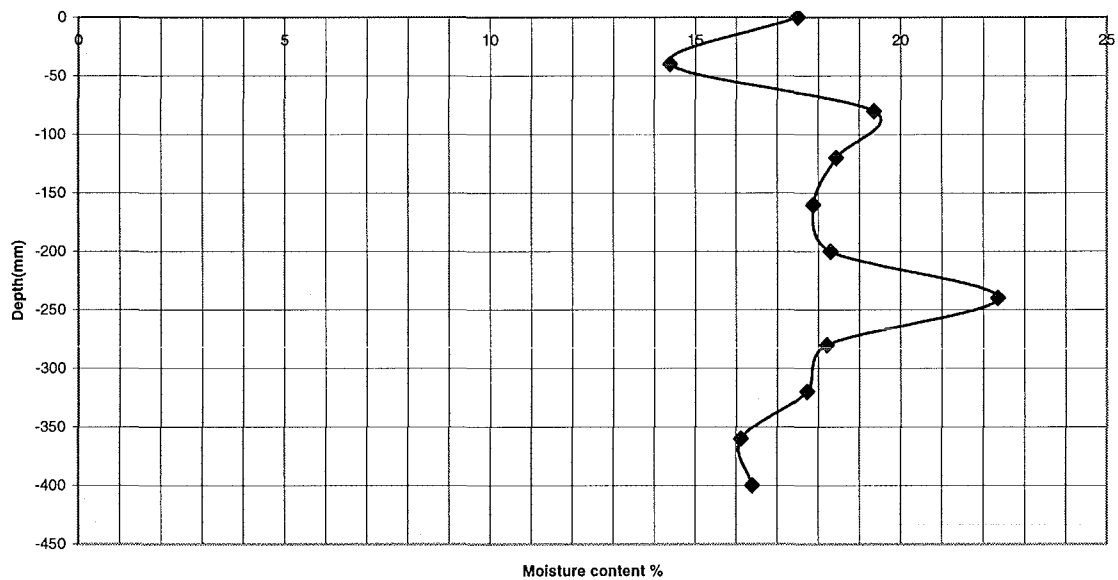
Hole H		16/2/2001				
Depth (mm)	Moisture content %	Tin + wet soil (g)	Tin + dry soil (g)	Mass of Moisture (g)	Mass of dry soil(g)	Weight of tin (g)
-10	12.00859	41.14	38.846	2.294	19.103	19.743
-40	19.15855	49.715	45.052	4.663	24.339	20.713
-80	19.06198	57.782	51.779	6.003	31.492	20.287
-120	18.37389	58.27	52.365	5.905	32.138	20.227
-160	17.24831	62.386	56.119	6.267	36.334	19.785
-200	16.89618	57.246	51.872	5.374	31.806	20.066
-240	16.04295	64.445	58.349	6.096	37.998	20.351
-280	16.06809	65.011	58.819	6.192	38.536	20.283
-320	16.54448	61.349	55.459	5.89	35.601	19.858
-360	17.1809	65.107	58.514	6.593	38.374	20.14
-400	17.12737	72.021	64.468	7.553	44.099	20.369

Moisture Gradient, hole H



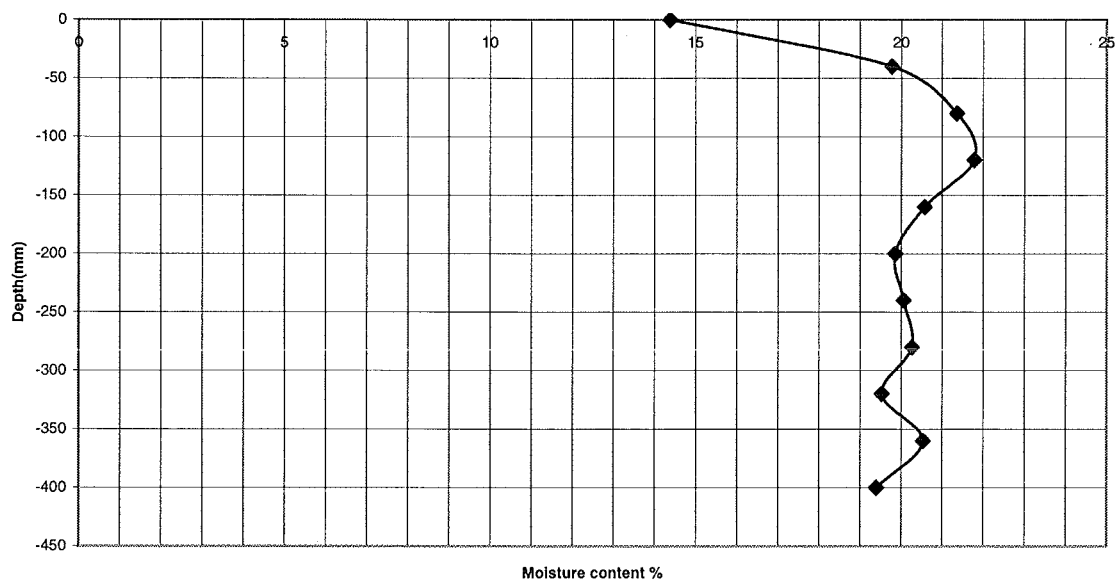
Hole I		17/3/2001				
Depth (mm)	Moisture content %	Tin + wet soil (g)	Tin + dry soil (g)	Mass of Moisture (g)	Mass of dry soil(g)	Weight of tin (g)
0	17.50367	35.189	31.972	3.217	18.379	13.593
-40	14.3809	60.013	54.164	5.849	40.672	13.492
-80	19.3659	52.183	45.916	6.267	32.361	13.555
-120	18.44138	47.168	41.988	5.18	28.089	13.899
-160	17.88708	54.239	48.093	6.146	34.36	13.733
-200	18.30416	45.806	40.923	4.883	26.677	14.246
-240	22.35437	62.226	53.392	8.834	39.518	13.874
-280	18.2098	48.226	42.843	5.383	29.561	13.282
-320	17.72952	51.74	46.049	5.691	32.099	13.95
-360	16.12627	68.183	60.638	7.545	46.787	13.851
-400	16.39184	61.593	54.903	6.69	40.813	14.09

Moisture Gradient, hole I



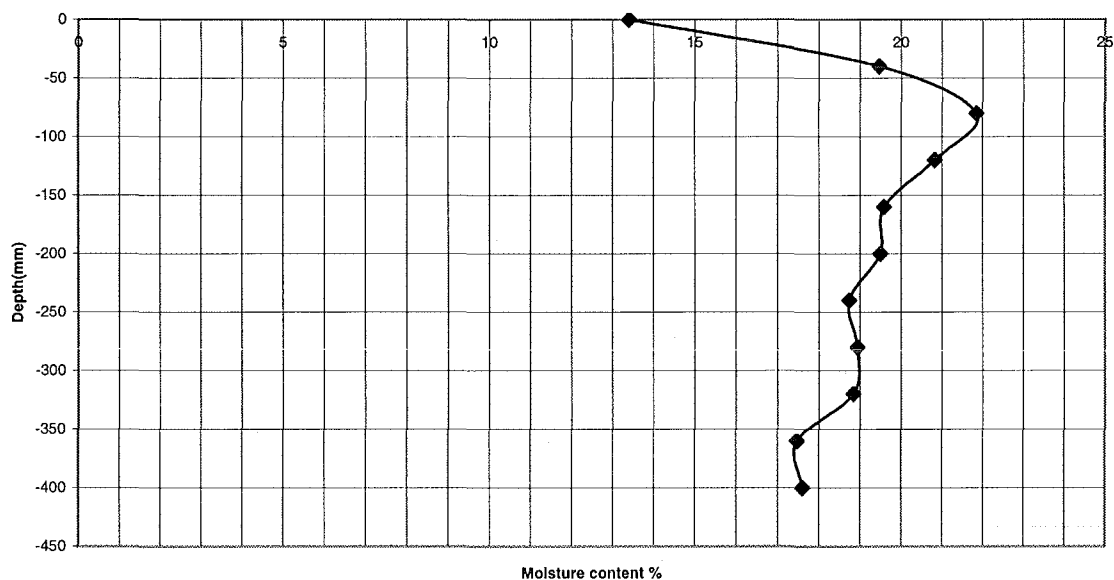
Hole J		30/3/2001				
Depth (mm)	Moisture content %	Tin + wet soil (g)	Tin + dry soil (g)	Mass of Moisture (g)	Mass of dry soil(g)	Weight of tin (g)
0	14.37743	131.653	118.485	13.168	91.588	26.897
-40	19.77802	44.453	39.41	5.043	25.498	13.912
-80	21.36129	49.661	43.447	6.214	29.09	14.357
-120	21.78001	65.898	58.833	7.065	32.438	26.395
-160	20.57053	50.143	43.992	6.151	29.902	14.09
-200	19.84925	47.33	41.8	5.53	27.86	13.94
-240	20.06021	84.323	74.595	9.728	48.494	26.101
-280	20.2616	70.931	63.48	7.451	36.774	26.706
-320	19.52428	48.704	42.95	5.754	29.471	13.479
-360	20.53508	47.965	42.17	5.795	28.22	13.95
-400	19.39209	82.435	73.35	9.085	46.849	26.501

Moisture Gradient, hole J



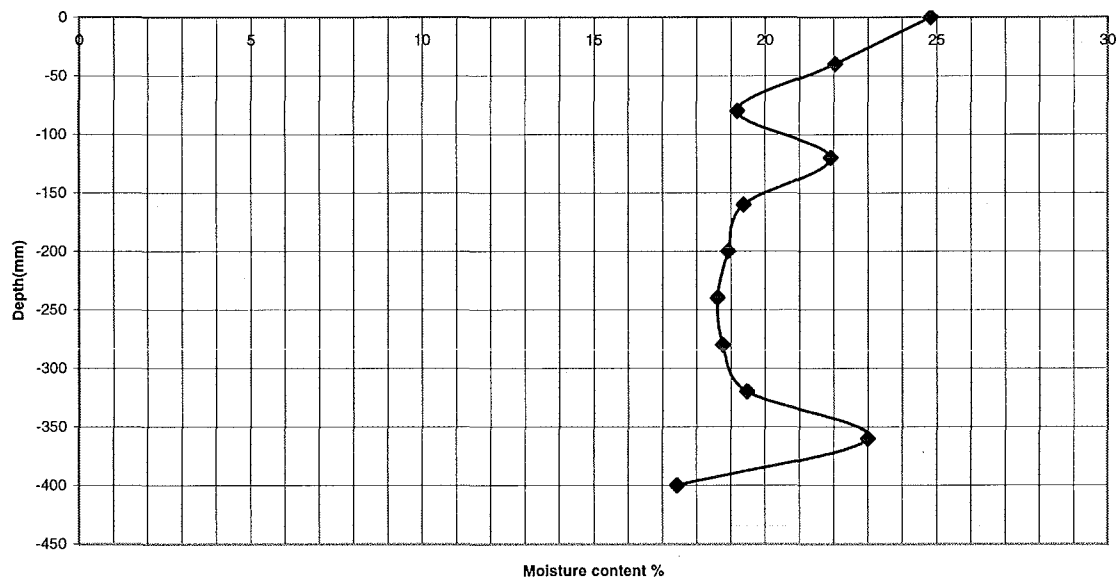
Hole K 20/4/2001						
Depth (mm)	Moisture content %	Tin + wet soil (g)	Tin + dry soil (g)	Mass of Moisture (g)	Mass of dry soil(g)	Weight of tin (g)
0	13.40357	80.683	74.284	6.399	47.741	26.543
-40	19.46393	60.078	54.777	5.301	27.235	27.542
-80	21.8528	66.329	59.224	7.105	32.513	26.711
-120	20.82959	80.25	70.965	9.285	44.576	26.389
-160	19.58786	55.696	48.852	6.844	34.94	13.912
-200	19.49706	47.858	42.392	5.466	28.035	14.357
-240	18.73462	57.393	50.464	6.929	36.985	13.479
-280	18.93802	51.212	45.263	5.949	31.413	13.85
-320	18.83501	55.332	48.768	6.564	34.85	13.918
-360	17.47407	61.48	54.403	7.077	40.5	13.903
-400	17.60364	52.005	46.234	5.771	32.783	13.451

Moisture Gradient, hole K



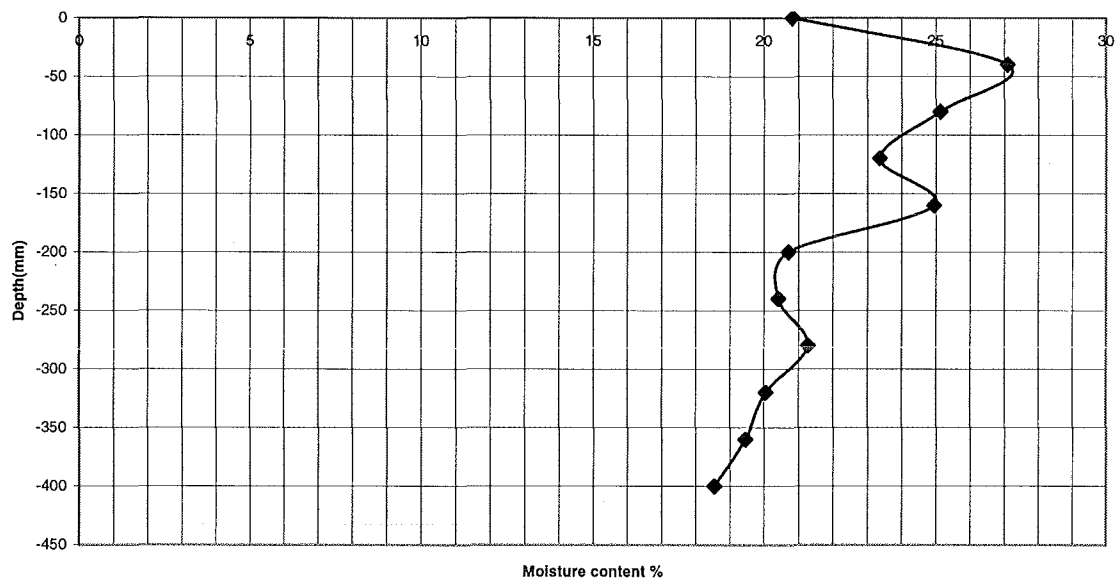
Hole L		8/5/2001				
Depth (mm)	Moisture content %	Tin + wet soil (g)	Tin + dry soil (g)	Mass of Moisture (g)	Mass of dry soil(g)	Weight of tin (g)
0	24.8315	57.097	48.513	8.584	34.569	13.944
-40	22.03796	46.137	40.343	5.794	26.291	14.052
-80	19.20226	47.33	41.89	5.44	28.33	13.56
-120	21.912	53.13	46.004	7.126	32.521	13.483
-160	19.374	50.929	44.894	6.035	31.15	13.744
-200	18.92165	53.377	47.19	6.187	32.698	14.492
-240	18.61186	46.695	41.533	5.162	27.735	13.798
-280	18.76107	54.391	48.034	6.357	33.884	14.15
-320	19.47109	48.501	42.817	5.684	29.192	13.625
-360	23.01152	46.318	40.228	6.09	26.465	13.763
-400	17.42807	65.529	57.842	7.687	44.107	13.735

Moisture Gradient, hole L



Hole M		25/5/2001				
Depth (mm)	Moisture content %	Tin + wet soil (g)	Tin + dry soil (g)	Mass of Moisture (g)	Mass of dry soil(g)	Weight of tin (g)
0	20.82446	43.882	38.603	5.279	25.35	13.253
-40	27.10222	37.886	32.713	5.173	19.087	13.626
-80	25.12518	49.585	42.309	7.276	28.959	13.35
-120	23.3544	62.652	53.413	9.239	39.56	13.853
-160	24.94507	44.757	38.513	6.244	25.031	13.482
-200	20.71543	41.534	36.739	4.795	23.147	13.592
-240	20.417	47.119	41.459	5.66	27.722	13.737
-280	21.27678	56.918	49.419	7.499	35.245	14.174
-320	20.05499	67.524	58.626	8.898	44.368	14.258
-360	19.44666	64.715	56.428	8.287	42.614	13.814
-400	18.54705	44.772	39.957	4.815	25.961	13.996

Moisture Gradient, hole M



Appendix – E

The procedure for preparation and analysis of samples is described in Ward (2000). In addition to the process described in Ward's thesis, was the analysis of the clay size fraction. In this case the slurry was taken from the settling tube of the pipette analysis (section 4.3) at the 8-hour extraction point (0.002mm). This replaced the process of mixing Ethanol with a small amount of sample in an agate mortar to produce slurry. The process is as otherwise stated.

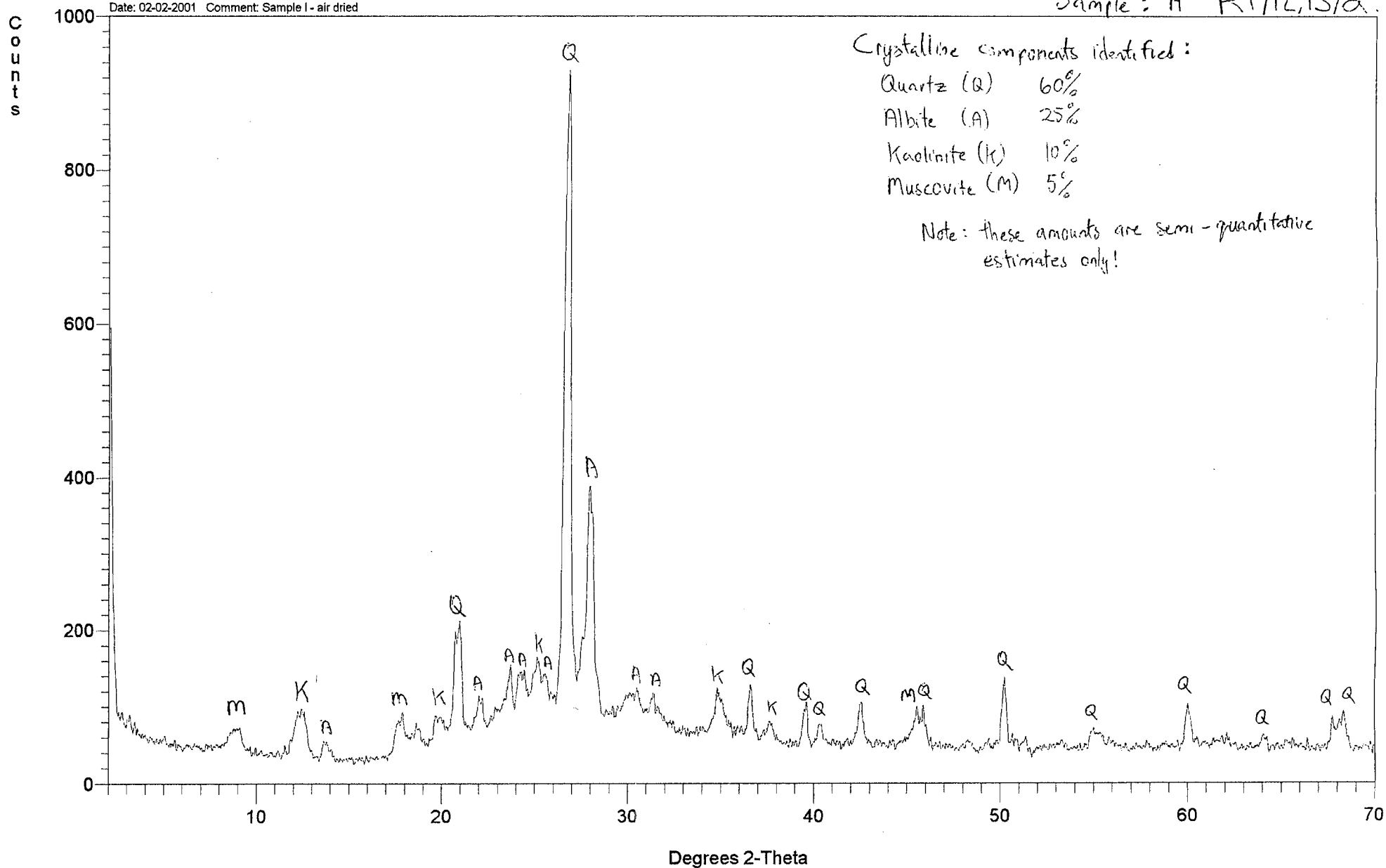
Date: 02-02-2001 Comment: Sample 1 - air dried

Sample: A R1/12,13/a

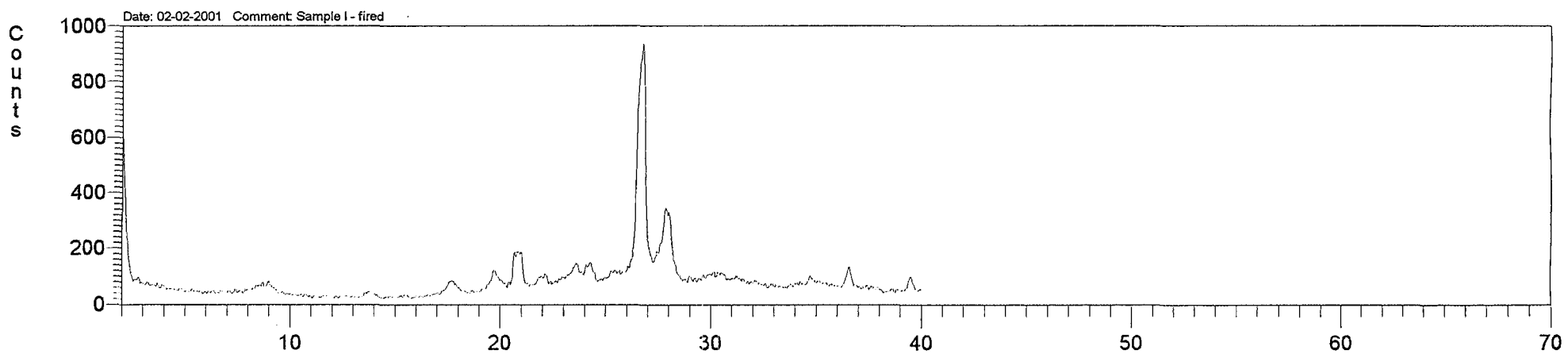
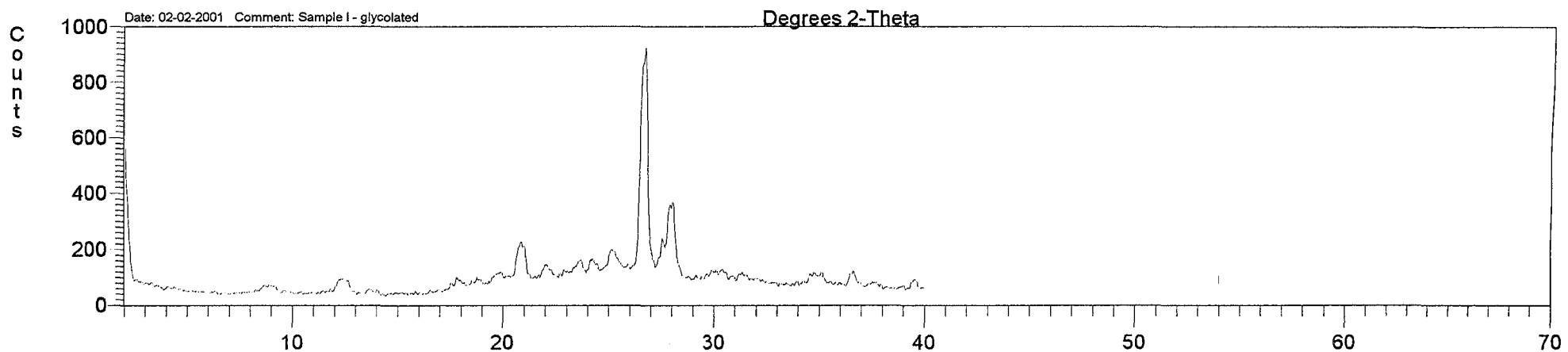
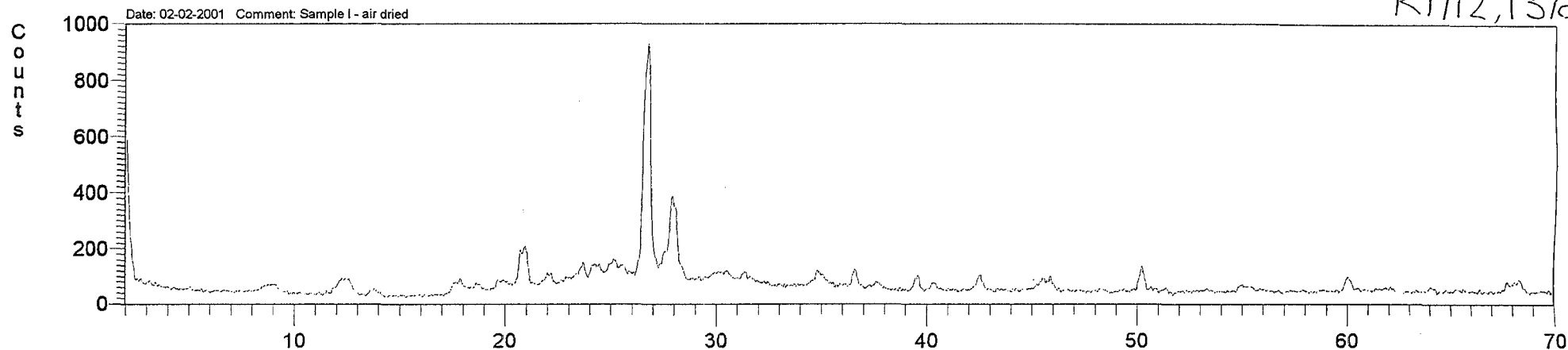
Crystalline components identified:

Quartz (Q)	60%
Albite (A)	25%
Kaolinite (K)	10%
Muscovite (M)	5%

Note: these amounts are semi-quantitative estimates only!



R1/12,13/a

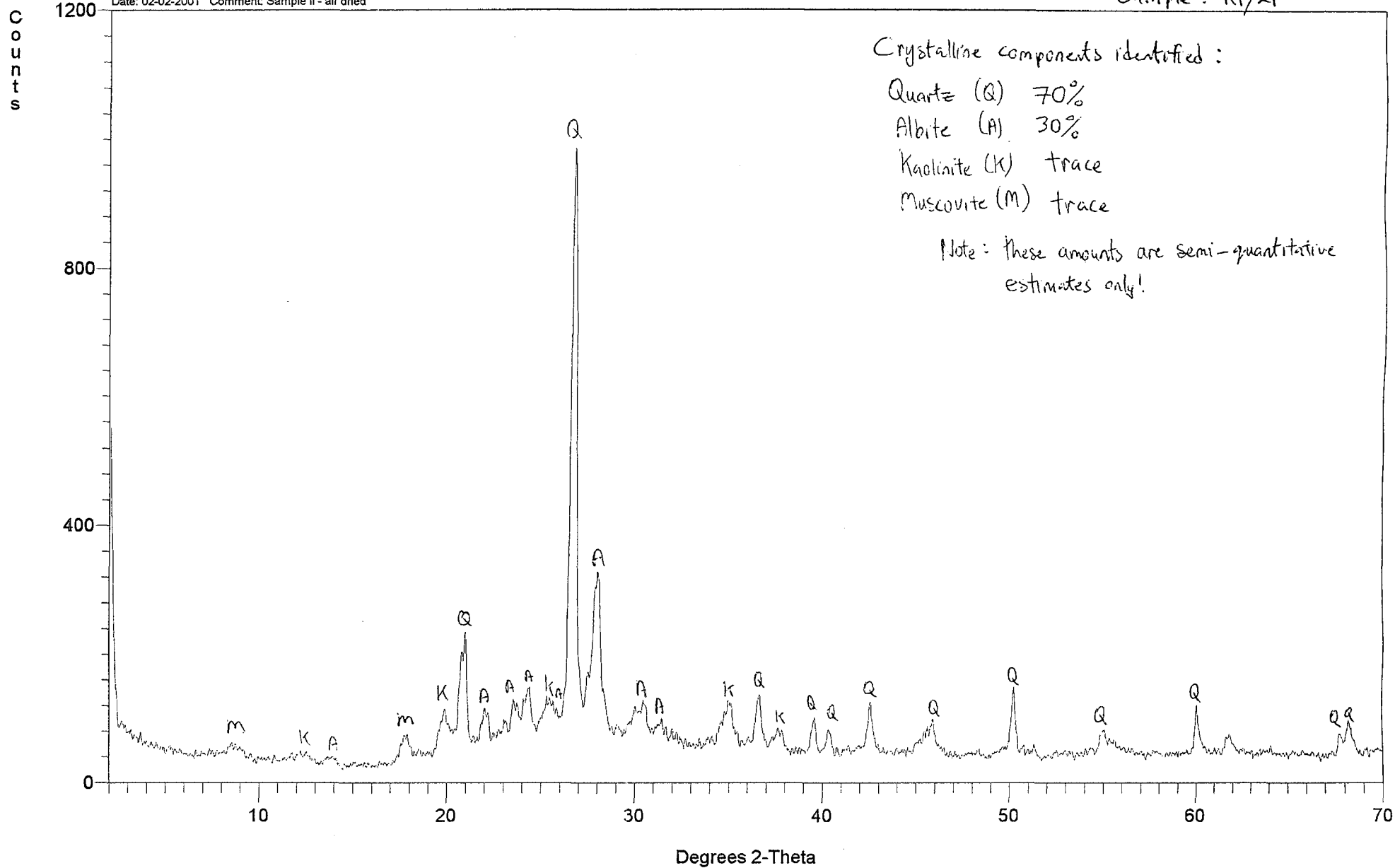


E-3

Sample R1/12,13/a

Sample: R1/21

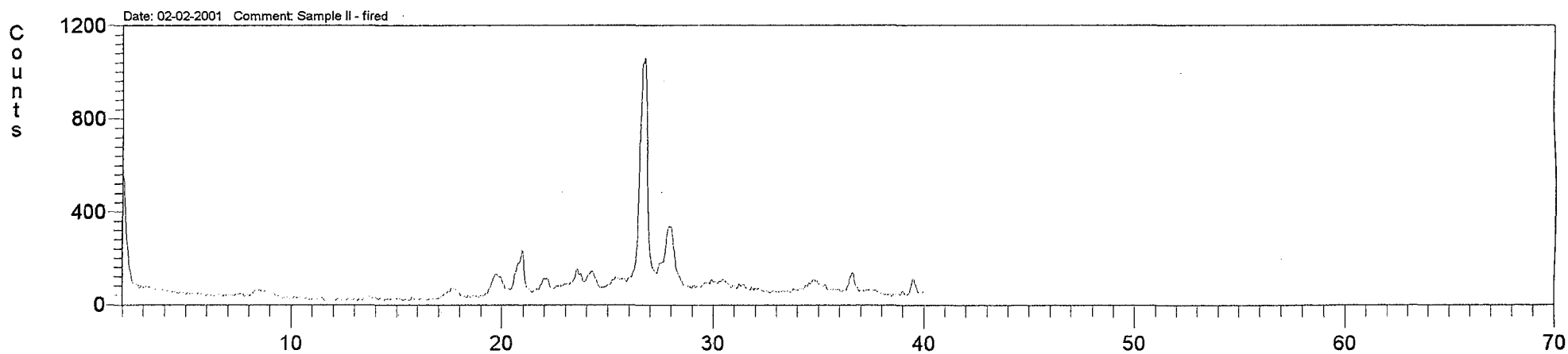
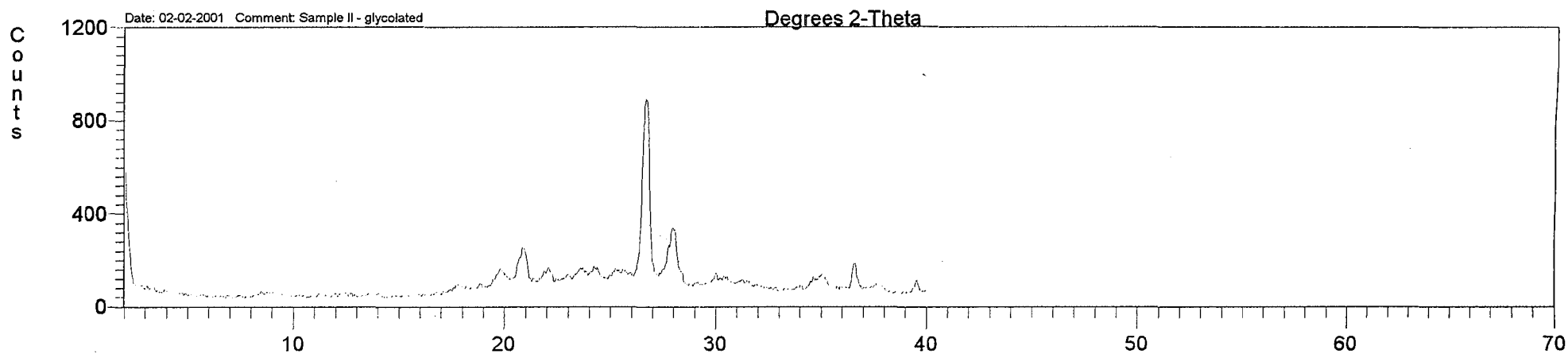
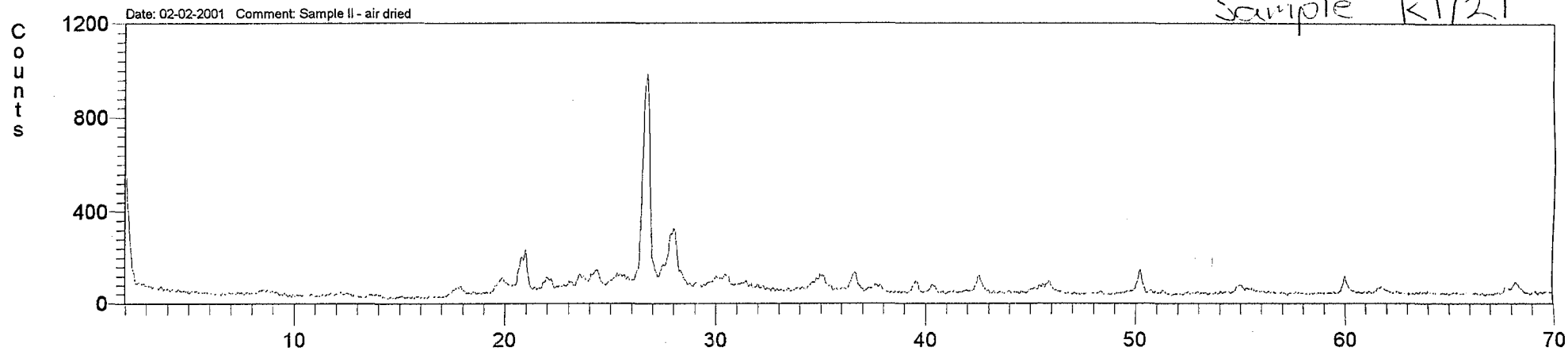
Date: 02-02-2001 Comment: Sample II - air dried



E-4

Sample R1/21

Sample R1/21



E-5

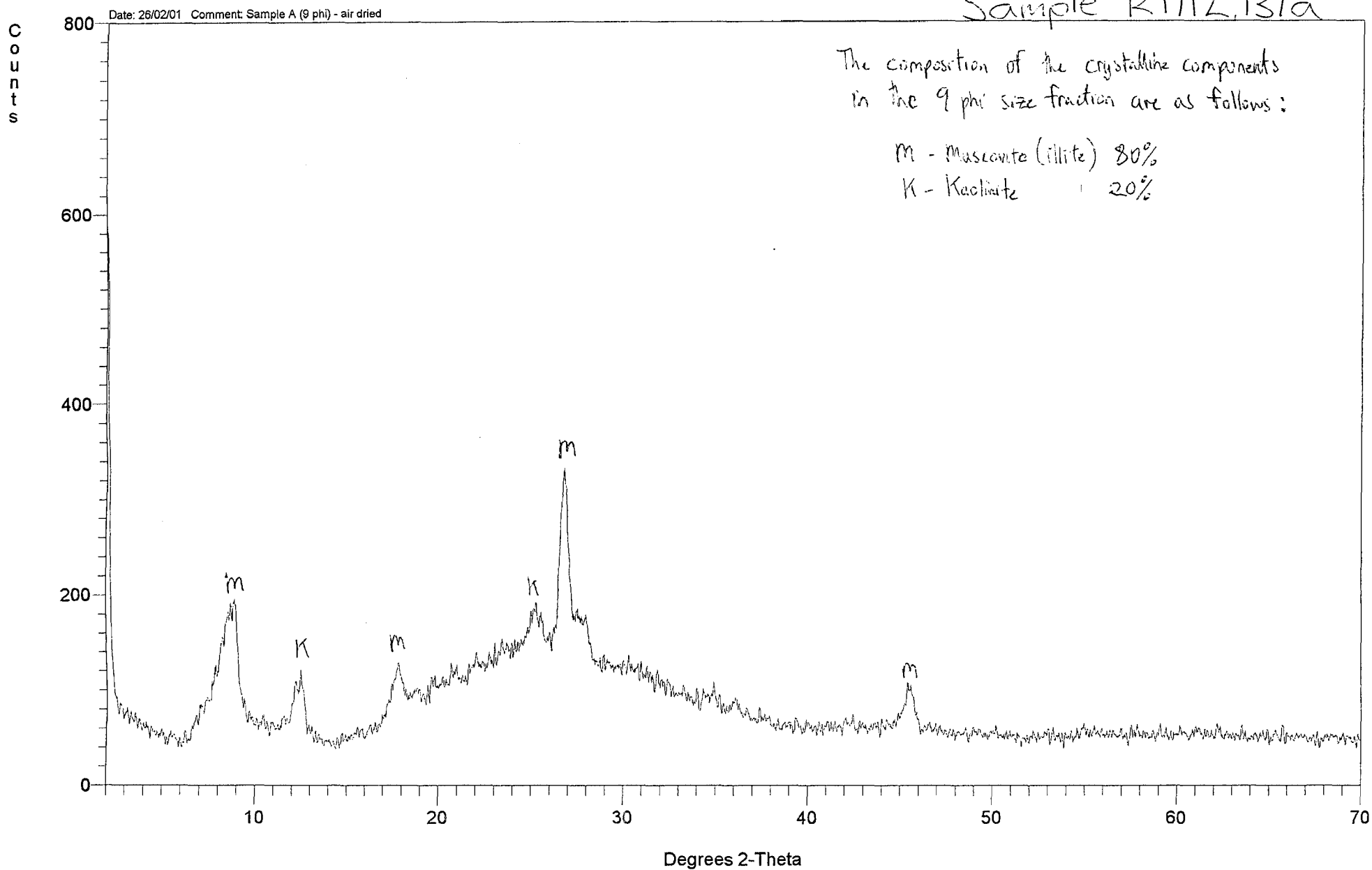
Sample R1/21

Sample R1/12.13/a

The composition of the crystalline components
in the 9 phi size fraction are as follows:

m - muscovite (illite) 80%

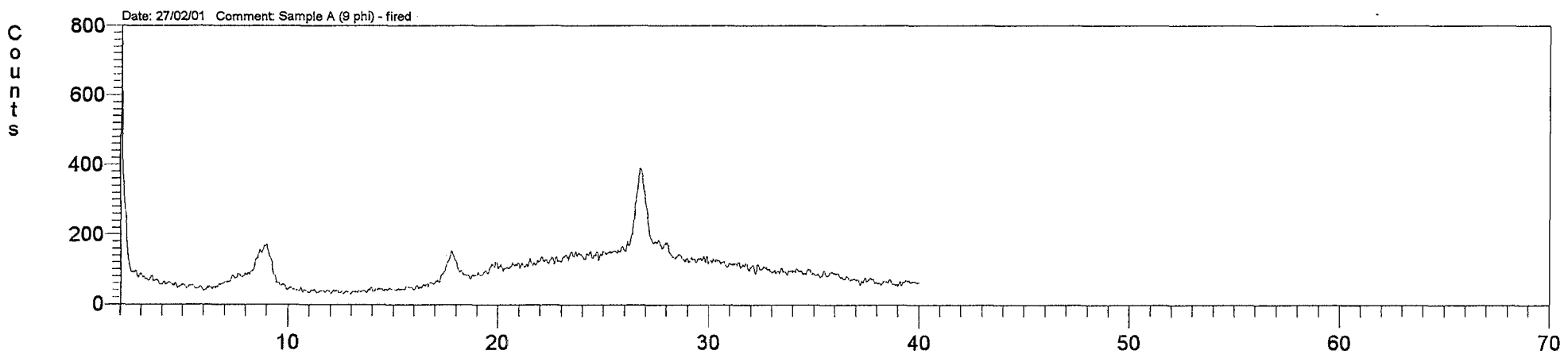
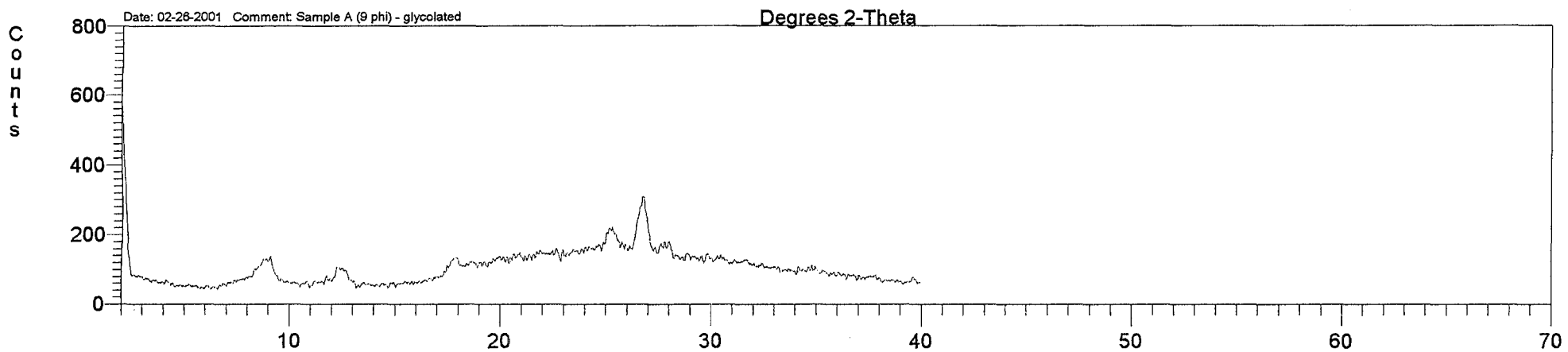
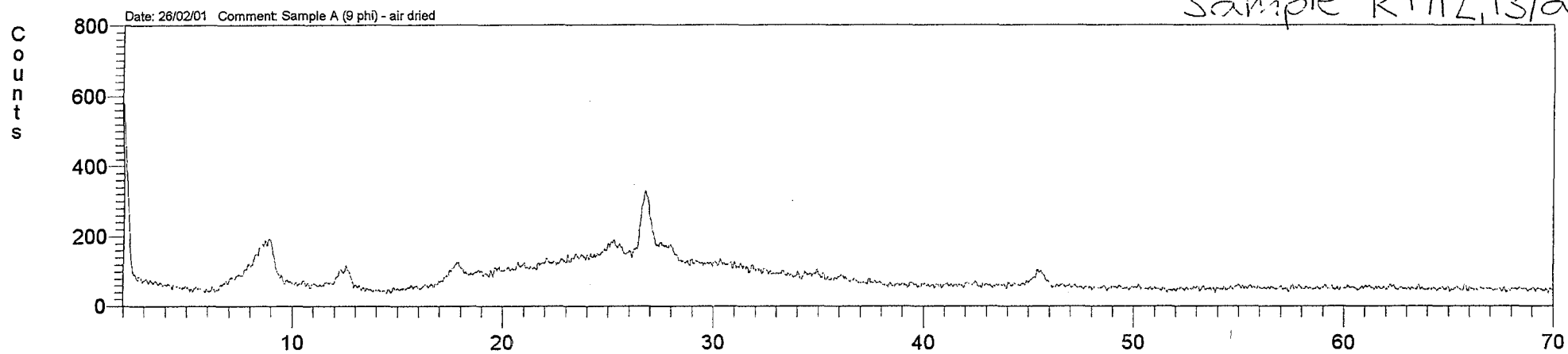
K - Kaolinite 20%



E-6

Sample R1/12.13/a

Sample K112,13/a



E-7

Sample R1/12,13/a

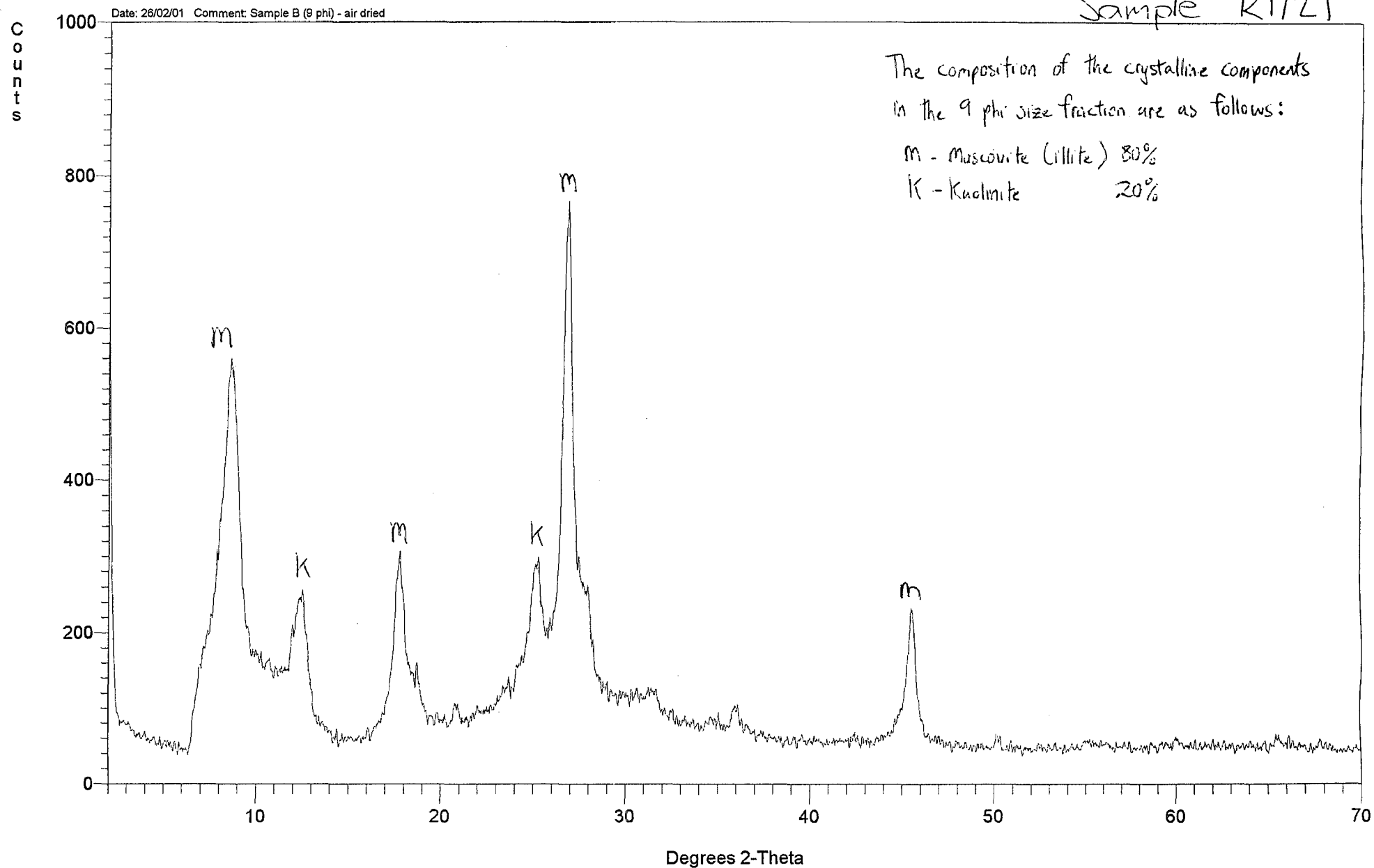
Sample R1/21

Date: 26/02/01 Comment: Sample B (9 phi) - air dried

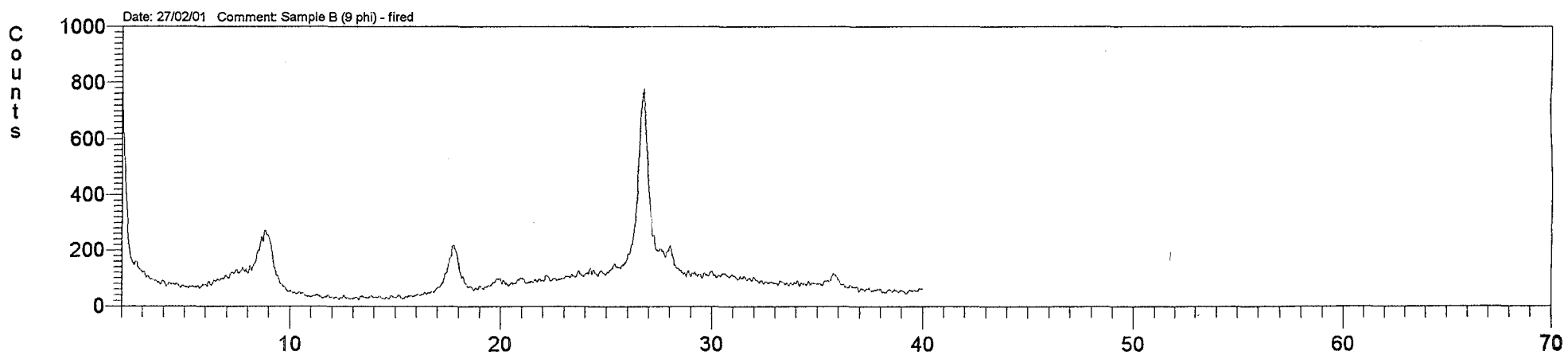
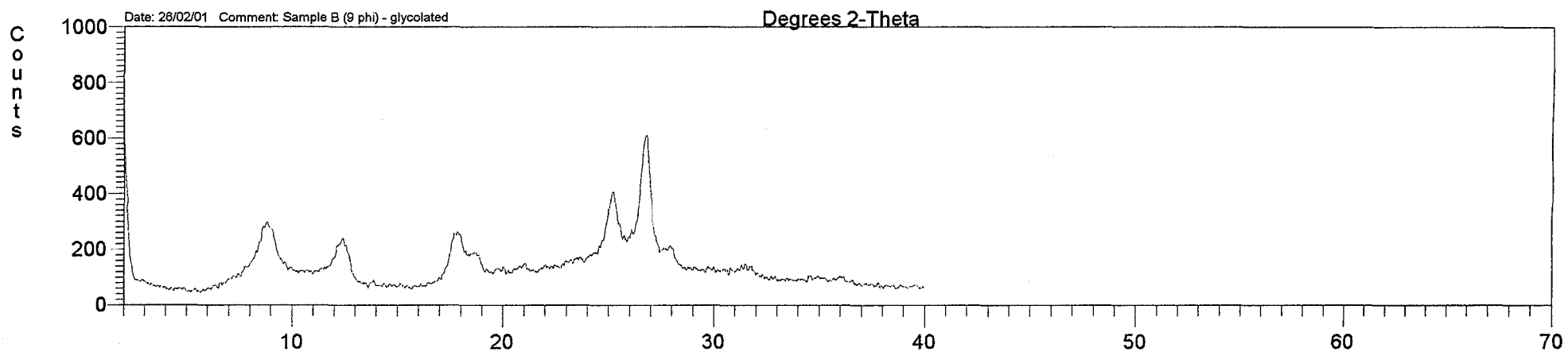
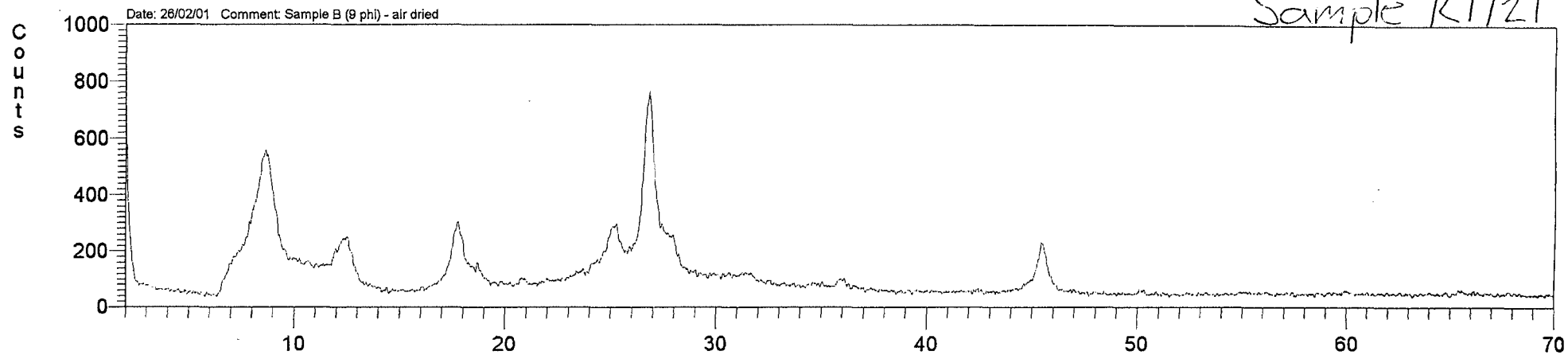
The composition of the crystalline components
in the 9 phi size fraction are as follows:

m - muscovite (illite) 80%

k - kaolinite 20%



Sample R1/21

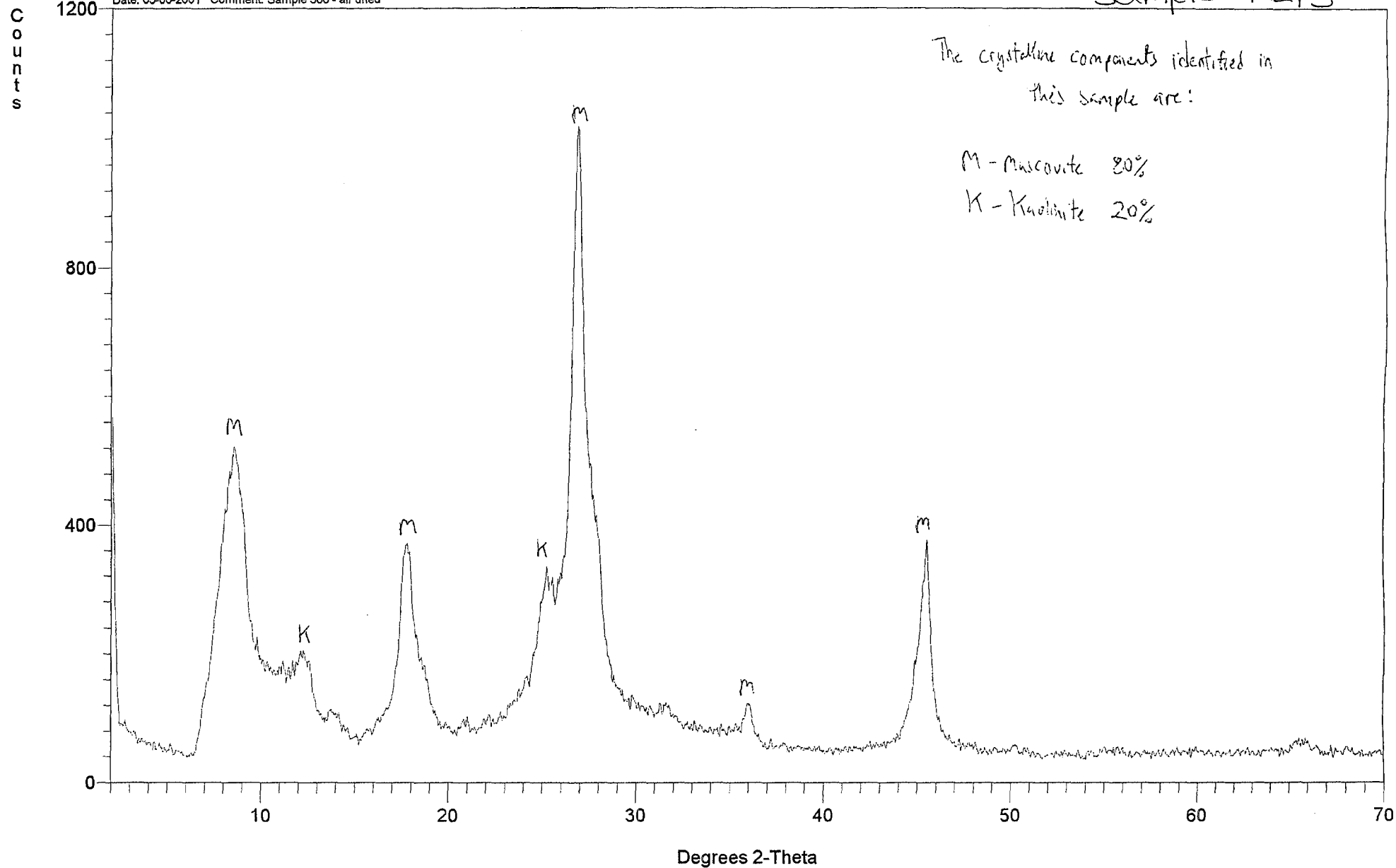


E-9

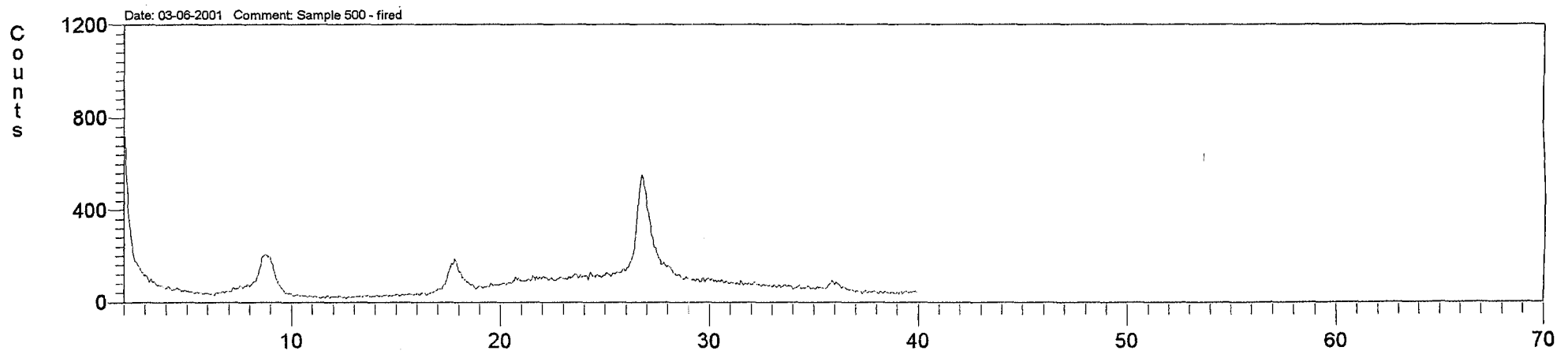
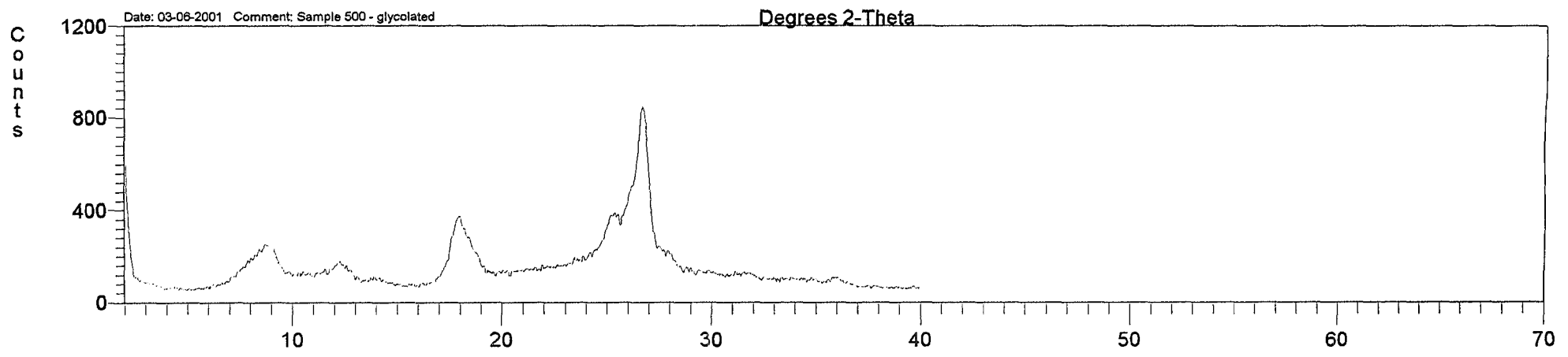
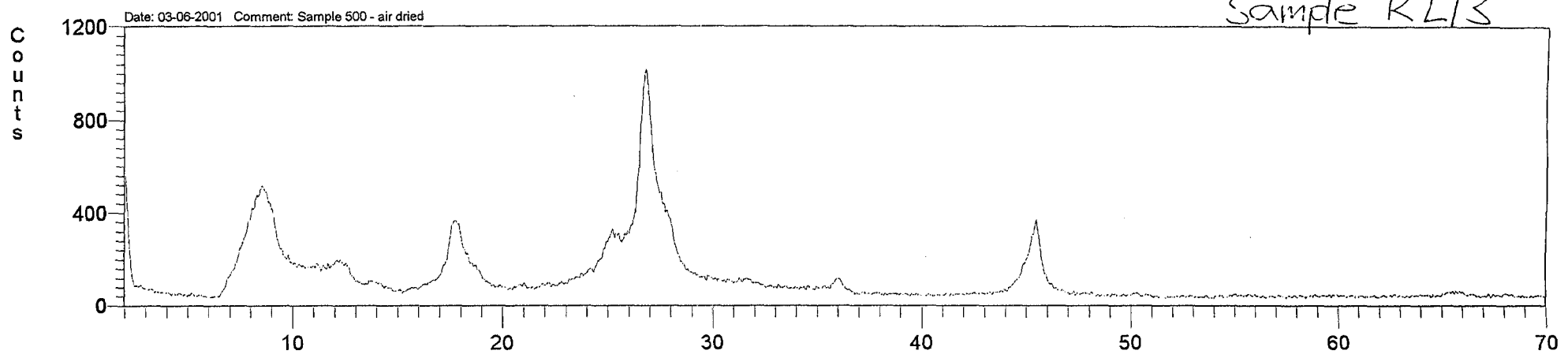
Sample R1/21

Sample R2/3

Date: 03-08-2001 Comment: Sample 500 - air dried



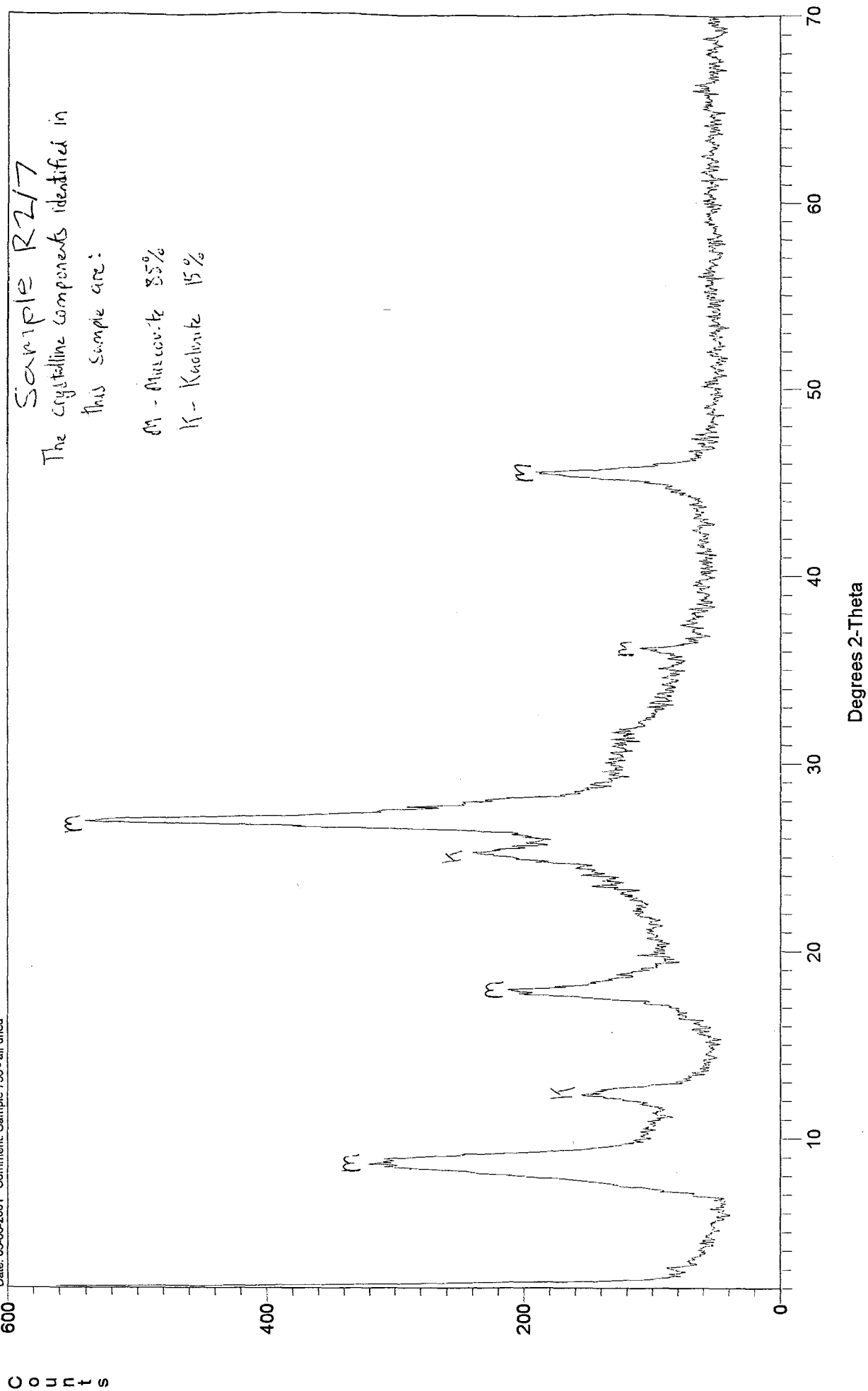
Sample K2/3



E-11

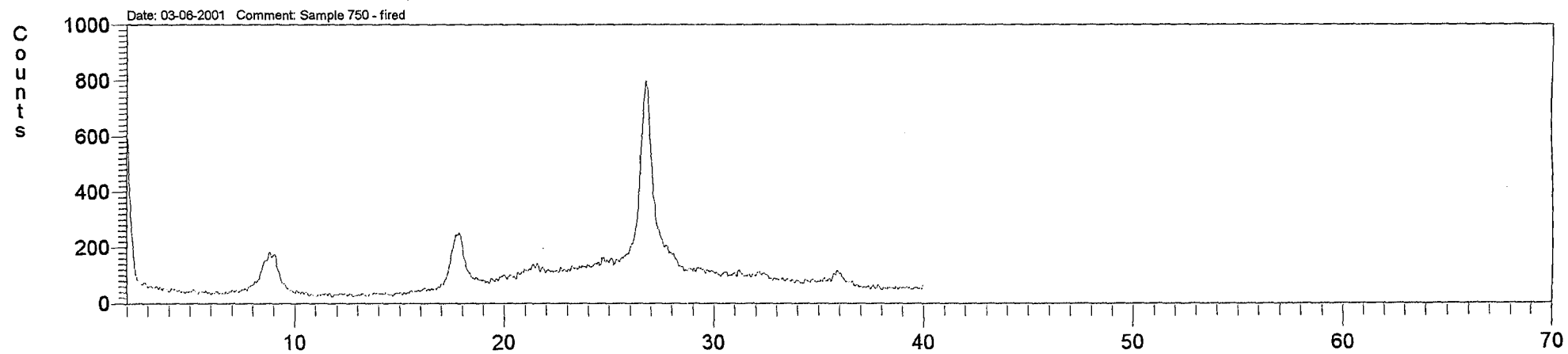
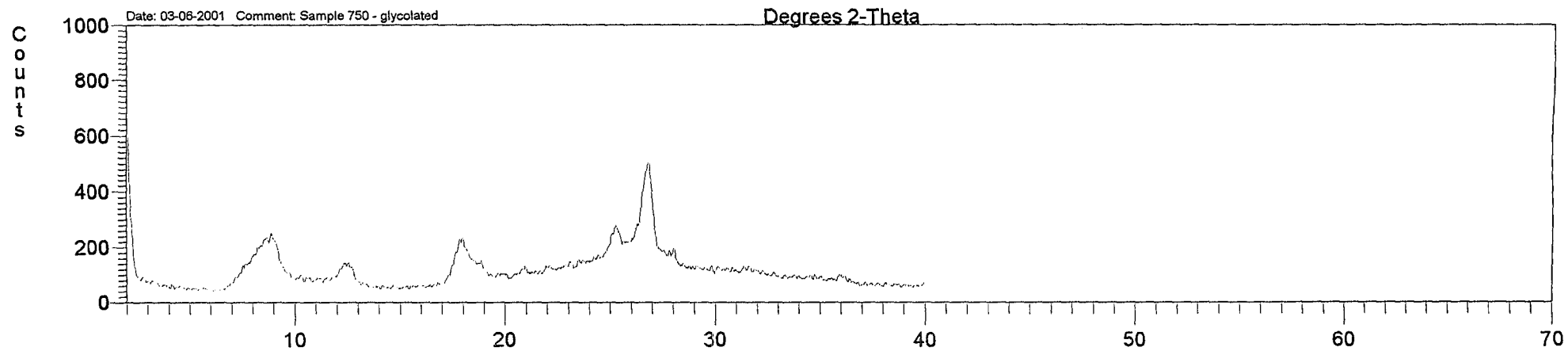
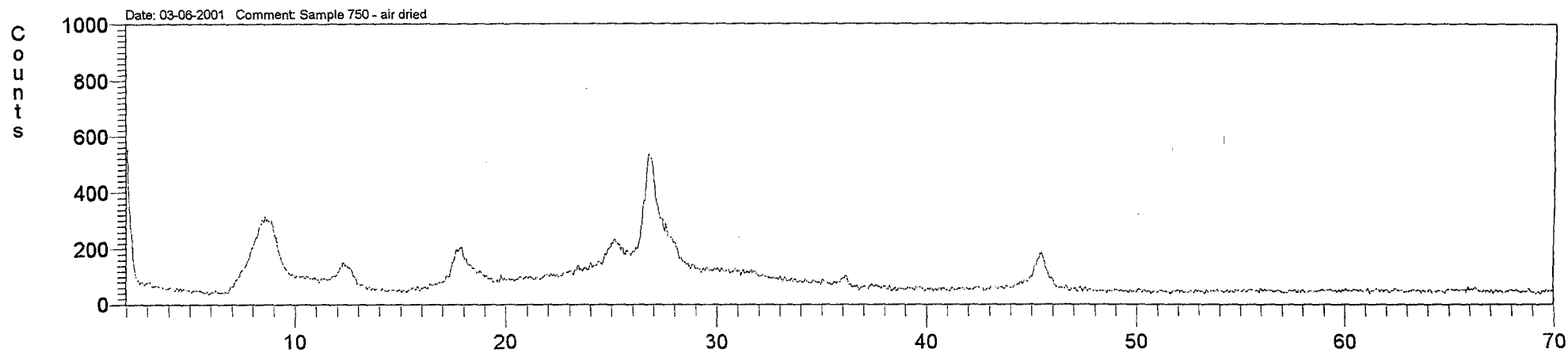
Sample R2/3

Date: 03-06-2001 Comment: Sample 750 - air dried



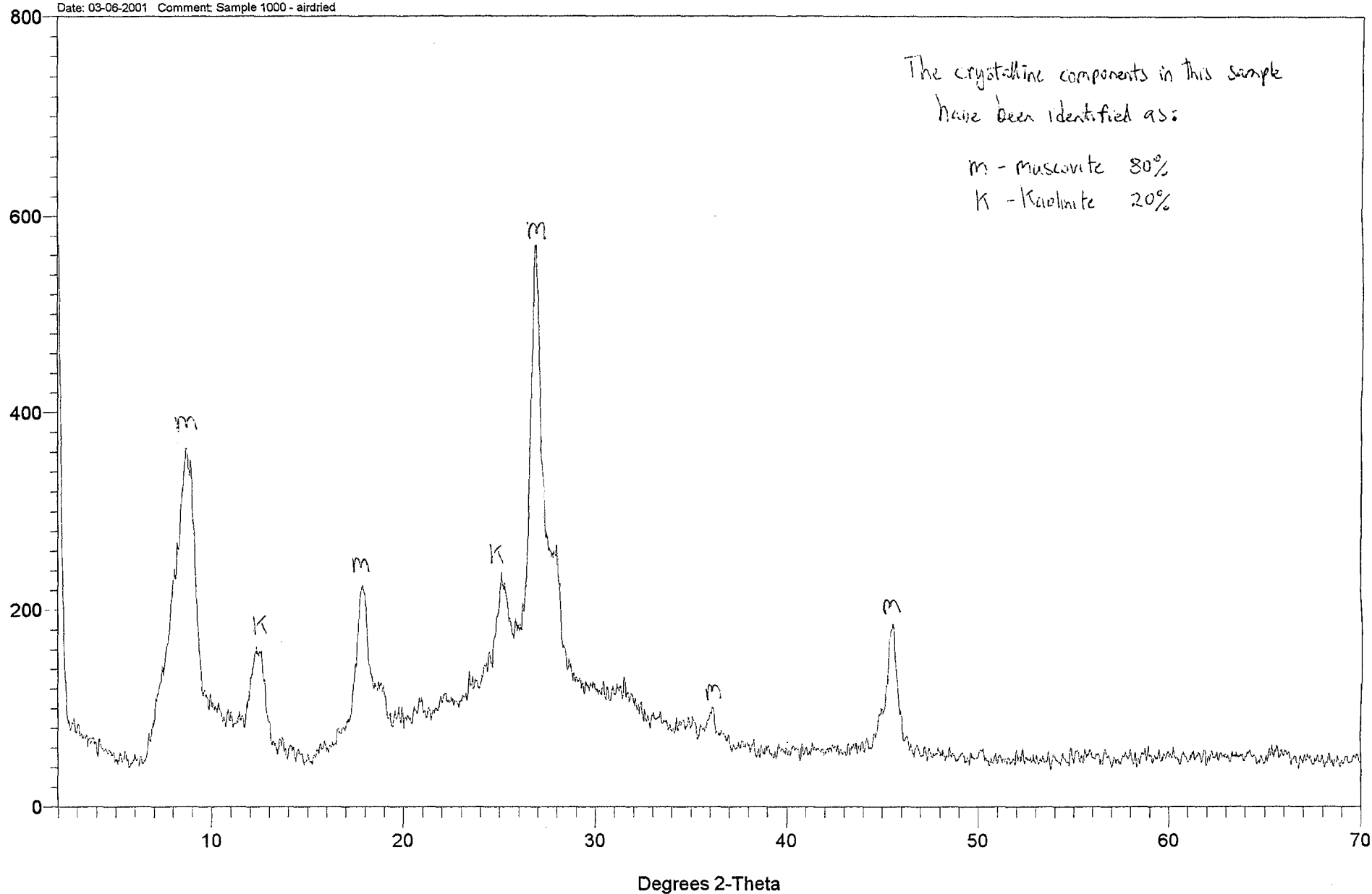
E-13

Sample R2/7



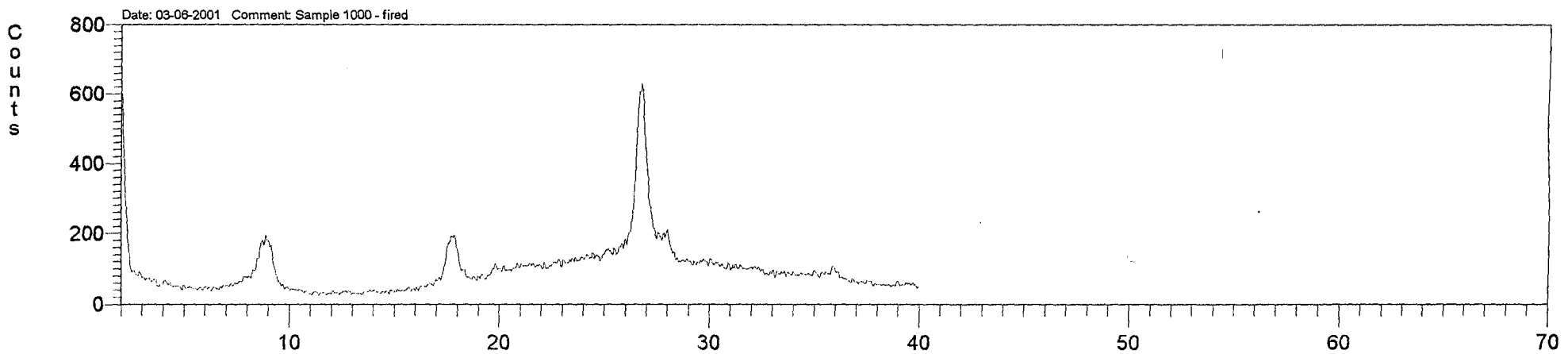
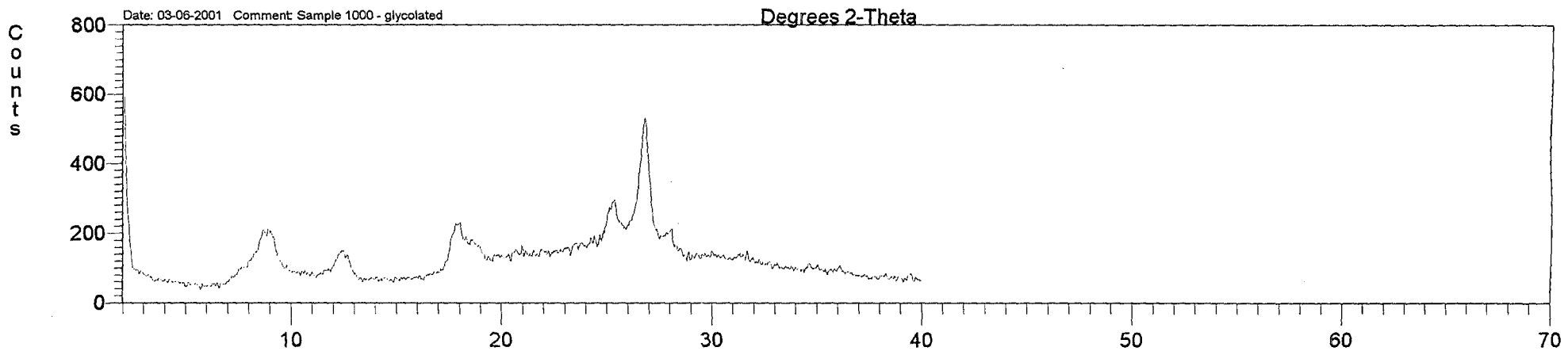
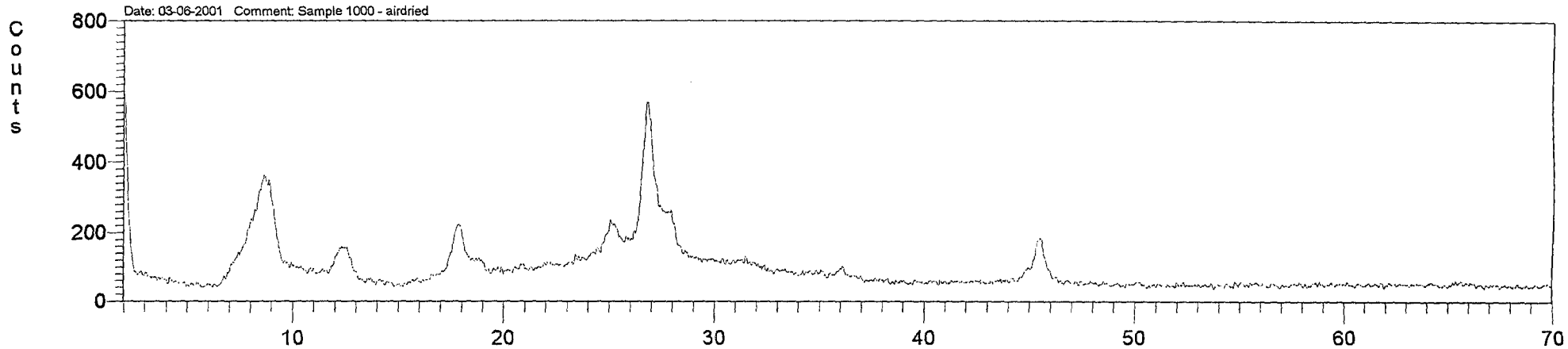
Date: 03-06-2001 Comment: Sample 1000 - airdried

C
O
U
N
T
S



E-14

Sample R2/11

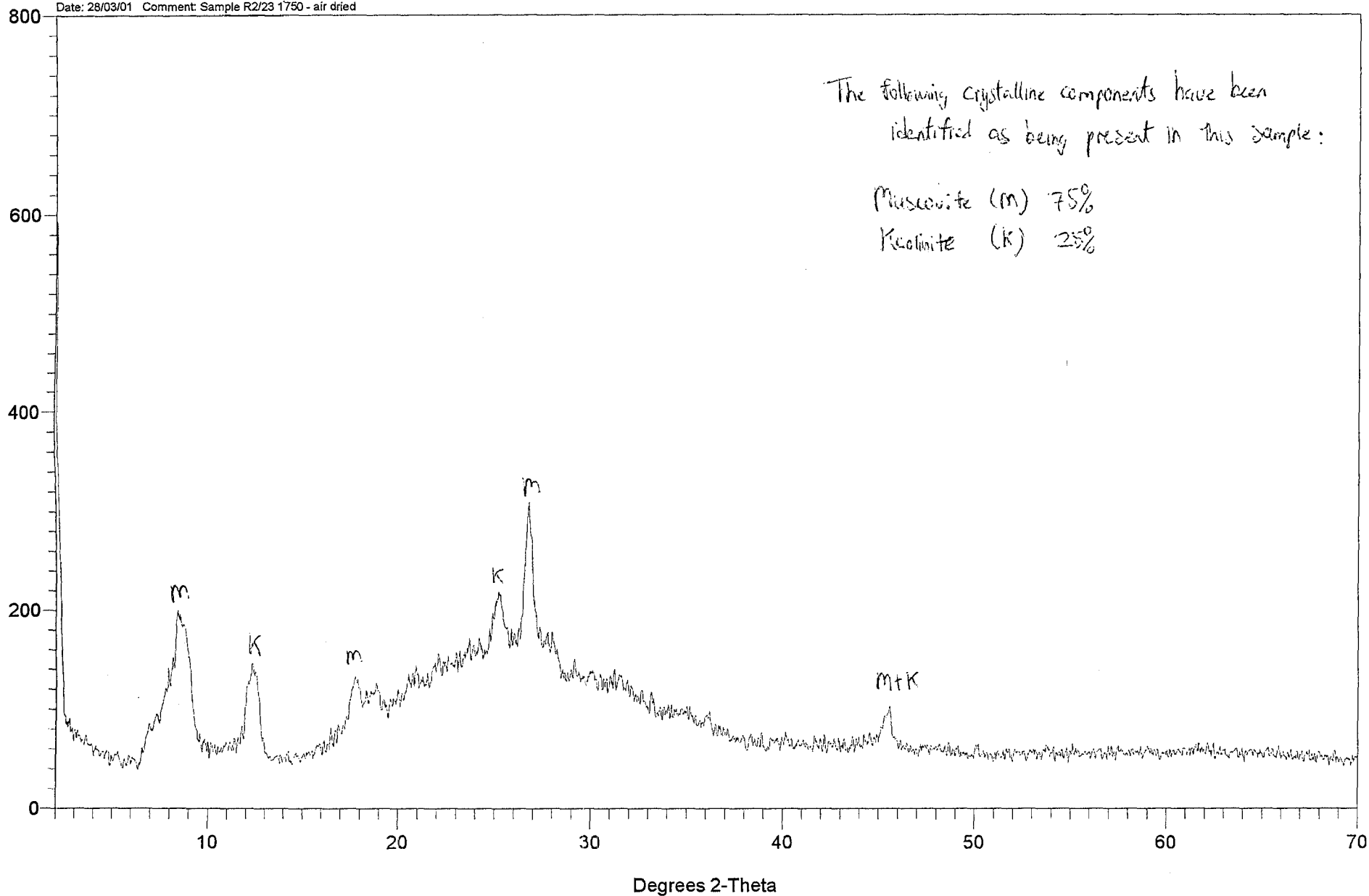


E-15

Sample R2/11

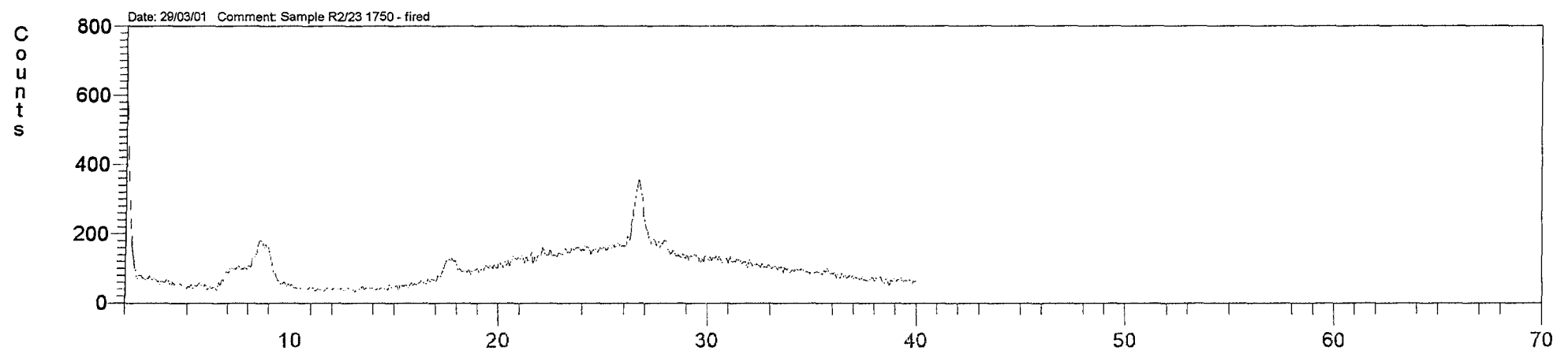
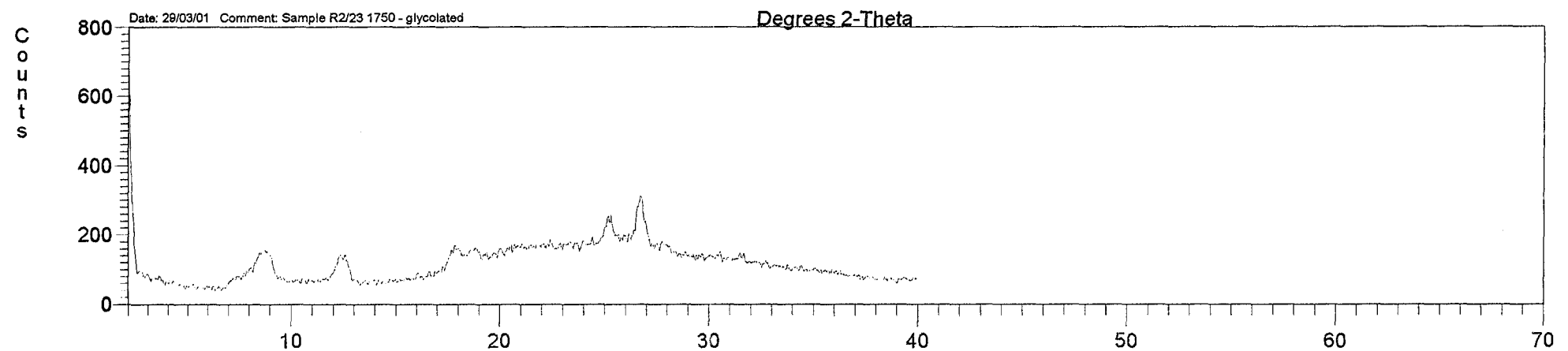
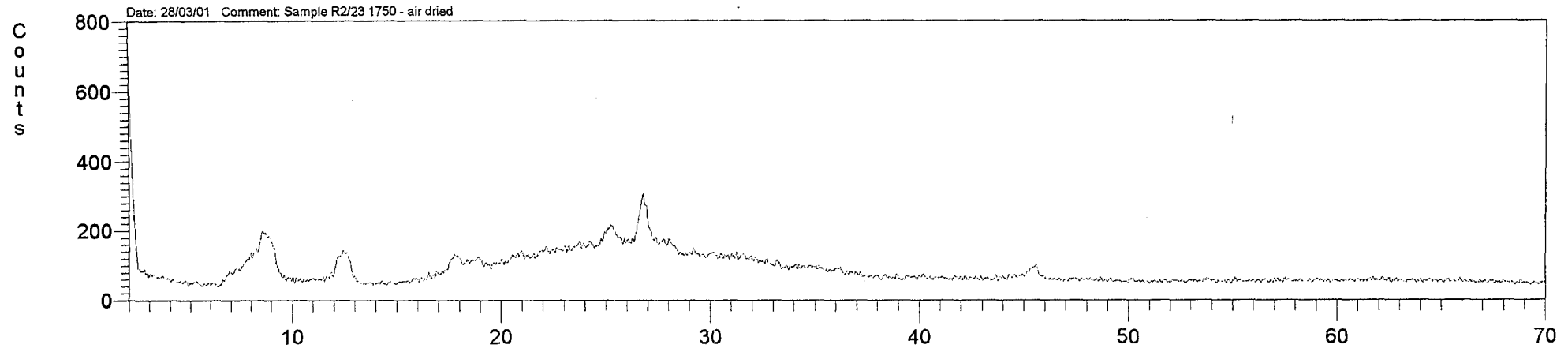
C
o
u
n
t
s

Date: 28/03/01 Comment: Sample R2/23 1750 - air dried



E-17

Sample R2/23



Appendix – F

Laboratory Testing

Method for Dry/Bulk Density and Confined Vertical Swell Tests

Dry density and partly-saturated bulk density were obtained using the samples that were recovered in long (170-190 mm) 35 mm diameter tubes from the trenches during excavation. Once the samples were brought to the laboratory, they were weighed at their *insitu* moisture content (partly saturated), and measurements of the length and diameter of the samples within the tube were taken. The sample was then placed in an oven at a temperature of $105 \pm 1^\circ\text{C}$ until dry. Once dry, the sample was weighed and measured before extraction from the tube, after which the empty tube was weighed so the weight of soil both dry and wet could be calculated and compared. To calculate volume of the wet and dry samples the equation for the volume of a cylinder was used.

$$V = \Pi R^2 L \quad \text{Equation 4.1}$$

V = Volume of Cylinder

Π = Pie

R = Radius

L = Length of cylinder

With both weight and volume the density can be easily calculated using the following equation.

$$\text{DryDensity} = \frac{M_s}{V_t} \quad \text{Equation 4.2}$$

$$(\text{Partially Saturated}) \text{ BulkDensity} = \frac{M_s + M_w}{V_a + V_w + V_s} \quad \text{Equation 4.3}$$

$$(\text{Fully Saturated}) \text{ BulkDensity} = \frac{M_s + M_w}{V_s + V_w} \quad \text{Equation 4.4}$$

M_s = Mass of Solids

V_t = Volume total

M_w = Mass of Water

V_a = Volume of air

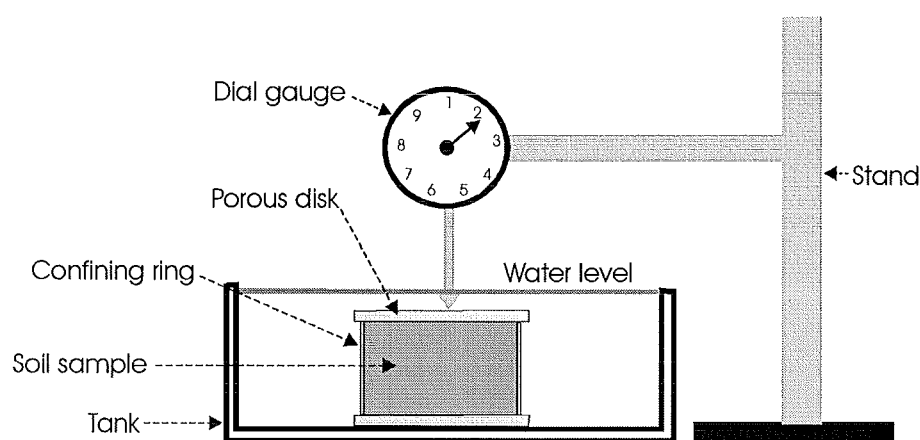
V_w = Volume of water

V_s = Volume of Solid

Partially saturated densities were calculated from long tube samples and tested at *insitu* moisture content, while fully saturated samples were taken after vertical swell tests were performed (see below).

Samples used for vertical swell tests were recovered in short (90mm long) 35mm diameter tubes. The sample was then extracted from the recovery tube and pushed into a shorter, 30 mm tube. Two 30 mm tube samples were produced (deformation of sample can occur at this stage). One was trimmed immediately, then weighed, measured, and placed into the testing tank (Figure A.5.1).

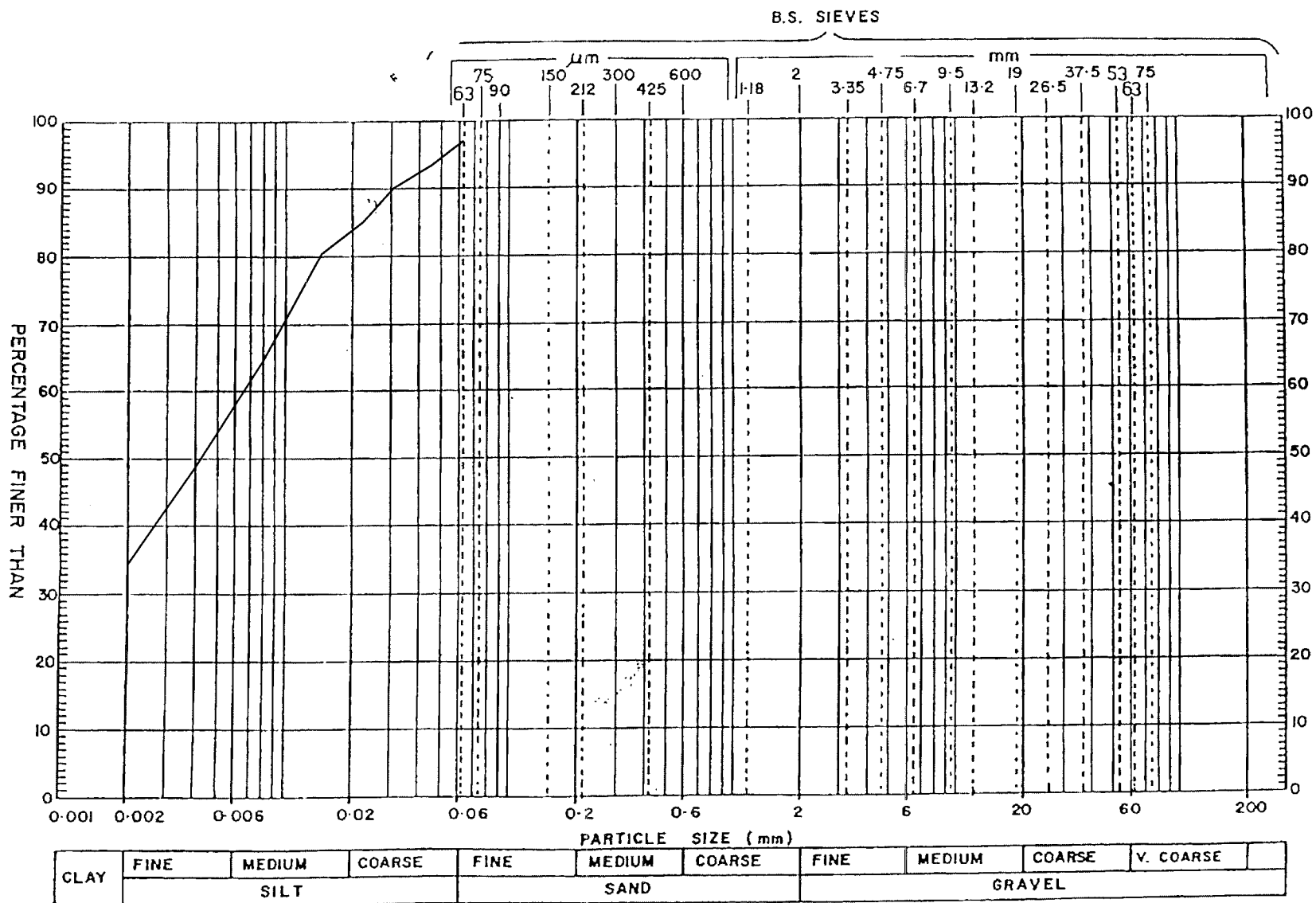
Figure A.5.1 Vertical Swell Apparatus



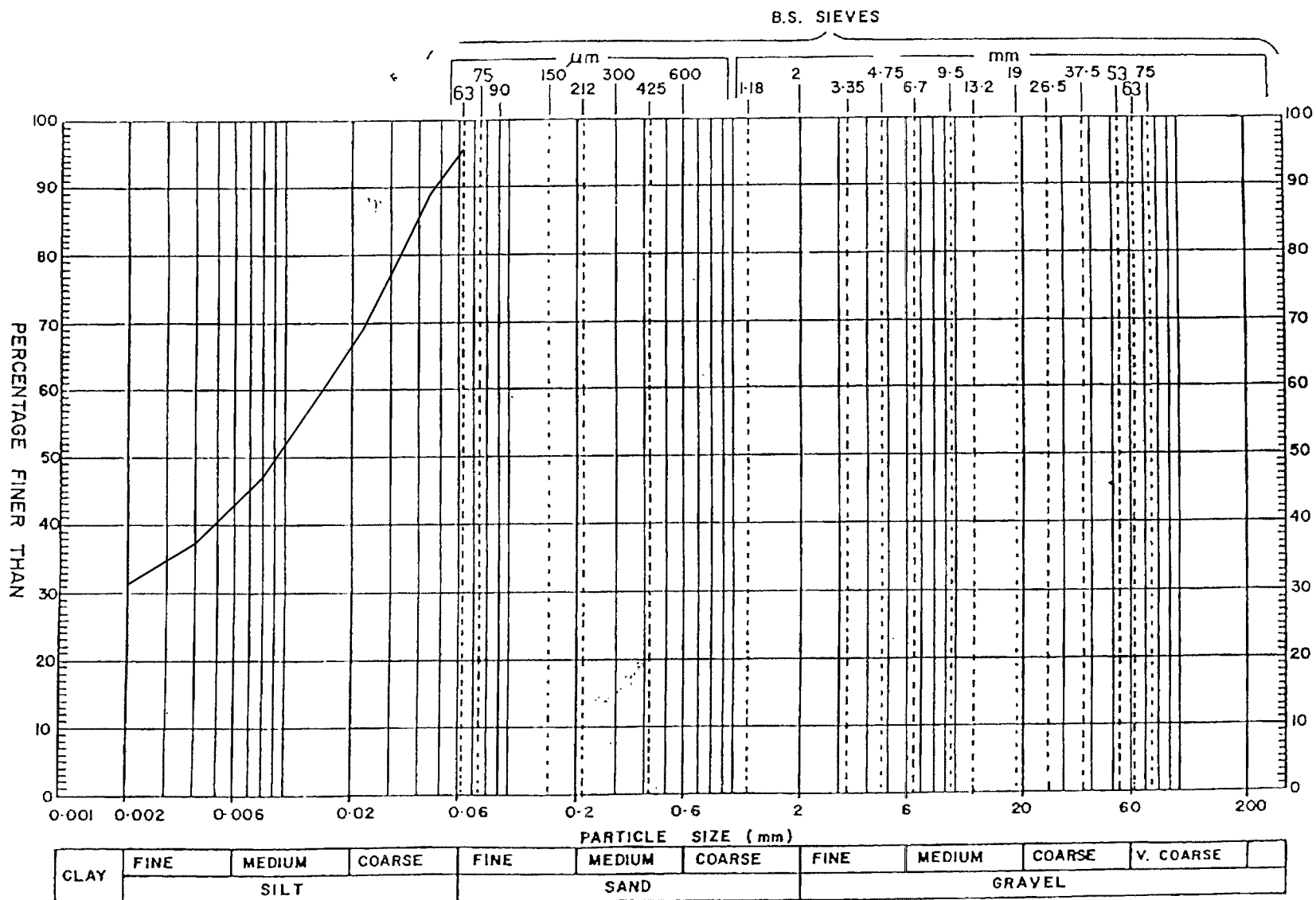
The dial gauge would be read before any water was placed in the dish and then after 24 hours to get a total swell measurement from which, percentage swells could be calculated. Once the sample was removed from the dish it would also be weighed so bulk density could be calculated.

The second sample would be trimmed conservatively at either end and then dried in an oven heated to 40 degrees Celsius. Once dry, the sample was trimmed using a file to produce two flat even surfaces. It was then weighed and measured, before being placed in the vertical swell apparatus. It should be noted that upon drying the soil shrinks away from the confining tube both in a vertically and horizontally. This gives the sample room to swell that cannot be measured by the vertical swell apparatus. While this should be taken into consideration, this occurrence should not be viewed as reducing the value of the results, as it is also part of the natural cracking process of soil.

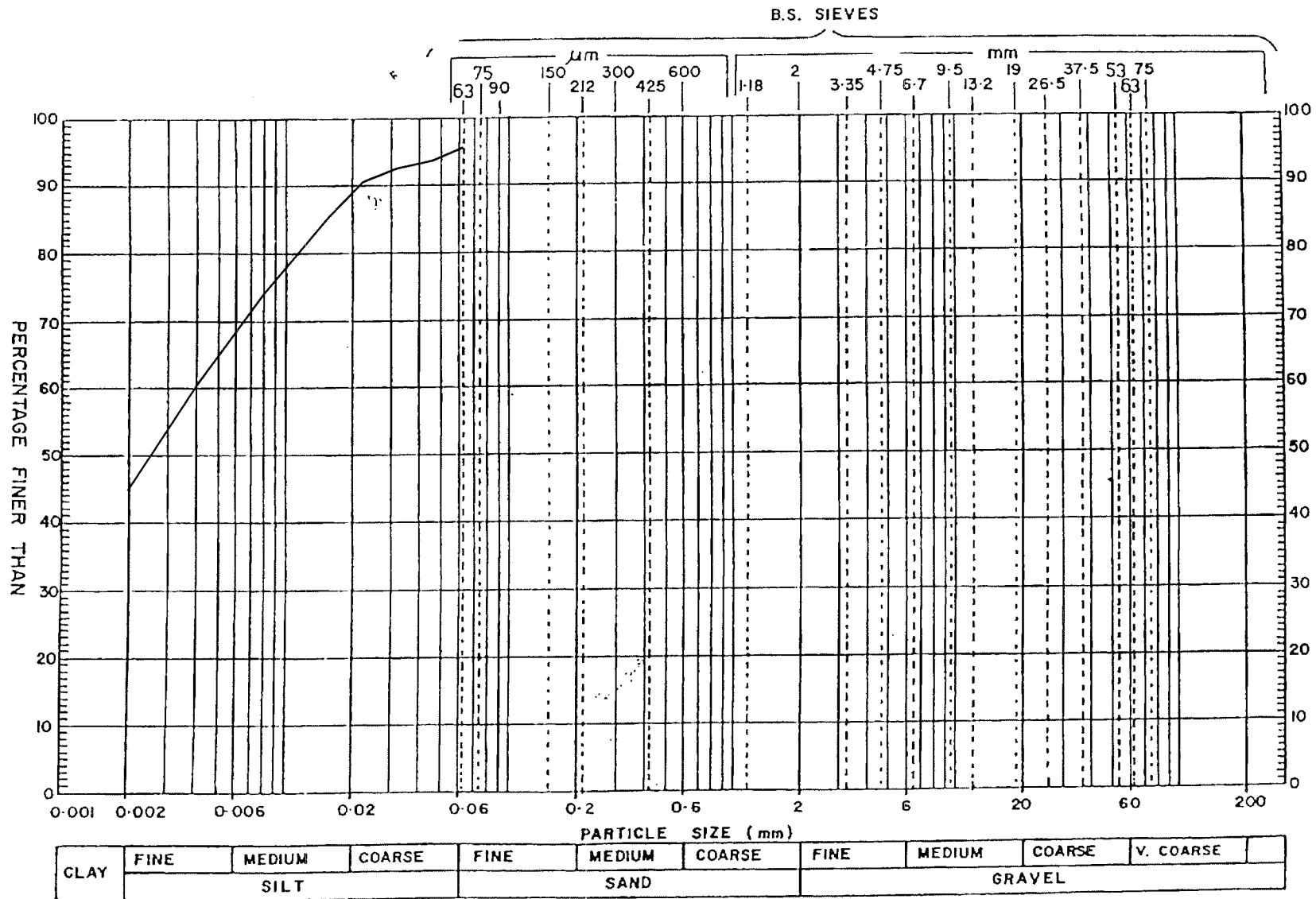
Determination of the Particle-Size Distribution For the < 0.063mm Material



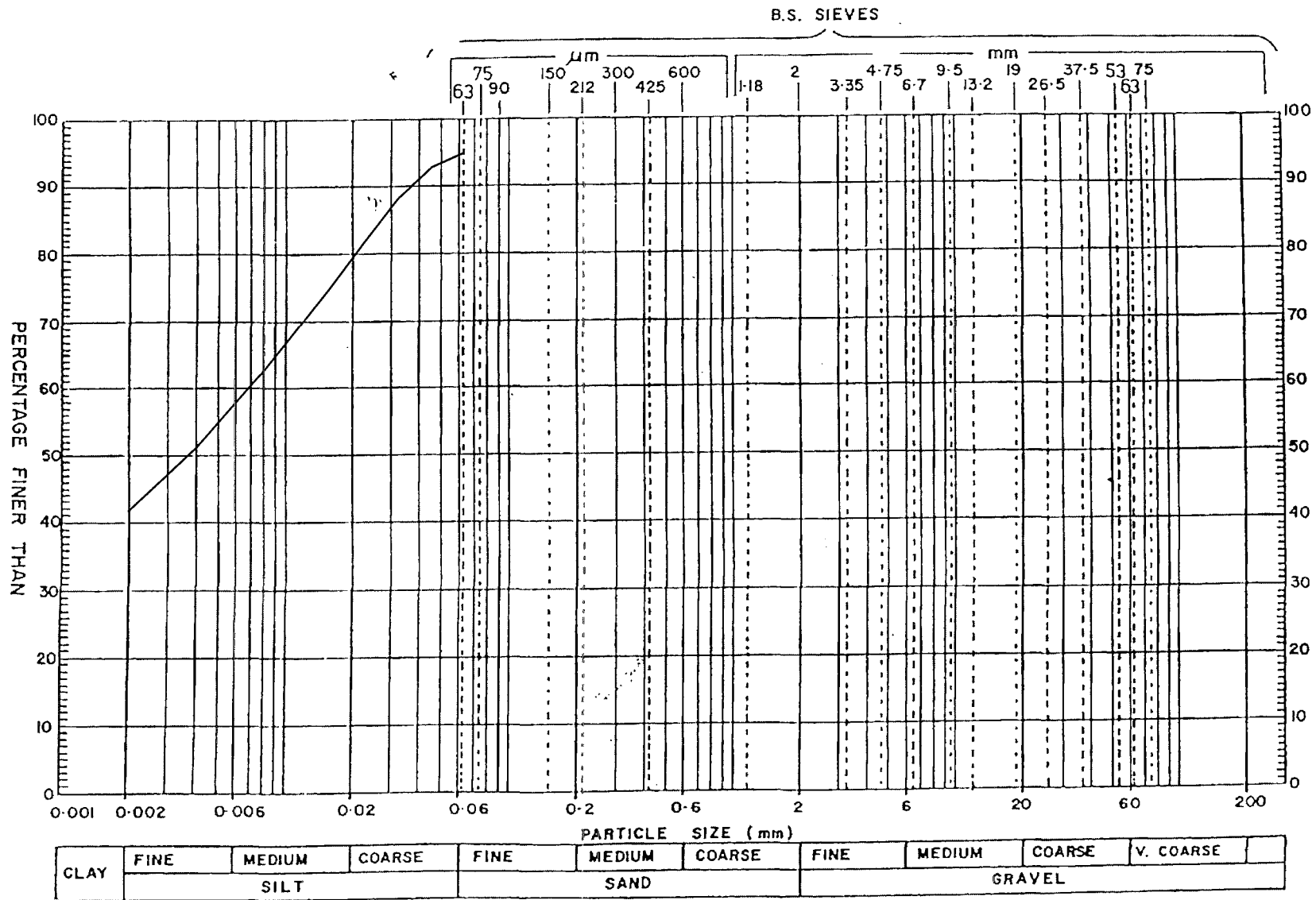
Determination of the Particle-Size Distribution For the < 0.063mm Material



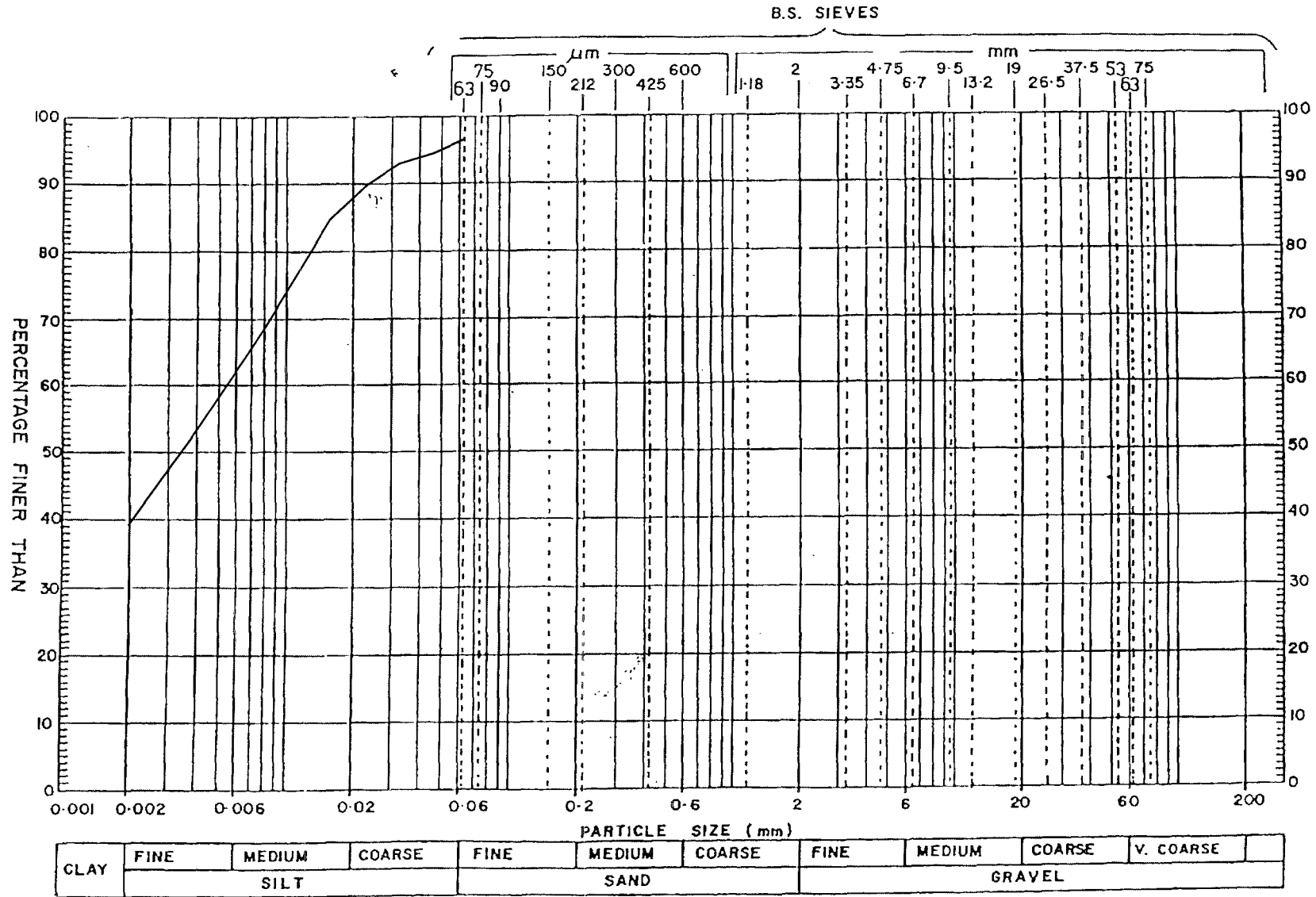
Determination of the Particle-Size Distribution For the < 0.063mm Material



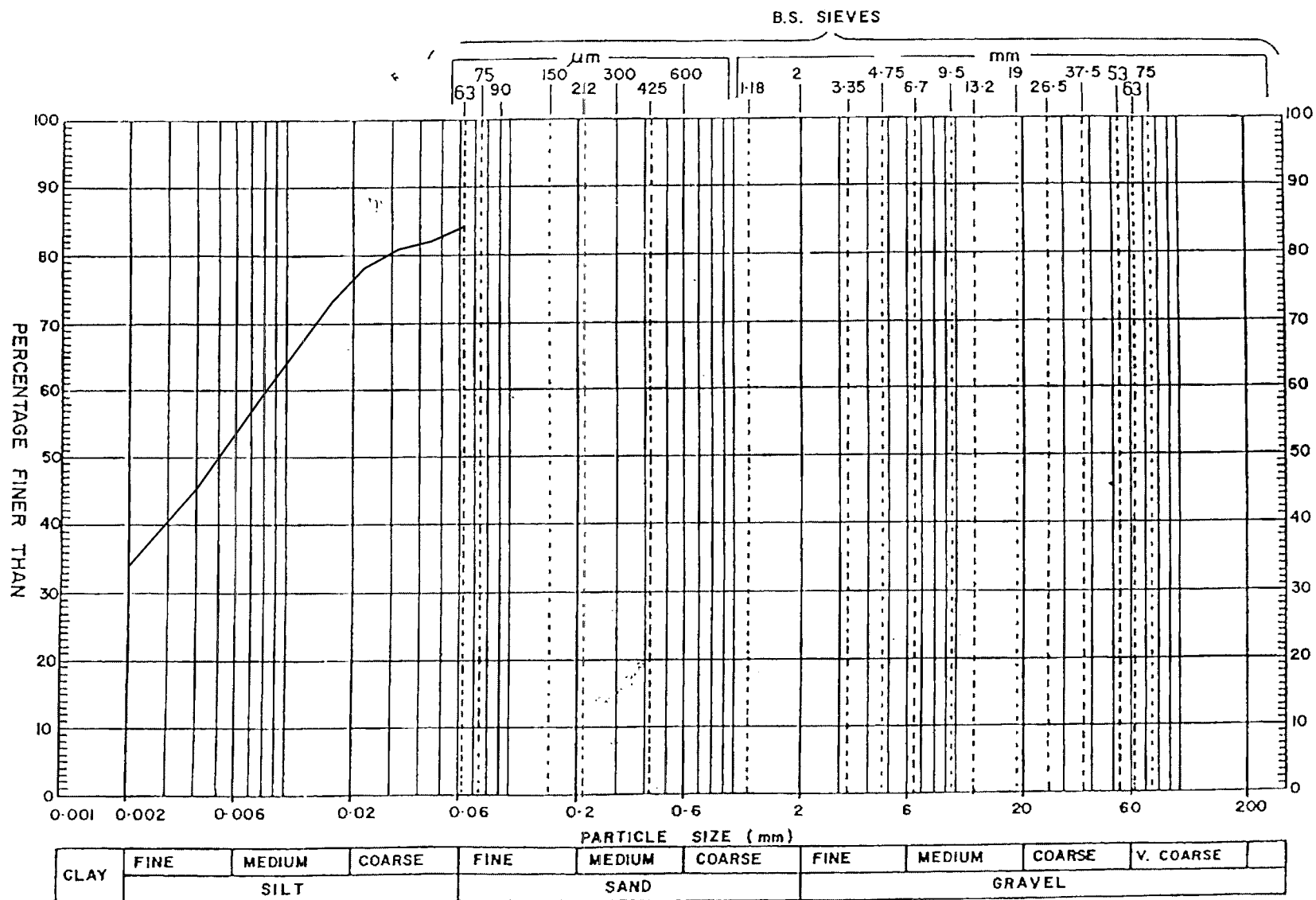
Determination of the Particle-Size Distribution For the < 0.063mm Material



Determination of the Particle-Size Distribution For the < 0.063mm Material



Determination of the Particle-Size Distribution For the < 0.063mm Material



Determination of the Particle-Size Distribution For the < 0.063mm Material

